10-23-2023 10:00 AM

Role and regulation of galectin-12 in the context of cellular differentiation

Rada Tazhitdinova, *Western University*

Supervisor: Timoshenko, Alexander V., *The University of Western Ontario*

A thesis submitted in partial fulfillment of the requirements for the Master of Science degree in Biology

Abstract

Galectin-12 is a tissue-specific galectin known for governing adipocyte differentiation and the regulation of lipogenesis. This study aimed to evaluate the role of galectin-12 in the differentiation of myeloid and breast cancer cell lines. All-trans retinoic acid (ATRA) and dimethyl sulfoxide (DMSO) were found to differentiate acute myeloid leukemia HL-60 cells into functionally distinct phenotypes of neutrophils which had opposite changes in *LGALS12*. Neutrophilic differentiation also led to the inhibition of galectin-12 secretion, and an increase in lipid droplet accumulation. Galectin-12 secretion was found to be influenced by a modulator of autophagy, suggesting the involvement of secretory autophagy. Galectin-12 (*LGALS12*) gene expression and secretion levels were also found to be *O*-GlcNAc-independent. In breast cancer cell lines, a subtype-specific upregulation of *LGALS12* was observed upon ATRA-induced differentiation in triple negative (basal B) MDA-MB-231 cells. These findings point to the role of galectin-12 as a tissue-specific biomarker of cellular differentiation.

Keywords

Galectin-12, *LGALS12*, cell differentiation, all-trans retinoic acid, *O*-GlcNAcylation, neutrophils, HL-60 cells, breast cancer, MDA-MB-231 cells, unconventional secretion.

Summary for Lay Audience

Cancer cells acquire features of stemness that help them grow uncontrollably or migrate to new sites. This stemness can potentially be reversed through drug treatments by inducing cell differentiation. Galectins are a family of sugar-binding proteins involved in the regulation of cell growth, death and differentiation. Galectin-12 is a tissue-specific galectin that is primarily found in adipocytes where it plays a role in cell differentiation and the regulation of lipid storage. I aimed to examine the role of galectin-12 in cell differentiation using two models, myeloid and breast cancer cell lines. First, I used acute myeloid leukemia HL-60 cells which can be differentiated into neutrophil-like cells using the chemical agents all-trans retinoic acid (ATRA) or dimethyl sulfoxide. Neutrophils are white blood cells that contribute to the immune response against invading pathogens. Galectin-12 was found to have opposite changes in expression upon neutrophilic differentiation with the two agents. This suggests that galectin-12 can be used as a marker to distinguish the two different populations of neutrophils produced. Galectins can also be secreted out of cells where they carry out signaling by binding to sugars on the cell surface. Galectin-12 was found to have its secretion blocked upon the differentiation of HL-60 cells into neutrophils. Four breast cancer cell lines were differentiated into epithelial-like cells with ATRA. An upregulation of galectin-12 gene expression was observed in MDA-MB-231 cells. This suggests that galectin-12 could act as a tumor suppressor gene or marker of select subtypes of breast cancer. Galectins and their activity can also be influenced by a protein modification known as *O*-GlcNAcylation which is often altered during differentiation. Galectin-12 was found to function in an *O*-GlcNAc-independent manner in both myeloid and breast cancer cell lines. Together, these findings provide new insight into the role and regulation of galectin-12 in cell differentiation.

Co-Authorship Statement

Section 1.5 Breast cancer contains materials from a manuscript currently available as a pre-print and co-authored with Dr. Alexander Timoshenko titled “The glycobiological landscape of breast cancer: insights into galectins and *O*-GlcNAc homeostasis-related genes” on Research Square at https://doi.org/10.21203/rs.3.rs-898135/v1. I contributed to the methodology, investigation, formal analysis, and writing under the supervision of Dr. Alexander Timoshenko.

Sara Cristiano conducted the scopoletin assays and collaborated on the *FPR1* gene expression analysis (Figure 9).

Joshua Yi provided assistance in the flow cytometry analysis of lipid droplets in HL-60 cells (Figure 17C, D).

Dr. Vladimir Zhurov assisted in the bioinformatics analysis of RNA-Seq data of HL-60 cells (Figure 10, Figure 16, Table 4).

Acknowledgments

First, I would like to thank my supervisor Dr. Alexander Timoshenko. Thank you for your mentorship, ideas and consistent support over the years. I joined this lab as an undergraduate volunteer and have learned many skills that are fundamental to research throughout this experience. I would also like to thank my advisory committee, Dr. Sashko Damjanovski and Dr. Gregory Kelly for their guidance and feedback throughout my project.

Next, I would like to thank Dr. Vladimir Zhurov for his tremendous knowledge and guidance with the bioinformatics work involved in my project. Thank you for conducting the analysis of RNA-Seq data and guiding me in the write up for the methodology.

I would like to thank Joshua Yi and Dr. Rodney DeKoter for their help and guidance in conducting my flow cytometry experiments. Josh was always able to find time to help me with my work despite his own extremely busy schedule as a fellow graduate student. I wish him the best of luck in his own project.

Thank you to Dr. John Kelly and Dr. John Ronald for their help in the nucleofection of HL-60 cells. While I was not able to complete this portion of my project, I hope this work will be continued in the future to exciting results. I have gained valuable knowledge in genetic engineering through this experience.

I would also like to thank Sara Cristiano for her crucial contributions to this project. Sara dedicated tremendous time running scopoletin assays and investigating the different phenotypes of neutrophils. I am grateful we got to collaborate and work together during her time as a 4^{th} year thesis student.

A final big thank you to all the other members of the Timoshenko lab that I have worked with throughout my project, including Jennifer Kaminker, Kristina Laus, and Haya Tawfik. It was always a fun time with you girls.

Table of Contents

List of Tables

List of Figures

List of Appendices

List of abbreviations

3-MA	3-methyladenine
3T3-L1	Mouse pre-adipocyte cell line
AC	Ac-5SGlcNAc
Akt	Protein kinase B
AML	Acute myeloid leukemia
APL	Acute promyelocytic leukemia
ATRA	All-trans retinoic acid
CDK2	Cyclin dependent kinase 2
C/EBP	CCAAT enhancer binding protein
ConA	Concanavalin A
DAPI	4′,6-diamidino-2-phenylindole
CRD	Carbohydrate recognition domain
DEG	Differentially expressed gene
DMSO	Dimethyl sulfoxide
DON	6-diazo-5-oxo-L-norleucine
DPBS	Dulbecco’s phosphate buffered saline
EMT	Epithelial-mesenchymal transition
Erk	Extracellular signal-regulated kinase
ESCRT	Endosomal sorting complexes required for transport
ELISA	Enzyme linked immunosorbent assay
Fabp4	Fatty acid binding protein 4
fMLP	N-formylmethionine-leucyl-phenylalanine
FPR	Formyl peptide receptor
GFAT	Glutamine fructose-6-phosphate aminotransferase
GO	Gene ontology
HBP	Hexosamine biosynthesis pathway
HL-60	Human myeloid leukemia cell line
ICAM-1	Intercellular adhesion molecule 1
LBR	Lamin B receptor
LPS	Lipopolysaccharide
MDA-MB-231	Triple negative breast cancer cell line
NADPH	Nicotinamide adenine dinucleotide phosphate

NB4	Acute promyelocytic leukemia cell line
NCF1	Neutrophil cytosolic factor 1
NCF2	Neutrophil cytosolic factor 2
NET	Neutrophil extracellular trap
NF-κB	Nuclear factor κ-light-chain-enhancer of activated B cells
O-GlcNAc	*O*-Linked β-N-Acetyl-D-glucosamine
OGA	*O*-GlcNAcase
OGT	*O*-GlcNAc transferase
PKA	Protein kinase A
PKC	Protein kinase C
PPAR-γ	Peroxisome proliferator-activated receptor γ
PTEN	Phosphatase and tensin homolog
PTM	Post translational modification
RAR	Retinoic acid receptor
RAREs	Retinoic acid response elements
ROS	Reactive oxygen species
RXR	Retinoid X receptor
SREBP1	Sterol regulatory element binding transcription factor 1
TG	Thiamet G
VPS13C	Vacuole protein sorting 13 homolog C

Chapter 1

1 Introduction

1.1 Galectins

Galectins are a family of soluble proteins initially characterized by their binding affinity towards β-galactoside sugars (Johannes et al., 2018; Cummings et al., 2022). Galectins have conserved carbohydrate-recognition domains (CRDs) that are responsible for their glycan-binding abilities. There are 16 known mammalian galectin genes of which 12 are expressed in humans. Galectins can be grouped based on their CRD, with there being proto-type, tandem-repeat, and chimeric galectins (**Figure 1**). Proto-type galectins (galectin-1, -2, -7, -10, -13, -14, and -16) possess one CRD and can form homodimers or remain monomeric. In contrast, tandem-repeat galectins (galectin-4, -8, -9, and -12) have two CRDs that are attached through a peptide linker. Finally, galectin-3 exists as the sole chimeric galectin with one CRD and a N-terminal tail rich in proline, glycine and tyrosine that allows for oligomerization. Each galectin varies in their binding preferences and affinities to various glycans due to the structural differences within the family (Cummings et al., 2022).

The functions of galectins are cell type-specific and vary depending on their localization within or outside the cell. Due to this there can be redundancy in galectin function or antagonistic effects (Tribulatti et al., 2012). Certain galectins like -1, -3, and -8 have ubiquitous expression being found in many tissues, while others like -7, -12, -13, -14, -16 are highly tissue-specific (Tazhitdinova and Timoshenko, 2020). Galectins are synthesized in the cytosol and have broad subcellular localization being detected in the nucleus, mitochondria, lysosomes and various other vesicles. Galectins lack a signal sequence for export through the endoplasmic reticulum-Golgi system and therefore are secreted out of cells through unconventional mechanisms (Popa et al., 2018). Extracellularly, galectins function primarily through carbohydrate-dependent binding of their CRD with cell surface glycoproteins and glycolipids leading to cross-linking and cell-cell/cell-matrix interactions

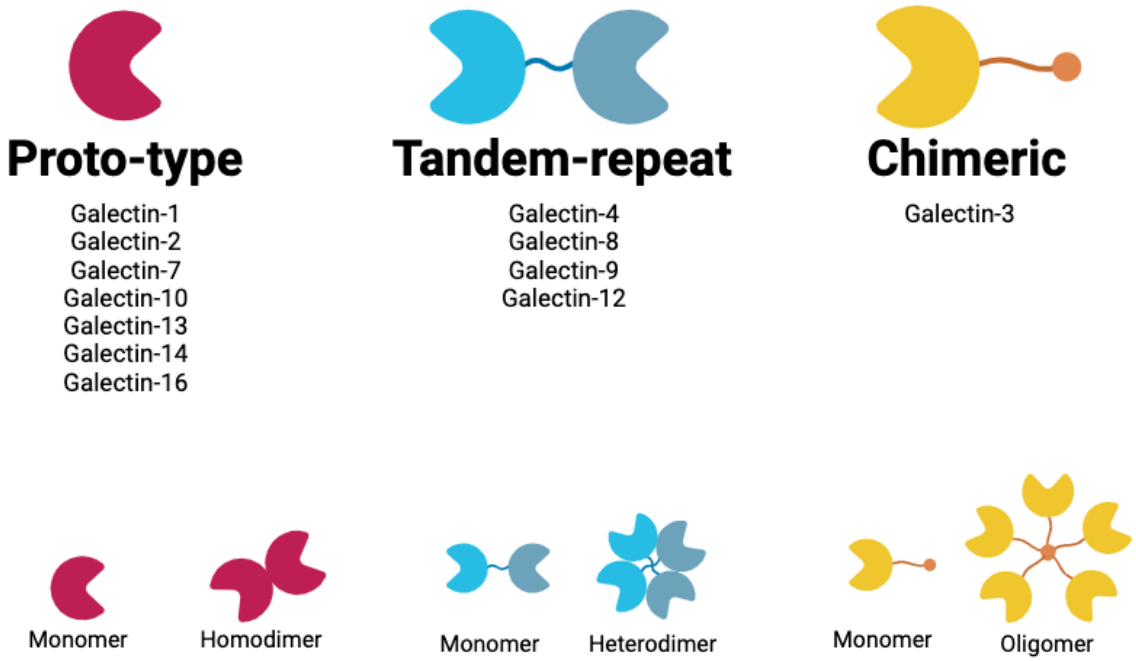

Figure 1. Classification of the galectin family.

Galectins are classified by their CRDs. Proto-type galectins contain one CRD, tandem-repeat have two CRDs joined by a peptide linker, and galectin-3 represents the only chimeric galectin with one CRD and an N-terminal tail. Figure was adapted from (Liu et al., 2023) and created using BioRender.

or transmembrane signaling (Johannes et al., 2018; Modenutti et al., 2019). Intracellularly, they interact with cytosolic and nuclear proteins typically through carbohydrate-independent mechanisms regulating gene expression and protein activity (Yang et al., 2008).

Ultimately, galectins can activate signaling pathways and modulate various fundamental biological processes including cellular differentiation, growth, apoptosis, migration and RNA transcription. Given this, galectins have been implicated in cell stress, inflammation and diseases like cancer (Timoshenko, 2015). The involvement or dysregulation of galectins in these conditions allows them to serve as biomarkers or clinical targets.

1.1.1 Unconventional secretion of galectins

Galectin protein peptides lack the signal sequence for transport to the endoplasmic reticulum (ER) and are therefore not secreted out of cells using the conventional ER-Golgi system but instead through unconventional means (**Figure 2**) that vary within the galectin family. Direct translocation through the plasma membrane has been a suggested mechanism of galectin-1 secretion (Schäfer et al., 2004; Popa et al., 2018). Previous work has shown galectin-1 and fibroblast growth factor 2 (FGF-2) to be secreted using plasma membrane-derived inside-out vesicles where the lumen of the vesicle resembles the extracellular space. Similarly, galectin-3 has been shown to spontaneously pass through the lipid bilayer observed through spectrophotometric methods, interacting with polar lipids (Lukyanov et al., 2005). Evidence also suggests that both galectin-1 and -3 accumulate at the plasma membrane which could reflect one step in the process of direct translocation. However, this accumulation may also reflect budding of the plasma membrane for secretion through microvesicles. In fact, microvesicular secretion of both galectin-1 and -3 has been shown experimentally (Cooper and Barondes, 1990; Hughes, 1999; Popa et al., 2018).

Other vesicular methods of secretion have been proposed including the use of exosomes and secretory autophagy through lysosomes/autophagosomes. Recently work has demonstrated that galectin-1 can be secreted from tumor-associated macrophages using toll-like receptor 2 (TLR2)-dependent secretory autophagy with the protein being packaged

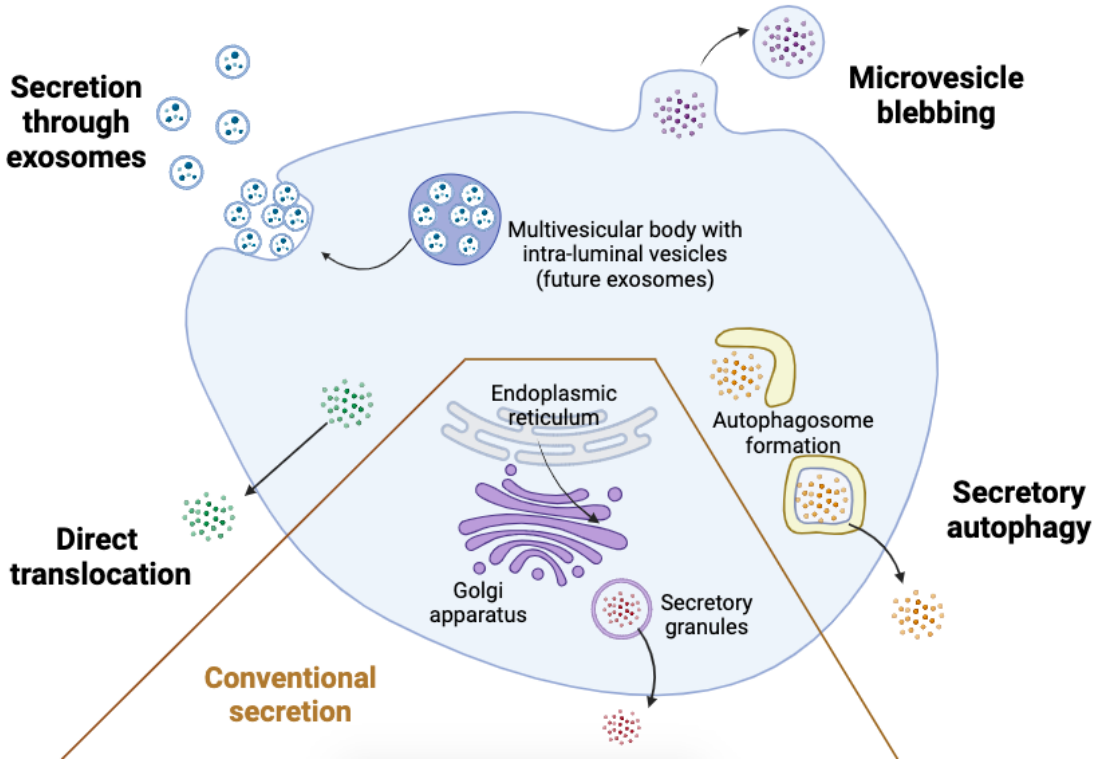

Figure 2. Potential mechanisms of unconventional secretion in the galectin family.

Galectins lack a signal sequence for secretion through the conventional ER-Golgi pathway and are thus secreted through unconventional means. These proposed mechanisms include direct translocation, the use of extracellular vesicles like exosomes and microvesicles, and secretory autophagy using autophagosomes/lysosomes. The figure was adapted from (Popa et al., 2018) and created using BioRender.

into autophagosomes (Davuluri et al., 2021). Furthermore, galectin-1, -3, -4, -8, and -9 have all been observed to associate with impaired or damaged vesicles like endosomes and lysosomes (Popa et al., 2018; Bänfer and Jacob, 2020). Galectin-8 itself is involved with regulating unconventional secretion of interleukin-1β through interaction with tripartite motif containing 16 (TRIM16) which binds cargo destined for secretory autophagy (Kimura et al., 2017). Galectin association with damaged vesicles could reflect the mechanism of secretion observed during cell stress, however it may not reflect what occurs during normal cell conditions (Popa et al., 2018). Galectin-3 and -4 have also been observed in undamaged endosomes, with galectin-4 playing a key role in lipid raft-based apical trafficking of proteins (Delacour et al., 2005; Popa et al., 2018).

Galectin-3 has been found within exosomes isolated from various cancers (bladder, colon, ovarian, etc.) and exosomes isolated from urine and saliva (Bänfer and Jacob, 2020). Thus, the presence of exosomal galectin-3 could serve as a biomarker for certain cancers (Bänfer and Jacob, 2020). The mechanism by which galectin-3 is packaged into exosomes has recently been identified with a conserved tetrapeptide motif in the N-terminal tail interacting with endosomal sorting complexes required for transport (ESCRT) machinery (Bänfer et al., 2018; Bänfer and Jacob, 2020). Exosomal recruitment of galectin-3 depends on interaction with the ESCRT components tumor susceptibility gene 101 (TSG101) and functional vacuolar protein sorting-associated protein 4A (VPS4A). Mutations of the tetrapeptide P(S/T)AP motif prevents release of exosomal galectin-3, supporting the notion that an intact N-terminal domain is required for secretion (Bänfer et al., 2018; Popa et al., 2018).

While exosomes are a proposed mechanism of galectin-3 secretion, the majority of secreted galectin-3 is free and not vesicle bound, suggesting several secretion mechanisms may be at play simultaneously (Stewart et al., 2017). Galectin-1 has also been observed on the surface of exosomes while galectin-9 in the lumen (Bänfer and Jacob, 2020). Exosomes are used for intercellular communication and merge into recipient cells releasing their luminal contents or attach to the cell surface to produce a signaling response (Edgar, 2016). Therefore, while the presence of galectins within or on the surface of exosomes has been

observed, it is not established if or how they are actually released from the exosomes into the extracellular space.

The regulation of galectin secretion is also poorly described. Given that galectins vary in both structure and cell-specificity, it can be difficult to extrapolate findings broadly to the whole family of proteins. Certain factors like nutrient availability, calcium, and serum levels can impact the level of galectin-3 secretion (Popa et al., 2018). Likewise, processes like cell differentiation can influence galectin flux out of cells. For example, extraembryonic endoderm differentiation of embryonic stem cells led to a significant increase in galectin-3 secretion (Gatie et al., 2022). Neutrophilic differentiation of human acute myeloid leukemia (AML) HL-60 cells with all-trans retinoic acid (ATRA) similarly elevated galectin-1, -3 and -9 secretion (McTague et al., 2022). Both cases were also marked by a drop in global *O*-GlcNAcylation upon differentiation creating a link between this post-translational protein modification and the regulation of galectin secretion.

1.2 Galectin-12

1.2.1 Structure, tissue distribution and localization

Galectin-12 (*LGALS12*) was identified by two groups independently in 2001 in human Jurkat T cells and human adipose tissue (Hotta et al., 2001; Yang et al., 2001), and has been linked to the regulation of various biological processes (**Figure 3**). It is a tandem-repeat galectin that is most homologous to galectin-8 but with weaker β-galactoside binding abilities (Hotta et al., 2001). Galectin-12 likely has tight regulation of expression and low mRNA stability due to its start codon being a weak translation initiator based on the Kozak rule and an AU-rich 3’ UTR (Yang et al., 2001). The promoter region also lacks a TATA-like sequence but contains binding sites for transcription factors SP1 and AP-2 (Hotta et al., 2001). There are five identified transcript variants of galectin-12 ranging from seven to nine exons with their variability in function and tissue distribution being currently unknown. The N-terminal CRD of galectin-12 is highly conserved while the C-terminal domain has divergence from other galectins. Like other galectins, galectin-12 is lactose-binding and is the first reported galectin with a preferential binding affinity for 3-fucosyla-

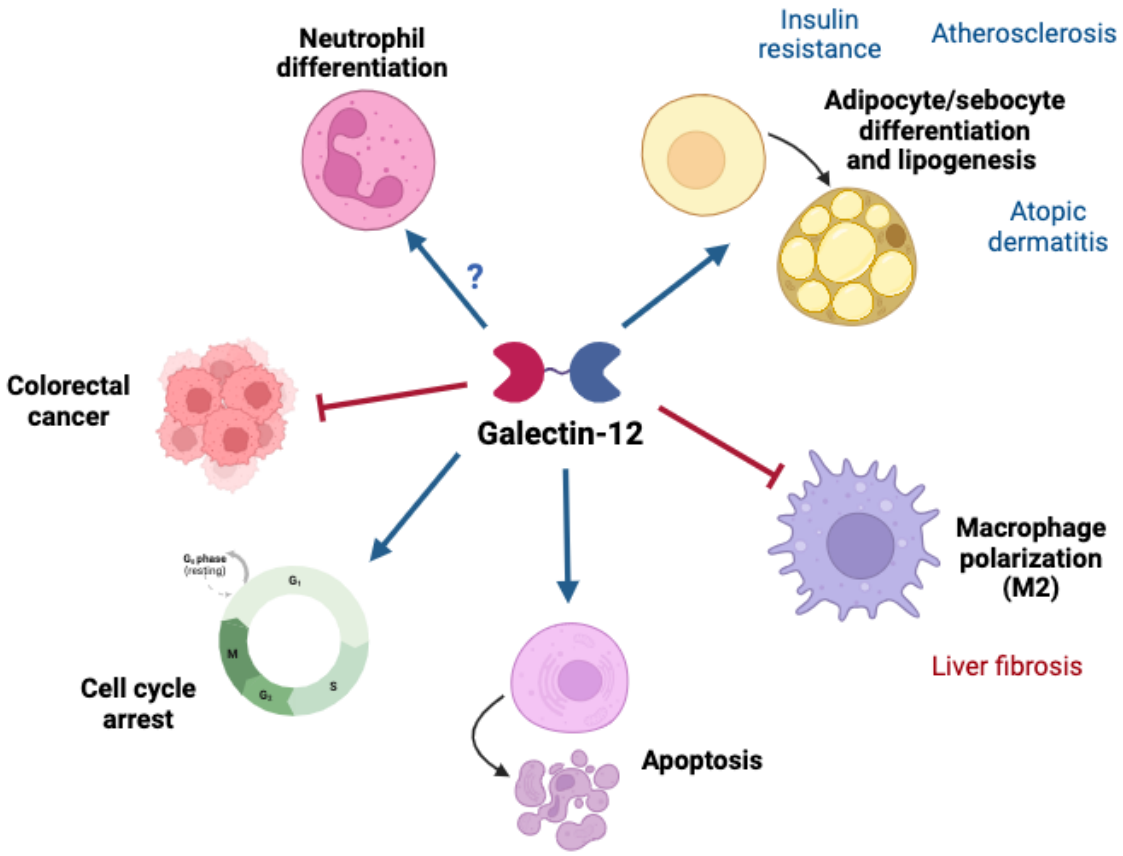

Figure 3. Proposed roles of galectin-12 in various biological processes and diseases.

Galectin-12 has been implicated to regulate the differentiation of various cell models like adipocytes, neutrophils, and sebocytes, as well as macrophage polarization. Galectin-12 has also been linked to cancer, apoptosis and cell cycle regulation. Some processes can be further linked to diseases and conditions like insulin resistance, atherosclerosis, dermatitis, and liver fibrosis. Blue arrows represent the promotion of this process/condition, while red represents inhibition by galectin-12. Figure was generated using BioRender.

ted structures (Yang et al., 2001; Maller et al., 2020). Galectin-12 is tissue-specific with low or negligible levels of mRNA detected in most human tissues. It is primarily found in adipose, myeloid, and breast tissues but also has modest detection in the heart, pancreas, spleen and thymus (Yang et al., 2001; Uhlén et al., 2015). It has been detected to some degree in cytosolic, nuclear, mitochondrial, low-density microsomal, and lipid droplet fractions (Hotta et al., 2001; Yang et al., 2011; Katzenmaier et al., 2018). However, galectin-12 primarily localizes to intracellular lipid droplets in adipocytes and predominantly on large droplets. Galectin-12 co-localizes with perilipin-1 on lipid droplets likely in a glycan-independent manner (Yang et al., 2011). Notably, galectin-12 was found primarily on the inner side of the lipid droplets while perilipin-1 on the membrane (Maller et al., 2020). The hydrophobic regions of galectin-12 may be the mechanism by which it localizes to lipid droplets. Negligible secretion of galectin-12 in cell culture media has been observed in mouse pre-adipocyte 3T3-L1 cells (Hotta et al., 2001; Yang et al., 2011).

Galectin-12 was first shown to play a role in cell cycle regulation. Upregulation of galectin-12 was observed in Jurkat T cells upon cell cycle synchronization at G_1/S. Similarly, ectopic expression of galectin-12 induced both cell cycle arrest at G_1/S and growth suppression in human cervical cancer HeLa cells (Yang et al., 2001). Furthermore, ectopic expression of galectin-12 in fibroblast-like COS-1 cells induced apoptosis and treatment of Zucker mice with peroxisome proliferator-activated receptor γ (PPAR-γ) ligand troglitazone which induces apoptosis led to an increase in *LGALS12* expression (Hotta et al., 2001).

1.2.2 Galectin-12 in adipocytes and lipogenesis

Galectin-12 has been shown to be necessary for adipocyte differentiation *in vitro* and is linked to lipolysis regulation. Adipocytes are primarily involved with modulating lipid metabolism and serve as energy stores in the body through synthesis of triglycerides (Duncan et al., 2007). These cells also play an important role in glucose/insulin sensitivity. An increase in galectin-12 at the gene and protein level was observed upon contact inhibition-induced growth arrest of 3T3-L1 pre-adipocytes (Yang et al., 2004). Subsequent stimulation with an adipogenic differentiation cocktail (3-isobutyl-1-methylxanthine,

dexamethasone and insulin) led to a brief downregulation of galectin-12 and then a sustained strong upregulation.

Transcription factors CCAAT/enhancer-binding protein β (C/EBP-β) and δ begin the adipocyte differentiation pathway leading to activation of C/EBP-α and PPAR-γ (Yang et al., 2004). Knockdown of galectin-12 led to downregulation of C/EBP-β and thus C/EBP-α and PPAR-γ as well. This knockdown also produced a decrease in the amount of phosphorylated protein kinase B (Akt), cAMP response element-binding protein (CREB) and extracellular signal-regulated kinase (Erk) which function upstream of C/EBP-β. This demonstrates that galectin-12 functions upstream of Akt and helps induce C/EBP-β activity (Yang et al., 2004). Ultimately, the knockdown of galectin-12 led to reduced lipid droplet production and a decrease in early (aP2) and late (adipsin) adipocyte differentiation markers. The levels of insulin receptor and insulin receptor substrate-1 (IRS-1) were also reduced upon galectin-12 knockdown suggesting galectin-12 also influences glucose/insulin homeostasis.

Beyond its involvement in adipocyte differentiation, galectin-12 is also a potent negative regulator of lipolysis (Yang et al., 2011). Galectin-12 deficient mice (*Lgals12*$^{-/-}$) had reduced whole-body lipid content and elevated energy expenditure. However, there was no reduction in the number of adipocytes but instead a reduction in adipocyte size. Similarly, no changes in expression of key adipose genes were observed suggesting adipose tissue development is not impacted as observed *in vitro* (Yang et al., 2011). *Lgals12*$^{-/-}$ mice had elevated lipolysis due to an increase in protein kinase A (PKA) phosphorylation and activation of adipocyte lipases. cAMP levels were also elevated in *Lgals12*$^{-/-}$ adipocytes suggesting galectin-12 acts upstream of PKA and regulates lipolysis by controlling intracellular cAMP levels. Galectin-12 deficiency also prevented the development of insulin resistance and glucose intolerance associated with weight gain in mice due to reduced adiposity. However, the role of galectin-12 in insulin sensitivity seems to be conflicting. Insulin resistance-inducing agents like isoproterenol, tumor necrosis factor α (TNF-α), insulin, and dexamethasone all downregulated *LGALS12* expression in differentiated 3T3-L1 cells (Fasshauer et al., 2002). In the case of isoproterenol this was

via β-adrenergic receptors and activation of G_s-proteins/adenylyl cyclase. Therefore, the suppression of galectin-12 could also be linked to induction of insulin resistance.

Vacuolar protein sorting 13 homolog C (VPS13C) was one of the first identified galectin-12-binding proteins in adipocytes, co-localizing on lipid droplets together (Yang et al., 2016). Both CRDs of galectin-12 are required for interaction with VPS13C. Like galectin-12, VPS13C expression was also upregulated during adipocyte differentiation. VPS13C is required for galectin-12 stability as it prevents it from being degraded through the lysosomal pathway. Knockdown of VPS13C in 3T3-L1 cells led to the suppression of adipocyte differentiation and accelerated galectin-12 protein degradation while its mRNA levels remained high.

Recently, galectin-12 has been shown to promote angiogenesis which supports adipose tissue expansion (Maller et al., 2020). 3T3-L1 cells under hypoxic conditions demonstrated an increase in galectin-12 expression. Recombinant galectin-12 was found to induce angiogenesis through binding to 3-fucosylated glycans on human umbilical vein endothelial cells (HUVEC) which promoted cell migration and generation of tubular structures. Additionally, *Lgals12*$^{-/-}$ mice had a reduction in vascular networks compared to wild-type mice.

1.2.3 Galectin-12 in sebocytes

Galectin-12 is expressed in both human and mouse sebocytes where it plays a role in differentiation and lipogenesis similar to what is observed in adipocytes (Harrison et al., 2007; Tsao, et al., 2022a; Tsao, et al., 2022b). Sebocytes produce a waxy substance known as sebum and are similar to adipocytes in terms of their high lipid content but are derived from different cell origins (Schneider and Paus, 2010). Human HaCaT keratinocyte cells induced towards sebocyte differentiation reported an increase in *LGALS12* expression (Tsao et al., 2022a). Galectin-12 silencing in human SZ95 sebocytes led to a decrease in proliferation while overexpression resulted in cell cycle progression with there being fewer cells observed in G_1 phase (Tsao et al., 2022b). Galectin-12 knockdown decreased expression of cell cycle regulators cyclin A1 and cyclin dependent kinase 2 (CDK2) along with PPAR-γ (Tsao et al., 2022b). It was suggested that galectin-12 positively regulates

sebocyte proliferation by promoting cyclin A1 and CDK2 expression via PPAR-γ activity. Galectin-12 regulates PPAR-γ gene expression and overexpression in SZ95 cells enhanced PPAR-γ transcriptional activity with both CRDs being necessary for this regulation.

Like in adipocytes, galectin-12 silencing decreases lipogenesis as observed in SZ95 and SEB-1 sebocytes (Tsao et al., 2022a). *Lgals12*$^{-/-}$ mice had reduced sebaceous gland size and growth upon androgen-stimulation in comparison to wild type mice (Tsao et al., 2022b). Additionally, *Lgals12*$^{-/-}$ mice had decreased levels of cholesterol esters, triglycerides, free fatty acids and cholesterol observed in the lipid content of the skin surface (Tsao et al., 2022a). Diacylglycerol *O*-acyltransferase 1 (DGAT1) and acetyl-coenzyme A synthetase 2 (ACS2) gene expression were downregulated in knockdown SZ95 cells and *Dgat1* was downregulated in the skin of *Lgals12*$^{-/-}$ mice. Both DGAT1 and ACS2 are PPAR-γ target genes and are involved with triglyceride biosynthesis.

Galectin-12 also regulates inflammation in the skin. Galectin-12 regulates interleukin-4 (IL-4)/STAT6 induced immune response through upregulation of PPAR-γ (Lin et al., 2023). IL-4 leads to upregulation of T helper 2 cell (Th2)-associated mediators like chemokine (C-C motif) ligand 26 (CCL26). *Lgals12*$^{-/-}$ mice had reduced sebaceous gland hyperplasia and a decrease in atopic dermatitis-like features. Galectin-12 also plays a role in suppressing ER stress in sebocytes, as its knockdown increased levels of activating transcription factor 4 (ATF4) and phosphorylated c-Jun N-terminal kinase (JNK). Triglyceride synthesis by DGAT1 can protect adipocytes against fatty acid-induced ER stress during lipolysis, thus galectin-12 likely also modulates ER homeostasis through PPAR-γ/lipid droplet formation (Chitraju et al., 2017; Lin et al., 2023). Overall, galectin-12 regulates immune response in skin and therefore may promote the development of Th2-mediated skin conditions.

1.2.4 Galectin-12 in macrophages

Galectin-12 has been shown to be expressed in both human and mouse macrophages (Lin et al., 2020; Wan et al., 2016). Macrophages are cells involved in inflammation that are highly plastic and functionally diverse (Funes et al., 2018). Macrophages undergo

polarization into M1 or M2 macrophages where M1 macrophages are classically activated and considered pro-inflammatory, while M2 are anti-inflammatory. Galectin-12 was found to be a pro-inflammatory protein in macrophages and supports M1 polarization. Galectin-12 expression was upregulated when macrophages are stimulated with lipopolysaccharide (LPS) and palmitic acid. Galectin-12 knockout did not impede the ability of cells to differentiate into macrophages. However, these cells demonstrated a drop in pro-inflammatory activity with a reduction of phagocytic activity and nitric oxide production in the presence of *Escherichia coli* (Wan et al., 2016).

Galectin-12 knockout in macrophages drove M2 polarization. This was supported by a decrease in pro-inflammatory M1 markers like interleukin-6, TNF-α, monocyte chemoattractant protein-1 (MCP-1), and chemokine ligand 1 (CXCL1) and an increase in M2 markers like CD163 and CD206 upon activation (Lin et al., 2020; Wan et al., 2016). Galectin-12 knockout induced M2 polarization by regulating nuclear factor κB (NF-κB) and activator protein 1 (AP-1) signaling pathways. Knockout cells had reduced phosphorylation of IκB kinase α/β, Akt and Erk which led to reduced NF-κB and Erk activation and thus less pro-inflammatory cytokine/chemokine production (Wan et al., 2016). Using galectin-12 knockout-conditioned media also improved insulin sensitivity in 3T3-L1 cells.

Galectin-12 may also serve as a therapeutic target for combatting atherosclerosis development. Foam cells are macrophages that accumulate lipid content by engulfing oxidized low-density lipoprotein which leads to plaque formation (Guerrini and Gennaro, 2019). *Lgals12*$^{-/-}$ mice had lower leptin levels and decreased foam cell formation in bone-marrow derived macrophages with reduced lipid content (Lin et al., 2020). The decrease in lipid accumulation was also linked to an increase in cholesterol efflux. Therefore, inhibition of galectin-12 could slow the development of atherosclerosis.

Galectin-12 is also implicated in non-alcoholic fatty liver disease where its knockdown promoted liver fibrosis (Lee et al., 2023). *Lgals12*$^{-/-}$ mice had increased cholesterol accumulation, downregulation of suppressor of cytokine signaling 3 (SOCS3), and elevated secretion of transforming growth factor β1 (TGF-β1). Above all, ablation of

galectin-12 ultimately led to the M2 polarization of Kupffer cells which can aggravate liver fibrosis. Using conditioned media from galectin-12 knockout macrophages also promoted myofibroblast differentiation of hepatic stellate cells, a hallmark of chronic inflammation-induced fibrosis.

1.2.5 Galectin-12 in colorectal cancer

LGALS12 is epigenetically silenced in colorectal carcinoma (CRC). No *LGALS12* transcript was detected in nine CRC cell lines however, *de novo* expression was induced upon sodium butyrate treatment in eight out of nine cell lines (Katzenmaier et al., 2014). Sodium butyrate is a known inducer of differentiation in CRC cells and also induces histone hyperacetylation. Similar findings were observed upon treatment with 5-Aza-dC, a demethylation agent which induced *de novo* expression in 5 out of 9 cell lines (Katzenmaier et al., 2017). Tissue samples of microsatellite unstable CRC patients were analyzed for *LGALS12* expression and a decrease in expression was observed when comparing primary tumor samples with adjacent normal tissue, with at least a two-fold decrease observed in 2/3^{rds} of patients tested (Katzenmaier et al., 2017). Another study examining the genetic profile of CRC categorized *LGALS12* as the only galectin where the majority of samples were classified as 'low expression' in contrast to other galectins which were typically over-expressed (Gopalan et al., 2016).

Interestingly, nucleocytoplasmic shuttling of galectin-12 was observed in a cell cycle-dependent manner in human CRC HCT116 cells (Katzenmaier et al., 2018). Galectin-12 also had speckle-like distribution in the nucleoli reminiscent to splicing factor-rich nuclear speckles (SC35 domains) suggesting a potential involvement in pre-mRNA splicing.

Ten galectin-12 candidate interacting proteins were recently identified including the neutral amino acid transporter SLC1A5, a protein involved with glutamine uptake and metabolism (Katzenmaier et al., 2019). Cancer cells rely on glutamine metabolism as a source of carbon for the tricarboxylic cycle and as precursors for nucleotide/lipid synthesis (Cluntun et al., 2017). Galectin-12 was identified as a novel inhibitor of glutaminolysis as binding of galectin-12 to SLC1A5 inhibited glutamine uptake in HCT116 cells. Thus, the

downregulation of galectin-12 in certain cancers may support tumor growth and dependence on glutamine.

1.2.6 Galectin-12 in neutrophils

LGALS12 downregulation is associated with poor overall survival in patients with AML (El Leithy et al., 2015). Over 80% of AML patients had downregulated *LGALS12* compared to healthy donors. Patients that had upregulated *LGALS12* had higher remission rates than those with downregulation. This downregulation of *LGALS12* is influenced by promoter methylation (Assem et al., 2023). All patients with no *LGALS12* expression had methylation of at least 7/11 CpG sites in the *LGALS12* promoter, with four sites identified that must remain unmethylated for expression. Patients with methylated promoters also had a higher mortality rate. Remarkably, *LGALS12* was found to be overexpressed only in acute promyelocytic leukemia (APL) but no other subtypes of AML (Xue et al., 2016). These findings point to a potential use of galectin-12 as a prognostic marker for AML or as a target for differentiation treatment-resistant patients in the case of APL.

The role of galectin-12 in neutrophilic differentiation seems to be variable with expression being cell line and stimuli-dependent. In human APL NB4 cells, galectin-12 knockdown led to an increase in ATRA-induced neutrophil-like differentiation (Xue et al., 2016). Similarly, galectin-12 was downregulated at both the gene and protein level upon dimethyl sulfoxide (DMSO)-induced neutrophil-like differentiation of AML HL-60 cells (Vinnai et al., 2017).

In the NB4 cells, neutrophilic differentiation was accompanied by an increase in intracellular lipid droplet content. Lipid droplets can be used in neutrophils as stores for cytokines and the number of lipid droplets increases in leukocytes upon inflammation in the body (Melo and Weller, 2016). Knockdown of galectin-12 led to enhanced neutrophil-like differentiation but also impaired lipid droplet production (Xue et al., 2016). A downregulation of PPAR-γ, phosphorylated CREB, and C/EBP α/β were also observed linking back to the adipocyte pathway previously discussed. However, recent work using the ATRA model of neutrophilic differentiation in HL-60 cells reported an upregulation of galectin-12 at the gene level (McTague et al., 2022). Therefore, it is still uncertain whether

galectin-12 stimulates or inhibits neutrophilic differentiation. These findings may also suggest the generation of different phenotypes of neutrophil-like cells with different gene expression profiles and functions.

1.3 *O*-GlcNAcylation

Recent findings indicate that galectin expression and localization may be influenced by the post-translational protein modification *O*-GlcNAcylation (Sherazi et al., 2018; Mathew et al., 2022)**.** *O*-GlcNAcylation is a process that involves the *O*-linked attachment of an *N*-acetyl-D-glucosamine (*O*-GlcNAc) sugar to serine and threonine residues of intracellular proteins (Yang and Qian, 2017). This is governed by *O*-GlcNAc transferase (OGT) which adds the sugar and *O*-GlcNAcase (OGA) which removes it, respectively (**Figure 4**). UDP-GlcNAc is the final product of the hexosamine biosynthetic pathway (HBP) and serves as the donor substrate for *O*-GlcNAcylation, making the rate limiting enzyme glutamine-fructose-6-phosphate amidotransferase (GFAT) another key player in *O*-GlcNAc homeostasis (Laczy et al., 2009).

O-GlcNAc homeostasis is linked to diseases like cancer since *O*-GlcNAcylation responds heavily to nutrient availability and cellular stress (Yang and Qian, 2017; Hanover et al., 2018). 3-5% of glucose in cancer is diverted to the HBP and thus cells can use UDP-GlcNAc as a nutrient/energy availability sensor for downstream processes (Akella et al., 2019). Indeed, many cancers like breast, lung, liver pancreas and others have elevated levels of *O*-GlcNAcylation and aberrant activity of OGT/OGA (Lee et al., 2021).

O-GlcNAcylation can impact gene expression, protein signaling and secretion influencing processes like differentiation. For instance, both transcription factors C/EBPβ and PPARγ can be modified with *O*-GlcNAc leading to regulation of adipocyte differentiation (Li et al., 2009; Ji et al., 2012). Alterations in *O*-GlcNAcylation during differentiation have been observed in a wide range of cell types. Oftentimes, this is a decrease in overall *O*-GlcNAcylation as observed in keratinocytes, neurons, muscle and myeloid cells suggesting high *O*-GlcNAcylation can be a marker of stemness (Tazhitdinova and Timoshenko, 2020). However, there are also cases where *O*-GlcNAcylation is elevated following differentiation

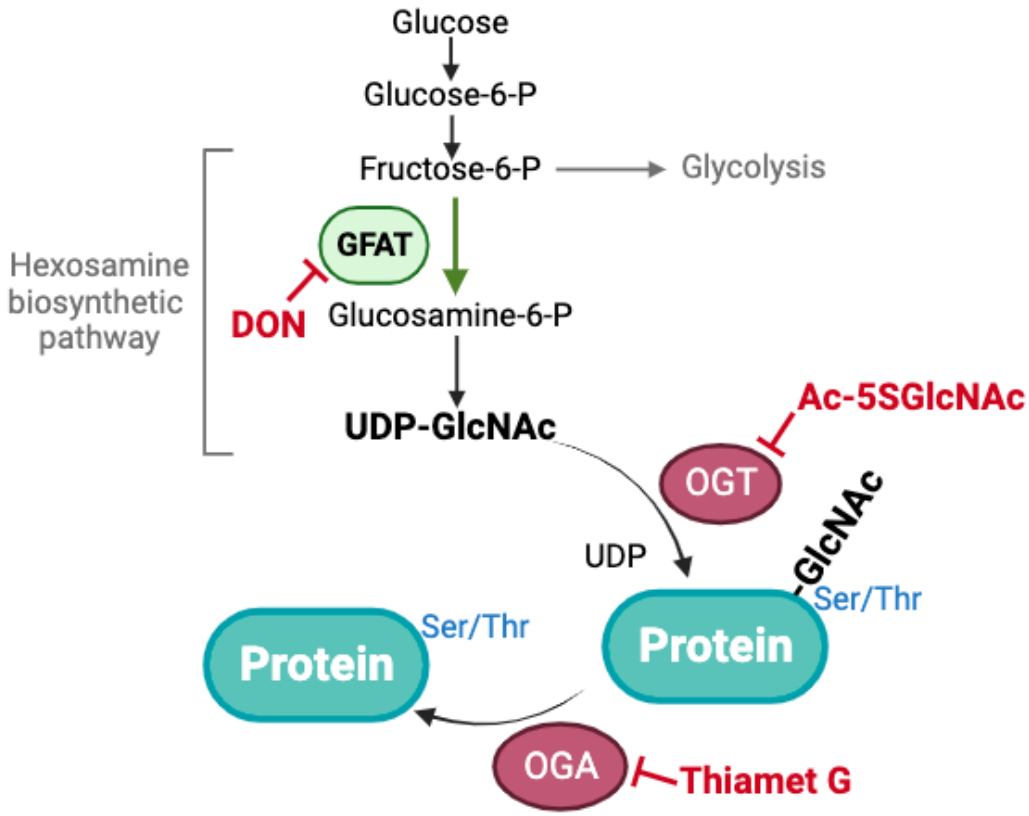

Figure 4. Regulation of *O*-GlcNAcylation.

The sugar substrate for *O*-GlcNAcylation is generated through the hexosamine biosynthetic pathway. This sugar can be added and removed from serine/threonine residues of intracellular proteins by OGT and OGA, respectively. Chemical inhibitors can be used to block key steps in *O*-GlcNAcylation. This includes inhibition of the rate-limiting enzyme GFAT by 6-diazo-5-oxo-L-norleucine (DON), OGA by thiamet G, and OGT by Ac4-5S-GlcNAc (AC). Figure was adapted from (Baudoin and Issad, 2015) and generated using BioRender.

like in adipocytes, chondrocytes and osteoblasts. *O*-GlcNAcylation also competes with phosphorylation because both PTMs target the same amino acid residues (Hart et al., 2011). Both PTMs have cycling enzymes that can be modified by the other modification, leading to extensive cross-talk between the two processes.

All human galectins have predicted serine/threonine residues that could be *O*-GlcNAcylated based on *in silico* analysis (Tazhitdinova and Timoshenko, 2020). As previously mentioned, there is a drop in *O*-GlcNAcylated proteins upon myeloid differentiation and this is accompanied by various changes in galectin levels. Therefore, increasing evidence points to the fact that there is a relationship between galectin expression/localization and *O*-GlcNAc homeostasis. HL-60 cells treated with chemical inhibitors of *O*-GlcNAc cycle enzymes demonstrated changes in protein expression and secretion of several galectins (Sherazi et al., 2018; McTague et al., 2022). Inhibition of GFAT with 6-diazo-5-oxo-L-norleucine (DON) led to increased levels of galectin-1 and -3, and a drop in galectin-9 in HL-60 cells (McTague et al., 2022). Similar but weaker effects were observed with specific OGT inhibitor Ac45S-GlcNAc (AC) suggesting GFAT inhibition is also influencing other processes like *N*-linked glycosylation which uses the same donor substrate. Treatment with DON also increased the level of secreted galectin-1, -3, -9, and -10 in the supernatant of HL-60 cells. Indeed, recent work has demonstrated galectin-3 secretion is sensitive to *O*-GlcNAcylation (Mathew et al., 2022). It was found that the secreted galectin-3 was primarily deglycosylated when comparing to cytosolic galectin-3. Furthermore, OGA knockout mouse embryonic fibroblast cells had impaired galectin-3 secretion and similar findings were observed in HeLa cells with siRNA knockdowns. The authors suggested that galectin-3 first needs to be *O*-GlcNAcylated in the N-terminal tail, then deglycosylated for secretion out of cells as mutations to predicted *O*-GlcNAcylation sites also impacted secretion. The effect of *O*-GlcNAcylation on galectin-12 levels is still to be properly addressed. Previously, both inhibition of OGA with Thiamet G (TG) and GFAT with DON led to an upregulation of *LGALS12* which is paradoxical as these produce opposite changes in *O*-GlcNAcylation levels (Sherazi et al., 2018; McTague et al., 2022). Furthermore, the use of OGT inhibitor AC did not produce any significant changes in *LGALS12* gene expression and changes at the protein level have not yet been assessed.

1.4 HL-60 cells and human neutrophils

1.4.1 HL-60 cells and acute myeloid leukemia

The HL-60 cell line was immortalized in 1977 from a female patient with acute myeloid leukemia (Birnie, 1988). This cell line was initially characterized as acute promyelocytic leukemia (APL) M3 subtype using the French-American-British classification however, further morphological and genetic analysis re-classified it as acute myeloblastic leukemia with maturation (FAB-M2) (Dalton et al., 1988). APL FAB-M3 subtype is characterized by a t(15;17) translocation that produces a PML-RAR fusion protein leading to cells being arrested at the promyelocyte stage of myeloid differentiation. This fusion involves the promyelocytic leukemia gene (PML) and the retinoic acid receptor (RAR). Myeloid differentiation can be induced through the binding of ATRA and its derivatives to RAR (Dalton et al., 1988; Tasseff et al., 2017). This generates a heterodimer consisting of RAR with the retinoid X receptor (RXR) which then binds to retinoic acid response elements (RAREs) in the promoter region of relevant genes downstream and also mitogen-activated protein kinases (MAPK) activation (Pohl and Tomlinson, 2020). Thus, targeting RAR using ATRA to induce differentiation has become the leading treatment for APL and has improved long-term survival with 80-90% of cases going into remission (Stahl and Tallman, 2019).

Despite the fact that HL-60 cells lack the t(15;17) translocation, these cells are still sensitive to ATRA-induced differentiation making them an effective model to study myeloid differentiation. HL-60 cells can be induced to differentiate into granulocytes like neutrophils using agents such as DMSO, ATRA, and dimethyl formamide (DMF) and eosinophils using sodium butyrate (Breitman et al., 1980). HL-60 cells can also undergo monocytic differentiation using vitamin D or phorbol esters (Birnie, 1988). ATRA and DMSO are the two best established models of inducing neutrophilic differentiation in HL-60 cells (**Figure 5**). RAR-RXR activation with ATRA induces an upregulation of p21 which then inhibits cyclin E and CDK2 leading to cell cycle arrest at G_1/S transition (Mar and Quackenbush, 2009; Congleton et al., 2011). DMSO does not induce neutrophilic differentiation through the retinoic acid signaling pathway, but instead upregulates

phosphatase and tensin homolog (PTEN) through activation of NF-κB (Mar and Quackenbush, 2009). This ultimately leads to the upregulation of p27 which also inhibits cyclin E and CDK2 resulting in cell cycle arrest as observed with ATRA.

1.4.2 Neutrophils

Neutrophils are cells of the innate immune system and are the most abundant leukocytes in circulation. They are the first line of defense against invading pathogens and act as modulators of inflammation. Neutrophils are produced in the bone marrow from hematopoietic stem cells and enter into circulation once mature where they can then be targeted to sites of infection or inflammation (Rosales, 2018). As neutrophils mature they acquire a signature lobulated nuclear morphology. This flexible and lobular nucleus allows for fast migration to squeeze past endothelium into infected tissues (Manley et al., 2018).

Neutrophils can protect the body against microorganisms through release of granules, neutrophil extracellular traps (NETs) and phagocytosis. Degranulation involves the release of granules into the extracellular space or phagosome which contain various antimicrobial proteins that help degrade the pathogen and protect the cell against damage including myeloperoxidase, lysozyme, serine proteases, and defensin, among others (Mayadas et al., 2014). NETs can also be used by neutrophils in a process dubbed NETosis to trap pathogens for degradation. The cells release chromatin fibers containing antimicrobial proteins to immobilize and ‘trap’ the pathogen (Mayadas et al., 2014; Manda-Handzlik et al., 2018). Alongside the chromatin there is also release of granules which together kill the pathogen.

Phagocytosis with generation of reactive oxygen species (ROS) is the most studied mechanism of defense in neutrophils. The NADPH oxidase complex becomes activated due to pro-inflammatory cytokines like interleukin-8 or the presence of pathogens. This complex consists of five subunits: nuclear cytosolic factor 1 (NCF1/p47^{phox}), 2 (NCF2/p67^{phox}), and 4 (NCF4/p40^{phox}), and cytochrome B subunits (p22^{phox}, Nox2/gp91^{phox}). Activation consists of phosphorylation of all NADPH oxidase subunits, activation of Ras-related C3 botulinum toxin substrate 2 (Rac2), and finally translocation

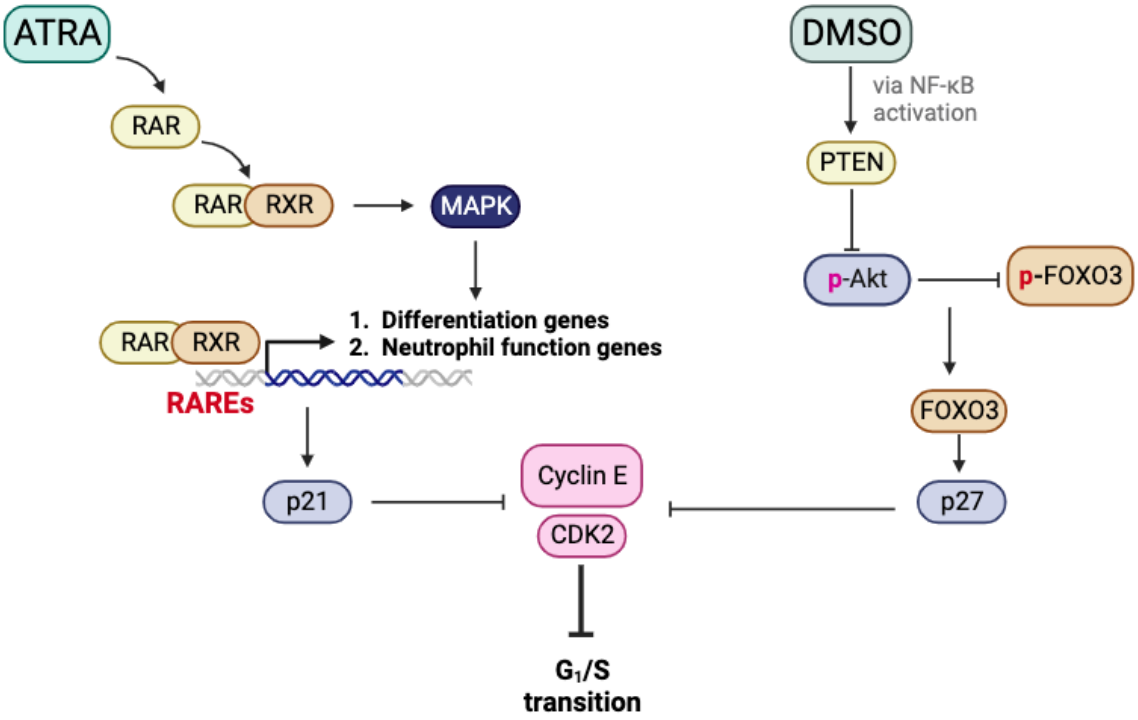

Figure 5. Neutrophilic differentiation of HL-60 cells induced by ATRA and DMSO.

ATRA binds to RAR which leads to the production of an RAR-RXR heterodimer that can bind to RAREs on target genes, inducing differentiation. DMSO leads to the upregulation of PTEN through NF-κB activation which leads to a downregulation of Akt phosphorylation. This blocks the phosphorylation of FOXO3, which allows it to act as a transcription factor in the nucleus. Both pathways lead to cell cycle arrest at G_1/S. The figure was adapted from (Lawson and Berliner, 1999; Mar and Quackenbush, 2009) and generated using BioRender.

of the cytosolic subunits to the membrane. Once active, NADPH oxidase will reduce cytosolic O_2 into superoxide anions ($O_2^{\cdot-}$) through oxidation of NADPH. This superoxide is unstable and is quickly converted into hydrogen peroxide by superoxide dismutase in the phagosome (Nguyen et al., 2017; Belambri et al., 2018). The hydrogen peroxide is converted by myeloperoxidase into the reactive oxygen species hypochlorous acid (HOCl). This process of ROS production is dubbed respiratory burst and kills engulfed pathogens in the phagosome.

The NADPH oxidase complex can be activated *in vitro* by pathogen-associated molecular patterns or chemoattractants like N-formylmethionine-leucyl-phenylalanine (fMLP) that mimic bacterial cell wall components (Fillion et al., 2001) (**Figure 6**). fMLP binds to the formyl peptide receptor (FPR) on the cell surface activating protein kinase C (PKC) signaling through phospholipase C (PLC) activation. Similarly, other agents like phorbol 12-myristate 13-acetate (PMA) can traverse the plasma membrane activating PKC signaling directly. Calcium (Ca^{2+}) flux also plays an important role in respiratory burst as release of intracellular calcium induces activation of PKC therefore non-ionic detergents like digitonin that permeabilize the membrane can also be used to promote respiratory burst (Tanaka et al., 2001; Nguyen et al., 2017). Ultimately, the activation of PKC leads to phosphorylation of the NADPH oxidase subunits and subsequent complex activation (Belambri et al., 2018).

1.4.3 Different phenotypes of neutrophils

Neutrophils were once considered to be a homogenous cell population with the sole function of destroying invading pathogens. However, more work has established that neutrophils are a dynamic heterogenous cell population with diverse activity. Neutrophils change in phenotype as they spend time in circulation, shifting from being considered ‘fresh’ when they exit the bone marrow to ‘aged’ as they leave circulation back to the bone marrow or into tissues (Rosales, 2018). Neutrophils have a short life span of about 24 hours and acquire changes in surface markers as they age.

Different phenotypes of neutrophils are also associated with cancer. Using mice models, tumor-associated neutrophils began to be categorized as being anti-tumor (N1) or pro-

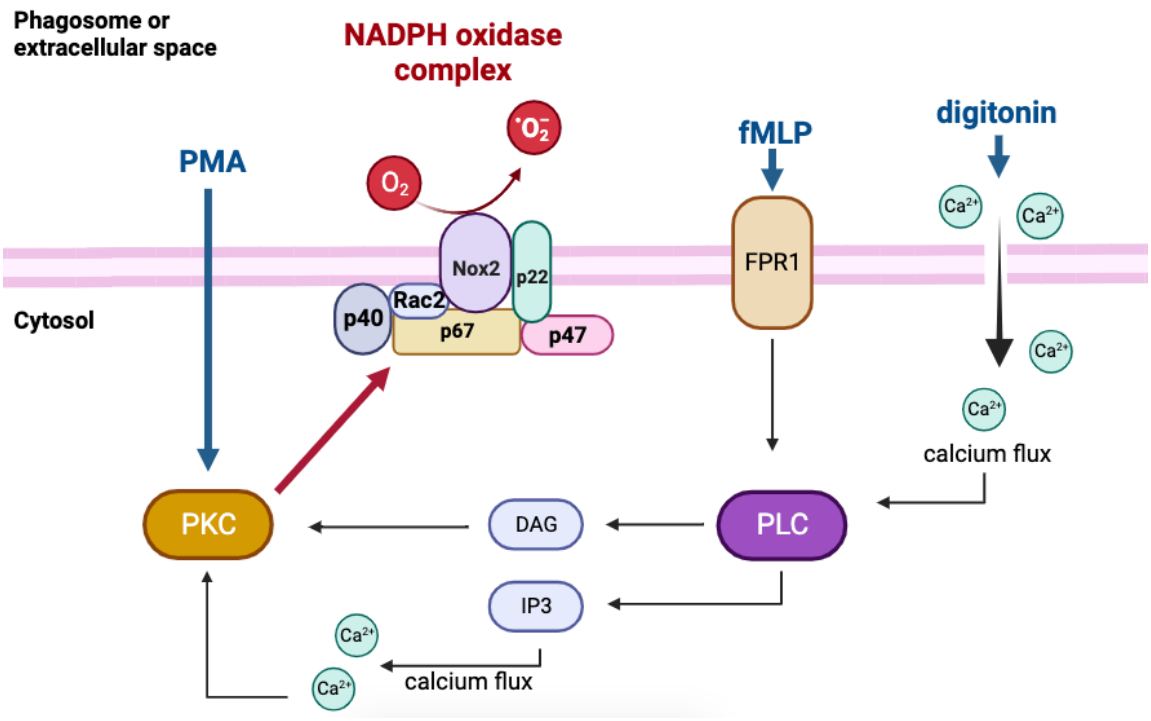

Figure 6. Activation of the NADPH oxidase complex using various stimuli.

The NADPH oxidase complex can be activated using stimuli like fMLP, PMA and digitonin. Digitonin causes calcium influx due to cell membrane permeabilization which activates PLC. fMLP binds to the FPR receptor on the cell surface which activates PLC and results in the generation of diacylglycerol (DAG) and inositol-triphosphate (IP3). PMA crosses the plasma membrane to directly activate PKC. All stimuli ultimately result in the activation of PKC which leads to the phosphorylation of subunits of the NADPH oxidase complex. When active, NADPH oxidase generates superoxide which is converted to hydrogen peroxide by superoxide dismutase. Figure was adapted using (Tanaka et al., 2001; Belambri et al., 2018) and created using BioRender.

tumor (N2), in a classification comparable to what is observed with macrophages (M1/M2) (Rosales, 2018). Furthermore, these neutrophils have some level of fluidity in phenotype as you can polarize them in the other direction. TGF-β can polarize N1 neutrophils towards an N2 phenotype, while interferon β (IFN-β) does the reverse. In cancer patients there is an elevated number of granulocytic myeloid-derived suppressors cells (G-MDSC) that resemble immature neutrophils and possess immunosuppressive functions by suppressing T and natural killer cell activity (Groth et al., 2021). Similarly, in circulation there exists populations of low-density (LDN) and high-density neutrophils as determined through density gradient centrifugation. An increase in the number of LDN is associated with tumor growth and progression because these cells possess impaired functionality and immunosuppressive properties (Rosales, 2018; Shaul and Fridlender, 2019). Overall, immature neutrophils seem to be functionally associated with pro-tumor effects. However, this has recently been debated as *ex vivo* studies have found T cell suppression executed primarily by mature neutrophils (Antuamwine et al., 2023). Neutrophil phenotype classifications are not well-defined and there is still much to be determined especially in human models.

Given that neutrophils vary phenotypically in circulation, it is not surprising then that the differentiation agent used can produce functionally diverse neutrophil-like cells. Prior work has found that ATRA is the most effective differentiation agent for HL-60 cells when comparing to DMSO and DMF. ATRA-differentiated cells had the greatest number of CD11 positive cells, a marker of mature neutrophils (Manda-Handzlik et al., 2018). This was further supported by ATRA-differentiated cells being the most mature morphologically based on the proportion of banded and segmented nuclei observed. These cells also had the highest phagocytic index and produced the greatest amount of ROS (Sham et al., 1995; Manda-Handzlik et al., 2018). ATRA also produced cells that had the ability to migrate further than those differentiated with DMSO (Sham et al., 1995). ATRA, DMSO, and DMF-differentiated cells also vary in their ability to produce NETs in response to PMA or calcium ionophore, with DMF cells being the only ones to respond to both stimuli (Manda-Handzlik et al., 2018). Similar findings were observed for generation of respiratory burst as all cells produced ROS in response to PMA but only DMF-

differentiated cells for stimulation with CI. ATRA-differentiated cells also produces little response to fMLP compared to DMSO due to the lack of expression of FPR receptor on the cell surface (Skubitz et al., 1982; Sham et al., 1995; Rincón et al., 2018). Together, these findings suggest that these cells represent functionally distinct phenotypes of neutrophils or are influenced by genetic limitations of the HL-60 cell line. Galectin-12 expression also seems to vary depending on the differentiation stimuli used therefore, it can be proposed that galectin-12 could serve as a marker of different neutrophil phenotypes.

1.5 Breast cancer

Breast cancer is the most commonly diagnosed cancer for women, which represents 25% of new diagnoses and 13% of the cancer deaths in Canada (Brenner et al., 2020). Comprehensive classification of tumors leads to individualized therapy, allowing for safer and more effective treatment. Breast tumors are categorized into five main molecular subtypes (luminal A, luminal B, HER2-enriched, basal-like, and normal-like) using immunohistochemistry and gene expression profiling centered on estrogen receptor (ER), progesterone receptor (PR), and human epidermal growth factor 2 receptor (HER2) status (Perou et al., 2000; Eliyatkin et al., 2015). To study these molecular subtypes of breast cancer, many human cell lines are available including, e.g., MCF-7 (ER+, PR+, HER2-), MDA-MB-231 (ER-, PR-, HER2-), MDA-MB-468 (ER-, PR-, HER2-), and SK-BR-3 (ER-, PR-, HER2+), among others (Dai et al., 2017).

Epithelial-mesenchymal transition (EMT) is a key process in tumor progression and metastasis involving epithelial cells gaining a mesenchymal phenotype. Changes in gene expression and various signaling pathways leads to the acquirement of a fibroblast-like phenotype and the ability to migrate due to the loss of cell-cell adhesion molecules like E-cadherin (Kalluri & Weinberg, 2009; Wang & Zhou, 2011). This is accompanied by an increase in expression of mesenchymal markers like N-cadherin and vimentin. Breast tumors that undergo EMT typically possess a basal-like phenotype with high potential for metastasis (Felipe Lima et al., 2016; Wang & Zhou, 2011). Other subtypes like luminal A/B and HER2-enriched maintain more of their epithelial features. The reverse process of

mesenchymal-epithelial transition (MET) occurs at secondary sites as circulating cells settle and form new tumors. Consequently, cells can be reverted back to their more differentiated epithelial state by undergoing MET. Differentiation therapy promoting MET will therefore prevent cancer progression and metastasis by allowing cells to function as their cell-of-origin.

As previously described, differentiation therapy with ATRA is the standard treatment for APL. Similar approaches are being tested for breast cancer. ATRA has been previously shown to induce differentiation of breast cancer stem cells (Ginestier et al., 2009; Yan et al., 2016). Treatment of radiation-resistant MCF-7/C6 cells with ATRA led to reduced invasiveness, migration and increase sensitivity to chemotherapy (Yan et al., 2016). This was marked by an increase in expression of the differentiation markers involucrin and syndecan-3. Similar findings were observed in MDA-MB-231 cells treated with ATRA and ATRA-derivatives with cells having reduced proliferation and migration (Wang et al., 2013). ATRA-induced MDA-MB-231 cell differentiation has been marked by an increase in expression of intercellular adhesion molecule 1 (ICAM-1) which has been previously used as a marker of human mammary epithelial cells, and a drop in phosphorylated Erk (Yu et al., 2019). MCF-7 and MDA-MB-435 cells treated with RRR-α-succinate (a vitamin E derivative) also induced differentiation like retinoids and this differentiation was also marked with an increase in ICAM-1 expression and involved Erk signaling (You et al., 2001). Interestingly, MCF-7 cells did not show an increase in ICAM-1 expression when treated with ATRA, suggesting stimuli and subtype specific differences in signaling exist (Yu et al., 2019). SK-BR-3 cells treated with ATRA also demonstrated increased epithelial differentiation and increased cell-cell adhesion strength (Byers et al., 1996). These findings point to potential clinical use of ATRA as an anti-cancer agent beyond APL.

Aberrant expression of numerous galectins has been linked to breast cancer. Galectin-1, -3, -9 in particular have been associated with promoting tumor progression, host immunity evasion and metastasis (Yasinska et al., 2019; Grazier and Sylvester, 2022). For example, surface-based galectin-9 protected tumor cells from T-cell induced death through suppression of host immune surveillance (Yasinska et al., 2019). In contrast, galectin-8 likely plays a protective role in breast cancer as low galectin-8 is a poor prognostic marker

(Grosset et al., 2016; Trebo et al., 2020). However, the findings surrounding galectin activity in breast cancer can be conflicting as a galectin can show both up and downregulations along with both pro- and anti-tumor effects in different studies (Thijssen et al., 2015; Ju et al., 2021). For instance, low galectin-3 has also been associated with poorer prognosis in node-positive patients (Ilmer et al., 2016). The heterogeneity of breast cancer as a disease likely makes the function of a particular galectin subtype-specific and context-dependent. The localization of the galectin either on the cell surface, intracellularly or in circulation also plays a factor. Ultimately, both tumor and circulating levels of galectins have potential clinical use as diagnostic or prognostic markers. To date, galectin-12 levels in breast tumors and in circulation of patients have not been evaluated. An *in silico* look at galectin-12 expression using The Cancer Genome Atlas cohort data found a large drop in *LGALS12* in all subtypes of breast cancer compared to normal tissue, with the largest downregulation in luminal B and basal-like tumors (Tazhitdinova and Timoshenko, 2021).

1.6 Hypothesis

Prior work using DMSO and ATRA as differentiation agents in myeloid cells produced opposite effects in galectin-12 expression, which may reflect different phenotypes of neutrophils being produced (Xue et al., 2016; Vinnai et al., 2017; McTague et al., 2022). Therefore, the overall role and regulation of galectin-12 in myeloid cell differentiation is still poorly defined. Additionally, galectins are secreted through unconventional mechanisms, and galectin-12 has been shown to co-localize to lipid droplets in adipocyte cells (Yang et al., 2011). To date, there is no information available about whether galectin-12 is secreted out of cells at all. Only negligible secretion was observed in 3T3-L1 adipocytes and secretion has not been examined in other cell models.

Recent findings suggest that galectin expression and secretion may be influenced by the post-translational protein modification *O*-GlcNAcylation. Like other members of the family, galectin-12 also has putative *O*-GlcNAcylation sites. Together, this proposes the existence of *O*-GlcNAc-dependent galectin regulation which may contribute to changes in expression and secretion observed during neutrophilic differentiation.

There are currently no publications that have evaluated the role of galectin-12 in breast cancer excluding one *in silico* approach by the Timoshenko lab (Tazhitdinova and Timoshenko, 2021). Galectin-12 expression in breast cancer patients was found to be strongly downregulated, suggesting galectin-12 may serve a protective role against tumorigenesis.

I hypothesize that galectin-12 is a tissue-specific biomarker of cellular differentiation including the polarization of neutrophils. I also hypothesize that galectin-12 expression and secretion are influenced by *O*-GlcNAc homeostasis and lipogenesis.

Objective 1: To study the molecular mechanisms and transcriptional regulation governing galectin-12 expression in HL-60 cells under two neutrophilic differentiation models.

Objective 2: To study the effects of inhibitors of *O*-GlcNAc cycle enzymes on the expression and secretion of galectin-12 in HL-60 cells.

Objective 3: To examine the role of extracellular vesicles and lipid droplets in the secretion of galectin-12.

Objective 4: To characterize the expression and secretion of *LGALS12* in breast cancer cell lines upon differentiation with ATRA.

Chapter 2

2 Materials and Methods

2.1 Chemicals and solutions

All-trans retinoic acid (ATRA) (R2625), 6-diazo-5-oxo-L-norleucine (DON) (D2141), horseradish peroxidase (P-8250), thiamet G (TG) (SML0244), DMSO (D26500), Dulbecco′s Phosphate Buffered Saline (D-PBS) with $MgCl_2$ and $CaCl_2$ (D8862), Immobilon Classico Western HRP substrate (WBLUC500), 3-isobutyl-1-methylxanthine (410957-250MG), scopoletin (S2500), digitonin (D141), oleic acid-albumin from bovine serum (O3008), isoproterenol-hydrochloride (I6504), concanavalin A (ConA) (C5275) and 3-methyladenine (3-MA) (189490) were purchased from Sigma-Aldrich Canada (Oakville, ON).

Mounting medium with DAPI (ab104139) was purchased from Abcam. D-PBS without $MgCl_2$ and $CaCl_2$ (311-425-CL), fetal bovine serum (FBS) 080-450, penicillin/streptomycin (450-201-EL), advanced cDNA synthesis kit (801-100-XR), human insulin recombinant solution (521-016-IL) and Iscove's Modification of Dulbecco's Modified Eagle Medium (IMDM) (319-105-CL) were purchased from Wisent Bio Products (Saint-Jean-Baptiste, QC). Mammalian Protease Inhibitor Cocktail (BS386), 2x RIPA Buffer IIII with EDTA and EGTA (pH 7.4) (RB4477), sodium azide (NaN_3) (S2002), bovine serum albumin (BSA) (AD0023), sodium orthovanadate (Na_3VO_4) (SB0869), Oil Red O (OD0395), and paraformaldehyde (PB0684) were purchased from BioBasic (Markham, ON).

Betulin (11041), HX 531 (20762), CD3254 (20870), GW 4869 (GW) (13127), and Y-27632 (10005583) were purchased from Cayman Chemical Company (Ann Arbor, MI). SsoAdvanced Universal SYBR® Green Supermix (1725274), and non-fat dry milk Blotting-Grade Blocker (1706404) were purchased from Bio-Rad (Mississauga, ON). Phorbol 12-myristate 13-acetate (PMA) (PMA168) and dexamethasone (DEX002) were purchased from BioShop. SYBR™ Safe DNA Gel Stain (S33102), BODIPY 493/503

(D3922), SYTOX™ Blue Dead Cell Stain (S34857), TRIzol® (15596018) and high glucose DMEM (11965092) were purchased from ThermoFisher Scientific (Mississauga, ON). Acryl/Bis™ 29:1 ULTRA PURE 40% (w/v) Solution (0311) was purchased from VWR Life Science. Froggarose LE Molecular Biology Grade Agarose (A87) and 2x Taq Frogga Mix (FBTAQM) were purchased from FroggaBio (Concord, ON).

OGT inhibitor 2-acetamido-1,3,4,6-tetra-O-acetyl-2-deoxy-5-thio-a-D-glucopyranose known as Ac-5SGlcNAc (AC) was synthesized in Dr. Vocadlo laboratory (Gloster et al., 2011) and kindly provided as per Material Transfer Agreement between Simon Fraser University and the University of Western Ontario.

2.2 Cell culture and treatments

2.2.1 Cell culture

Human acute promyelocytic leukemia HL-60 cells were cultured in IMDM (Wisent) supplemented with 10% fetal bovine serum (Wisent), 50 IU/mL penicillin, and 50 µg/mL streptomycin (Wisent) at 37°C and 5% CO_2. Mouse pre-adipocyte 3T3-L1 cells and human breast cancer cell lines MCF-7, MDA-MB-231, MDA-MB-468, and SK-BR-3 were cultured in high glucose DMEM (ThermoFisher Scientific) supplemented with 10% fetal bovine serum, 50 IU/mL penicillin, and 50 µg/mL streptomycin at 37°C and 5% CO_2. MCF-7 cells were also supplemented with 10 µg/mL of human recombinant insulin (Wisent). Adherent cell lines were passaged at 80% confluency while HL-60 cells were passaged prior to reaching a concentration of $1.0x10^6$ cells/mL.

2.2.2 Cell differentiation treatments

To induce neutrophilic differentiation, HL-60 cells were treated with either 1.3% DMSO or 1 µM ATRA for 72 hours starting at a concentration of $0.4x10^6$ cells/mL (Vinnai et al., 2017; McTague et al., 2022). To induce adipocytic differentiation, 3T3-L1 cells were grown in complete high glucose DMEM until confluency was reached. The cells were then maintained for an additional 48 hours to achieve contact-induced growth inhibition and reach a “post-confluency” state. Once post-confluent a differentiation cocktail was added

to cell medium including 0.5 mM 3-isobutyl-1-methylxanthine, 1 µM dexamethasone and 10 µg/mL human insulin (Yang et al., 2004). After 48 hours the differentiation medium was replaced with post-differentiation media consisting of complete DMEM supplemented with 10 µg/mL insulin. Once cells were in the post-differentiation medium further treatment and experimental work were conducted and the cells were maintained until day seven of differentiation. To induce epithelial-like differentiation, MCF-7, MDA-MB-231, MDA-MB-468 and SK-BR-3 cells were treated with 1 µM of ATRA for 72 hours, with medium replacement and ATRA supplementation after 48 hours.

2.2.3 Chemical stimulator/inhibitor treatments

To test the role of *O*-GlcNAcylation homeostasis in the regulation of galectin-12 expression, HL-60 cells were treated for 48-72 hours with 10 µM of TG (OGA inhibitor), 12.5 µM of DON (GFAT inhibitor), or 40 µM of AC (OGT inhibitor) and grown in 60 mm dishes. To examine the potential role of transcription factors (SP1, RXR-α, SREBP1) in *LGALS12* transcriptional regulation, cells were treated for 24 hours with 25-250 mM of mithramycin (SP1 inhibitor), 250-1000 nM of HX 531 (RXR-α inhibitor), 250-1000 nM of CD3254 (RXR-α stimulator), or 2.5-10 µM of betulin (SREBP1 inhibitor).

To test the mechanisms of unconventional secretion at play, HL-60 cells were treated with inhibitors of exosome formation, microvesicle formation, and secretory autophagy for 48 hours. Cells were treated with 20 µM of selective neutral sphingomyelin phosphodiesterase (N-SMase) inhibitor GW 4869 to block exosome formation (Hekmatirad et al., 2021). 10 µM of selective inhibitor of rho-associated protein kinase (ROCK) inhibitor Y-27632 was used to block microvesicle formation (Sapet et al., 2006). Finally, 2 mM of type III phosphatidylinositol 3-kinases (PI3K) inhibitor 3-MA was used to block secretory autophagy (Davuluri et al., 2021). Similarly, cells were treated for 48 hours with 100 µM of oleic acid or 10 µM of isoproterenol to stimulate and inhibit lipid droplet production, respectively.

2.3 Brightfield and fluorescence microscopy

To prepare HL-60 cells for fluorescence microscopy, the concentration of live cells was determined using the trypan blue exclusion assay and cells were diluted with D-PBS to a concentration of $0.5x10^6$ cells/mL. HL-60 cells were centrifuged for 5 min at 500 rpm using a Shandon Cytospin 2 centrifuge. HL-60 cell nuclei were stained with Fluoroshield mounting medium containing DAPI (Abcam). To stain for lipid droplets HL-60 cells were temporarily adhered to ConA-coated cell 30 mm suspension culture dishes (Sarstedt). The cell culture dishes were prepared in advance by their treatment with 2 mL of ConA solution (5 µg/mL in D-PBS) overnight at 4°C. Cell culture dishes were briefly washed with D-PBS before HL-60 cells were added and incubated for 1 hour at 37°C, followed with another brief wash to remove cells that did not adhere, after which BODIPY 493/503 (ThermoFisher Scientific) staining was applied.

A Leica DM IL LED brightfield inverted microscope was used for all phase-contrast and Integrated Modulation Contrast (IMC) microscopy with images captured using a Leica EC3 camera and LAS software (Leica). All fluorescence images were taken using a Zeiss Axio Imager A1 fluorescence microscope equipped with DAPI and FITC filter cubes. Images were captured using a high-resolution monochrome XCD-X700 CCD camera (Sony Corporation) with Northern Eclipse 8.0 software (Empix Imaging).

2.3.1 BODIPY 493/503 lipid droplet staining

3T3-L1 or HL-60 cells were washed twice with D-PBS then incubated with a 2 µM BODIPY 493/503 solution in D-PBS for 15 min at 37°C (Qiu and Simon, 2016). Following the incubation, cells were washed with D-PBS twice, then fixed with 4% paraformaldehyde in D-PBS for 30 min at room temperature. The cells were washed with D-PBS an additional three times before mounting with Fluoroshield mounting medium containing DAPI.

2.3.2 Oil Red O lipid droplet staining

3T3-L1 cells were washed twice with D-PBS then fixed with 4% paraformaldehyde in D-PBS for 30 min at room temperature. Cells were then washed with distilled water twice

and incubated in a 3:2 isopropanol and distilled water solution at room temperature for 5 min (Kinkel et al., 2004). The isopropanol solution was then replaced with a 3:2 solution of 3 mg/mL oil red O in isopropanol and distilled water for 10 min. The cells were then washed with water five times before imaging.

2.3.3 ImageJ analysis

ImageJ was used to analyze nuclear morphology of DAPI-stained images. Images were converted to binary form using default B&W threshold settings. "Shape smoothing" plugin (version 1.2) was used to smoothen the binary image contours, with the relative proportions FDs (Fourier descriptors) % set at 7, and the absolute number FDs at 2. Apoptotic, overlapping and poorly contrasted nuclei were removed prior to morphology analysis, as well as any observed cellular debris. Nuclei in contact with each other that were not overlapping in the original images were separated using the paintbrush tool to avoid analysis as a singular cell. The "Analyze particles" feature was used to measure circularity ($\frac{4\pi\times Area}{Perimeter^2}$) and roundness ($\frac{4\times Area}{\pi\times Major\_axis^2}$) from a minimum to maximum range (0.00-1.00). Size exclusion criteria was set from (0.01-infinity) inch^2 to exclude noise and small particles.

For analysis of lipid droplets, counts were conducted using the "Cell counter" plugin (version 2.2.2). For each intact nucleus, the number of individual visible lipid droplets was counted to determine the number of droplets per cell.

2.4 RNA isolation, cDNA synthesis and PCR analysis

Total RNA was isolated using TRIzol (ThermoFisher Scientific) and quantified using a Nanodrop 2000c UV-Vis spectrophotometer (ThermoFisher Scientific) with a $A_{260/280}$ of >1.8 as a quality threshold. Reverse transcription of 500-1000 ng RNA was conducted using the Advanced cDNA Synthesis Kit (Wisent). PCR primers were synthesized using the UWO BioCorp OligoFactory (**Table 1**) and verified through BLAST. For endpoint PCR reaction mix (20 µL), 10 µL of 2x Taq FroggaMix (FroggaBio), 1 µM each of forward and reverse primer, 0.5 µl of undiluted cDNA template, and nuclease-free water were used. PCR products were loaded onto 2% agarose gels containing SYBR™ Safe (Thermo Fisher

Scientific) and run at 90 V for 50 min then imaged using a Molecular Imager GelDoc XR+ (Bio-Rad) with Image Lab software (Bio-Rad). Real-time PCR (RT-qPCR) was conducted using the CFX Connect real-time PCR system (Bio-Rad) with a two-step cycling regime (**Table 1**). The reaction mix (20 µL) consisted of 10 µL of SsoAdvanced Universal SYBR™ Green Supermix (Bio-Rad), 1 µM each of forward and reverse primer, 1 µl of 2-4x diluted cDNA template, and nuclease-free water. Relative mRNA levels were determined through the Livak ($2^{-\Delta\Delta Ct}$) method with *ACTB*, *RPL30* or *Gapdh* serving as reference genes (Livak and Schmittgen, 2001).

2.5 Protein isolation and immunoblotting

2.5.1 Protein isolation

A 5 mL suspension of HL-60 cells grown in 60 mm dishes was centrifuged at 300 *g* for 5 min and supernatant was collected with the cell pellet being washed twice with ice-cold D-PBS. Similarly, cell media for adherent cell lines was collected from 60 mm dishes and the cell monolayer was washed twice with ice-cold D-PBS. Cells were lysed on ice with 150-300 µL of RIPA buffer (10 mM Tris-HCl, 1% Triton X-100, 0.1% SDS, 500 µM EGTA, 0.1% sodium deoxycholate, and 140 mM NaCl) supplemented with 100 µM Na_3VO_4 and mammalian protease cocktail (800 nM aprotinin, 10 µM bestatin, 14 µM E-64, 10 µM leupeptin, and 15 µM pepstatin A, and 1 mM PMSF). The cells were incubated on ice for 10 min and then centrifuged at 10,000 *g* for 15 min. Total protein concentration was assessed using the DC™ Protein Assay Kit II (Bio-Rad) with a BSA standard and absorbance was measured at 690 nm on a BioTek 800 TS Absorbance Reader from Agilent Technologies (Santa Clara, CA).

2.5.2 Immunoblotting

Global *O*-GlcNAcylation was assessed using a Bio-Dot microfiltration apparatus as previously described (Sherazi et al., 2018). To each well, 4 µg of total protein (in D-PBS) was loaded per well (200 µL volume) onto 0.2 µm nitrocellulose membrane pre-wetted with Tris-buffered saline (TBS). Proteins were transferred to the membrane through gravity filtration for 1.5-2 hours. The membrane was then blocked using 3% nonfat milk powder

Table 1. PCR primer sequences.

Gene name	Sequence 5'-3'	Size (bp)	2 step cycling	PMID reference
ACTB	F - TCAGCAAGCAGGAGTATGACGAG R - ACATTGTGAACTTTGGGGGATG	265	95°C (5 s) 62°C (25 s)	30504378
FPR1	F - CCAAACCAGTGACACAGCTACC R - CAGCCTAACTCAAGGTGAGACG	131	95°C (5 s) 62°C (25 s)	Origene
ICAM1	F - AGCGGCTGACGTGTGCAGTAAT R - TCTGAGACCTCTGGCTTCGTCA	115	95°C (5 s) 62°C (25 s)	Origene
LBR	F - AGTATAGCCTTCGTCCAAGAAGA R - CAAAGGTTCTCACTGCCAGTT	99	95°C (5 s) 60°C (25 s)	27336722
LGALS12	F - TGTGAGCCTGAGGGACCA R - GCTGAGATCAGTTTCTTCTGC	111	95°C (5 s) 62°C (25 s)	18202194
LGALS12 #2	F - GCCTGGGCAGGTCATCATAG R - GAGTTCTGTCTGCGAAGGAGG	125	95°C (5 s) 62°C (25 s)	36313453
LMNA	F - CTCCACATCTGCCTTAAAAC R - GCTAGCCTCTATAAAAGCAC	75	95°C (5 s) 60°C (25 s)	32698886
LMNB1	F - AAGCATGAAACGCGCTTGG R - AGTTTGGCATGGTAAGTCTGC	152	95°C (5 s) 60°C (25 s)	32180800
LMNB2	F - TGACCAGAACGACAAGGCG R - CCGAATGCGATCTTCAGCG	130	95°C (5 s) 60°C (25 s)	32180800
NCF1	F - GTCAGATGAAAGCAAAGCGA R - CATAGTTGGGCTCAGGGTCT	93	95°C (5 s) 62°C (25 s)	23147401
NCF2	F - GGTGCCCCTTTCAGAAGACA R - AAAGCCTTGGTCACCCACTG	100	95°C (5 s) 60°C (25 s)	27078885
RPL30	F - TTCTCGCTAACAACTGCCCA R - TGCCACTGTAGTGATGGACAC	90	95°C (5 s) 62°C (25 s)	34593877
RXRA	F - ACATGCAGATGGACAAGACG R- TCGAGAGCCCCTTGGAGT	78	95°C (5 s) 60°C (25 s)	30216632
SP1	F - TACCCCTACCTCAAAGGAACAG R - AACATACTGCCCACCAGAGACT	97	95°C (5 s) 60°C (25 s)	28332021
SREBF1	F - CGGAACCATCTTGGCAACAGT R - CGCTTCTCAATGGCGTTGT	141	95°C (5 s) 60°C (25 s)	32218693
Fabp4	F - GATGAAATCACCGCAGACGACA R - ATTGTGGTCGACTTTCCATCCC	101	95°C (5 s) 62°C (25 s)	26070408
Gapdh	F - CATCACTGCCACCCAGAAGACTG R - ATGCCAGTGAGCTTCCCGTTCAG	153	95°C (5 s) 62°C (25 s)	Origene
Lgals12	F - AGGACTGGTCTTGAAAGAGCCG R - GCCAGTGTTCTGTCTGTGAAGG	101	95°C (5 s) 62°C (25 s)	Origene

in TBS-T (TBS with 5% Tween 20) for one hour at room temperature. Membranes were probed with mouse monoclonal pan-specific *O*-GlcNAc (RL2) (**Table 2**) antibody overnight at 4°C. The following day membranes were probed with goat anti-mouse IgG HRP-conjugated secondary antibody for one hour at room temperature followed by imaging. For western blots, cell lysate (10-25 µg total protein) was mixed with 4x SDS loading buffer (2% (w/v) SDS, 0.04% β-mercaptoethanol) and boiled for five min. SDS-PAGE was conducted using a 10% Mini-PROTEAN TGX and ran at 90 V. Proteins were transferred to 0.22 µm PVDF membrane (Sigma-Aldrich) at 20 V overnight at 4°C in methanol buffer (25 mM Tris, 190 mM glycine, 20% methanol). The following day blocking and incubation with primary and secondary antibodies (**Table 2**) were conducted as described above. To image the membranes, a Chemidoc XRS system (Bio-Rad) with Quantity One software was used with the Immobilon Classico chemiluminescent HRP detection agent (Sigma-Aldrich).

2.6 Enzyme-linked Immunosorbent Assay (ELISA)

Intracellular and extracellular levels of human and mouse galectin-12 were measured as instructed by Novus Biologicals ELISA kits (NBP2-76718, NBP2-76719), while extracellular galectin-3 was measured using a SimpleStep ELISA kit from Abcam (ab269555). Undiluted cell supernatant was used while cell lysate was diluted up to 50-fold, depending on initial protein concentration. Absorbance was measured at 450 nm using a BioTek 800 TS Absorbance Reader from Agilent Technologies.

2.7 Flow cytometry

HL-60 cells were differentiated with ATRA or DMSO for 72 hours then cell concentration and viability were assessed using the trypan blue exclusion test. Cells were washed with D-PBS then stained with 2 µM BODIPY 493/503 for 15 min at 37°C or left unstained to serve as negative controls. All cells were washed three times with FACS buffer (Ca^{2+}/Mg^{2+}-free D-PBS, 1% of 0.5M EDTA, 5 µg/mL BSA) then resuspended in FACS buffer at $1x10^6$ cells/300 µL. 1 µM SYTOX Blue (Thermo Fisher Scientific) was used as a dead-cell

Table 2. Primary and secondary antibodies used for immunoblotting.

Antigen	Source	Host	Type	Conjugate	Dilution	Catalog #
Galectin-12	Santa Cruz	Rabbit	Polyclonal	N/A	1:200	sc-67294
Galectin-12	Invitrogen	Rabbit	Polyclonal	N/A	1:500	PA5-113236
Galectin-12	Bioss	Rabbit	Polyclonal	N/A	1:500	BS-8413R
Galectin-12	Abnova	Mouse	Polyclonal	N/A	2 ug/mL	H0008532 9-B02P
O-GlcNAc (RL2)	Thermo Fisher	Mouse	Monoclonal	N/A	1:1000	MA1-072
β-actin (C4)	Invitrogen	Mouse	Monoclonal	N/A	1:200	sc-47778
Mouse IgG (H+L)	Thermo Fisher	Goat	Polyclonal	HRP	1:10000	A16066
Rabbit IgG (H+L)	Thermo Fisher	Goat	Polyclonal	HRP	1:10000	A16096

indicator. Cells were analyzed using a CytoFLEX S flow cytometer (Beckman Coulter) at the London Regional Flow Cytometry Facility (Robarts Research Institute) and results were analyzed using FlowJo.

2.8 Scopoletin assay for hydrogen peroxide generation

Hydrogen peroxide generation was measured in differentiated neutrophil-like HL-60 cells as described previously using scopoletin (McTague et al., 2022). HL-60 cells were centrifuged at 300 *g* for 5 min and resuspended at a concentration of $0.5x10^6$ cells/mL in D-PBS with Ca^{2+}/Mg^{2+}. Cells were added to a cuvette containing 1 µM scopoletin and 20 µg/mL horseradish peroxidase (HRP) which would generate a stable fluorescence signal. The fluorescence was measured using an AMINCO-Bowman Series 2 Luminescence Spectrometer with an excitation wavelength of 350 nm and emission wavelength of 460 nm. Once a stable fluorescence signal was achieved 1 µM of PMA, 100 nM of fMLP, or 2.3 µg/mL of digitonin was added to activate the NADPH oxidase complex and generate respiratory burst in the cells. The rate of hydrogen peroxide generation can be measured indirectly using the maximum slope of scopoletin oxidation by HRP calculated using R (Vinnai et al., 2017).

2.9 Bioinformatics analysis

PROMO and Harmonizome bioinformatics tools were used to identify transcription factors that potentially bind to the promoter region of the *LGALS12* gene (Messeguer et al., 2002; Farre, 2003; Rouillard et al., 2016). As a defined promoter for *LGALS12* is not established in the literature, a 10 Kb region prior to the start codon from Ensembl was used (RefSeq: NM_033101.4). PROMO analysis was run using version 8.3 of the TRANSFAC database with a dissimilarity index of 5%.

RNA-Seq data for ATRA/DMSO-differentiated HL-60 cells were obtained from the Gene Expression Omnibus (GEO) accessions GSE93996 and GSE103706. Reads were aligned to Genome Reference Consortium Human Build 38 release 108 genome assembly and annotation using STAR version 2.7.10a (Dobin et al., 2013) in two-pass mode with annotation, allowing only unique mapping, and up to five mismatches per read mapped.

Per gene read counts were generated using htseq-count (HTSeq framework version 1.99.2) in "union" mode (Anders et al., 2015). All subsequent analysis was conducted using R (R Core Team, 2022). Prior to differential gene expression analysis datasets were merged by ComBat for RNA-Seq counts using R package sva (Johnson et al., 2007; Leek et al., 2012). Genes expressed at the level at or above 1 fragment count per million in at least three samples were considered for the subsequent analysis. Differential gene expression analysis and estimation of $\log_2$ fold changes and false discovery rate (FDR) adjusted p-values (Benjamini and Hochberg, 1995) was conducted using voom (Law et al., 2014). Changes in gene expression were deemed significant at FDR-adjusted $p<0.01$ and $\log_2$ fold change of ±1 cut-offs.

Gene Ontology (GO) enrichment analysis was performed using topGO R package with the "weight01" algorithm and a weighted $p<0.05$ cut-off to generate the top GO terms for biological processes (BP), molecular function (MF), and cellular components (CC) for the list of DEGs (Alexa et al., 2006). Gene Set Enrichment Analysis (GSEA) was performed using piano and fgsea R packages (Väremo et al., 2013; Korotkevich et al., 2016). GSEA was conducted for BP, MF, and CC terms and visualized as networks plots comparing ATRA- and DMSO-differentiated cells. Only GO terms with a minimum of 20 annotated genes were considered for analysis. GSEA was also conducted for all lipid-related GO terms extracted from the Molecular Signatures Database (MSigDB) and normalized enrichment score was reported with significance cut-off at FDR-adjusted $p<0.05$ (Liberzon et al., 2011).

2.10 Statistical analysis

All statistical analyses were conducted using GraphPad Prism 6.0 for Mac (GraphPad Software, La Jolla California USA). One-way or two-way ANOVA with Tukey's or Dunnett's multiple comparisons test, or unpaired t-tests were conducted for comparison between treatment groups. A minimum of three biological replicates were used for all experiments. Data were presented as group mean with standard deviation and statistical significance designated at $p<0.05$.

Chapter 3

3 Results

3.1 Transcriptional regulation of *LGALS12* and characterizing different phenotypes of neutrophil-like HL-60 cells

3.1.1 *LGALS12* is differentially expressed between ATRA- and DMSO-induced neutrophil-like HL-60 cells

ATRA and DMSO are two established models of inducing neutrophil-like differentiation in HL-60 cells (Mar and Quackenbush, 2009). My first objective was to compare the two phenotypes produced by these models and the potential differences in galectin-12 regulation under these models. The neutrophilic differentiation of HL-60 cells with ATRA resulted in a significant increase in *LGALS12* expression (3.2-fold, $p<0.0001$), while neutrophil-like differentiation with DMSO led to a significant drop (3.7-fold, $p<0.01$) as observed through RT-qPCR analysis (**Figure 7A**). Both stimuli led to significant increases in gene expression of neutrophilic differentiation makers *NCF1* and *NCF2*. *NCF1* was upregulated 18.2-fold with ATRA ($p<0.001$) and 10.8-fold with DMSO ($p<0.01$) (**Figure 7B**), while *NCF2* was upregulated 2.7-fold with ATRA ($p<0.05$) and 5.7-fold with DMSO ($p<0.0001$) (**Figure 7C**).

Another established characteristic of neutrophil-like differentiation is a decrease in protein *O*-GlcNAcylation. Global *O*-GlcNAcylation levels in HL-60 cells were evaluated using immunodot blots and compared to cells treated with inhibitors of *O*-GlcNAc cycle components (**Figure 7D**). Densitometric analysis found a significant decrease in global *O*-GlcNAcylation levels upon differentiation with both ATRA ($p<0.01$) and DMSO ($p<0.0001$). As expected, cells treated with 40 µM of OGT inhibitor AC ($p<0.0001$) and 12.5 µM of GFAT inhibitor DON ($p<0.001$) both demonstrated significant decreases in global *O*-GlcNAcylation levels, while a significant increase was observed in cells treated with 10 µM of OGA inhibitor TG ($p<0.01$).

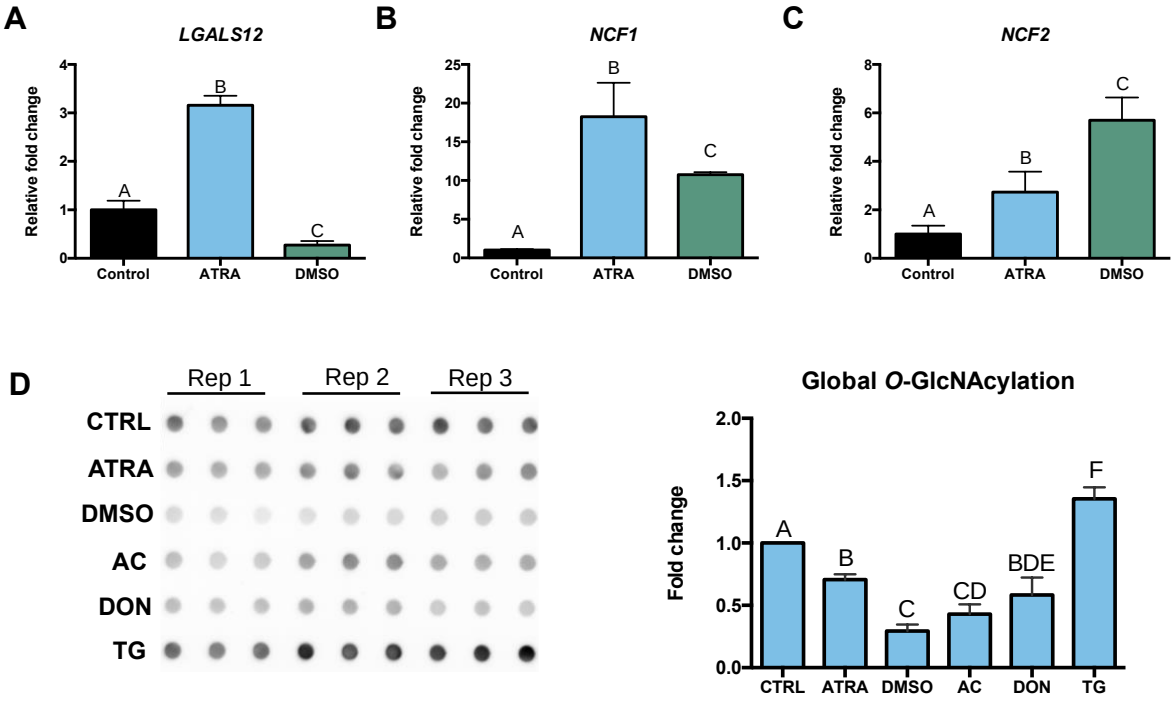

Figure 7. Neutrophil-like differentiation of HL-60 cells by ATRA and DMSO induce opposite changes in *LGALS12* expression.

HL-60 cells were differentiated with 1 µM ATRA or 1.3% DMSO for 72 h, (A) *LGALS12* and (B, C) neutrophilic differentiation markers *NCF1* and *NCF2* gene expression were quantified through RT-qPCR using the Livak method ($2^{-\Delta\Delta CT}$) with *ACTB* as a reference gene. (D) Global *O*-GlcNAcylation levels were measured using an immunodot blot for HL-60 cells treated with differentiation agents and *O*-GlcNAc cycle enzymes (AC, DON, TG) and compared relative to control cells. Data are presented as mean ± SD, n=3-5. Significant differences were determined using one-way ANOVA with Tukey's multiple comparisons test. Different letters between treatment groups represent significance where $p<0.05$, while any overlap in letters represents non-significance.

3.1.2 Neutrophil-like differentiation with both ATRA and DMSO leads to nuclear envelope remodeling

Neutrophil-like differentiation can also be assessed through changes in the nuclear morphology of cells. HL-60 cells grow in suspension and do not form aggregates (**Figure 8A**). Upon differentiation with ATRA or DMSO, HL-60 nuclei develop a lobulated and segmented morphology characteristic of neutrophilic cells (**Figure 8B**). ImageJ analysis of nuclear morphology measuring circularity and roundness found a significant decrease in circularity upon ATRA-induced differentiation ($p<0.0001$) but not DMSO (**Figure 8C**). However, a significant decrease in roundness was observed for both ATRA- and DMSO-induced differentiation ($p<0.0001$).

The nuclear lobulation observed is partially due to remodeling of the nuclear envelope influenced by various proteins including A-type and B-type lamins. The expression of five lamin-related genes were measured through RT-qPCR. Lamin B receptor (*LBR*) expression was significantly upregulated upon ATRA treatment (1.5-fold, $p<0.01$), but was significantly downregulated in DMSO-treated cells (1.9-fold, $p<0.01$) (**Figure 8D**). Meanwhile, DMSO-treated cells had a significant upregulation of lamin A/C (*LMNA*) expression (2.1-fold, $p<0.05$), while no significant changes were observed with ATRA (**Figure 8E**). Both ATRA and DMSO led to a significant drop in lamin B1 (*LMNB1*) expression (5.5-fold and 6.5-fold, $p<0.0001$) while lamin B2 (*LMNB2*) was significantly downregulated only upon ATRA-induced differentiation (3.7-fold, $p<0.05$) with no significant changes in DMSO-treated cells (**Figure 8F, 8G**).

3.1.3 Generation of respiratory burst differs between ATRA- and DMSO-differentiated HL-60 cells

Differentiated neutrophils undergo a respiratory burst in response to various stimuli producing ROS like superoxide, that is then converted to hydrogen peroxide (Belambri et al., 2018). Therefore, the reduction of scopoletin fluorescence via hydrogen peroxide production and HRP activity can serve as a valid measure of respiratory burst. I aimed to examine the differences in functional response of cells differentiated with ATRA and

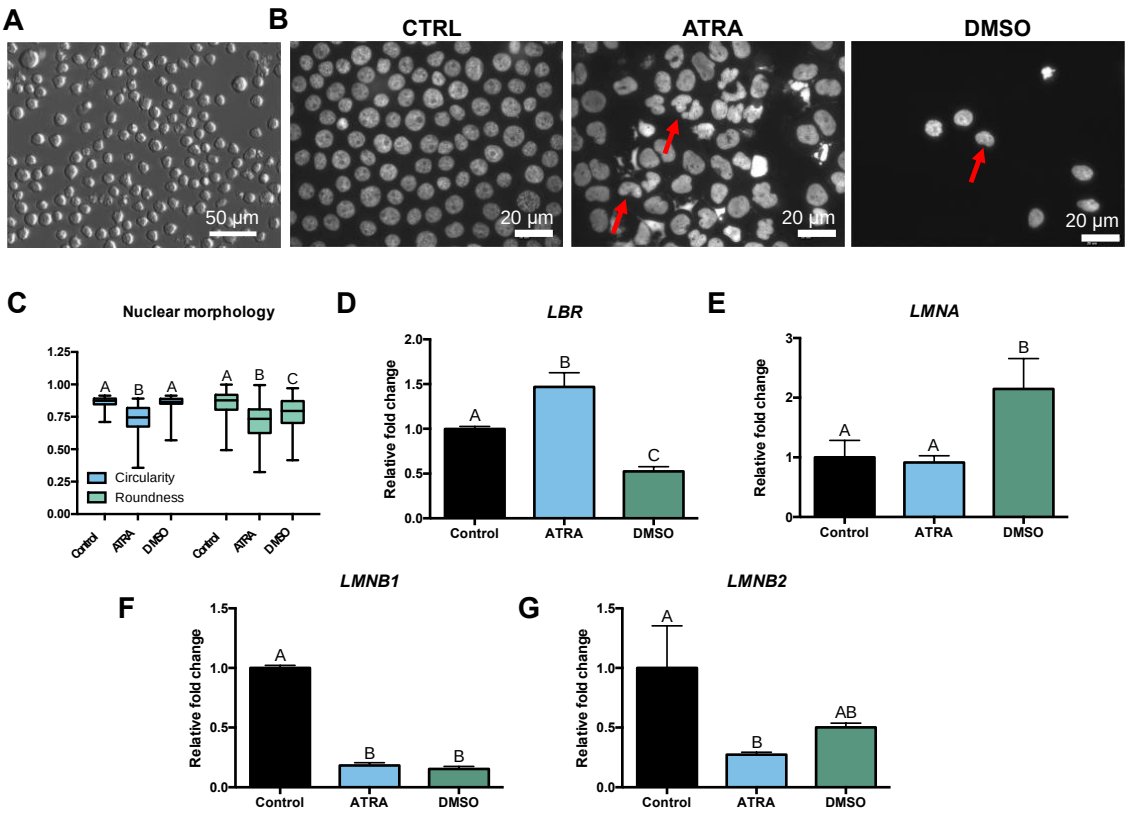

Figure 8. Neutrophil-like differentiation leads to changes in HL-60 cell nuclear morphology and expression of nuclear envelope genes.

HL-60 cells were differentiated with 1 µM ATRA or 1.3% DMSO for 72 h. (A) Overall cell morphology of undifferentiated HL-60 cells through brightfield IMC microscopy. DAPI-stained HL-60 cell nuclei were compared for (B) control, ATRA- and DMSO-treated cells with nuclear lobulation highlighted using red arrows. (C) Nuclear circularity and roundness were measured using ImageJ and significant differences were determined using two-way ANOVA with Sidak's multiple comparisons test and are represented as different letters for treatments, where $p<0.05$. The expression of nuclear envelope genes was examined through RT-qPCR using the Livak method ($2^{-\Delta\Delta CT}$) with reference gene *ACTB* for (D) *LBR*, (E) *LMNA*, (F) *LMNB1* and (G) *LMNB2*. Data are presented as mean ± SD, n=3-5. Significant differences were determined using one-way ANOVA with Tukey's multiple comparisons test and are represented as different letters for treatments, where $p<0.05$.

DMSO. I first looked at the gene expression of formyl peptide receptor 1 (*FPR1*) which is necessary for a response to fMLP. *FPR1* was found to be significantly upregulated in cells differentiated with DMSO (10.1-fold, $p<0.01$) but not ATRA (**Figure 9A**). Moreover, upon stimulation with fMLP the DMSO-differentiated cells showed a significantly higher ($p<0.01$) generation of hydrogen peroxide compared to both control and ATRA-differentiated cells (**Figure 9B**). In contrast, both ATRA- and DMSO-differentiated cells had similar levels of hydrogen peroxide generation when stimulated with PMA both being significantly higher than undifferentiated cells ($p<0.01$) (**Figure 9C**). Stimulation with digitonin led to similar outcomes as with fMLP where DMSO-differentiated cells had significantly higher hydrogen peroxide production than control and ATRA-differentiated cells ($p<0.01$) (**Figure 9D**).

3.1.4 ATRA and DMSO activate distinct neutrophilic differentiation pathways in HL-60 cells.

Differential gene expression analysis of ATRA- and DMSO-differentiated HL-60 cells was conducted using RNA-Seq data from GEO. Overall, DMSO led to the differential expression of more genes than ATRA (**Figure 10A**). In ATRA-treated cells there were 871 and 768 significantly upregulated and downregulated genes, respectively (minimum $\log_2$ fold change of ± 1, $p<0.01$). On the other hand, DMSO-treated cells had 1852 significantly upregulated and 2431 significantly downregulated genes. 562 upregulated and 584 downregulated genes were common to both treatments. Group network plots were created covering gene ontology terms related to biological processes (**Figure 10B, 10C**). Terms clustering around cell division were found to be significantly downregulated with DMSO but not ATRA ($p<0.01$). Similarly, terms clustering around DNA damage were also significantly downregulated in DMSO with fewer significant terms observed with ATRA. Transcription factors predicted to bind the promoter region of *LGALS12* were extracted from PROMO and Harmonizome. Transcription factors shown to have opposite changes in expression between ATRA and DMSO treatment in HL-60 cells were selected for further analysis (**Table 3**).

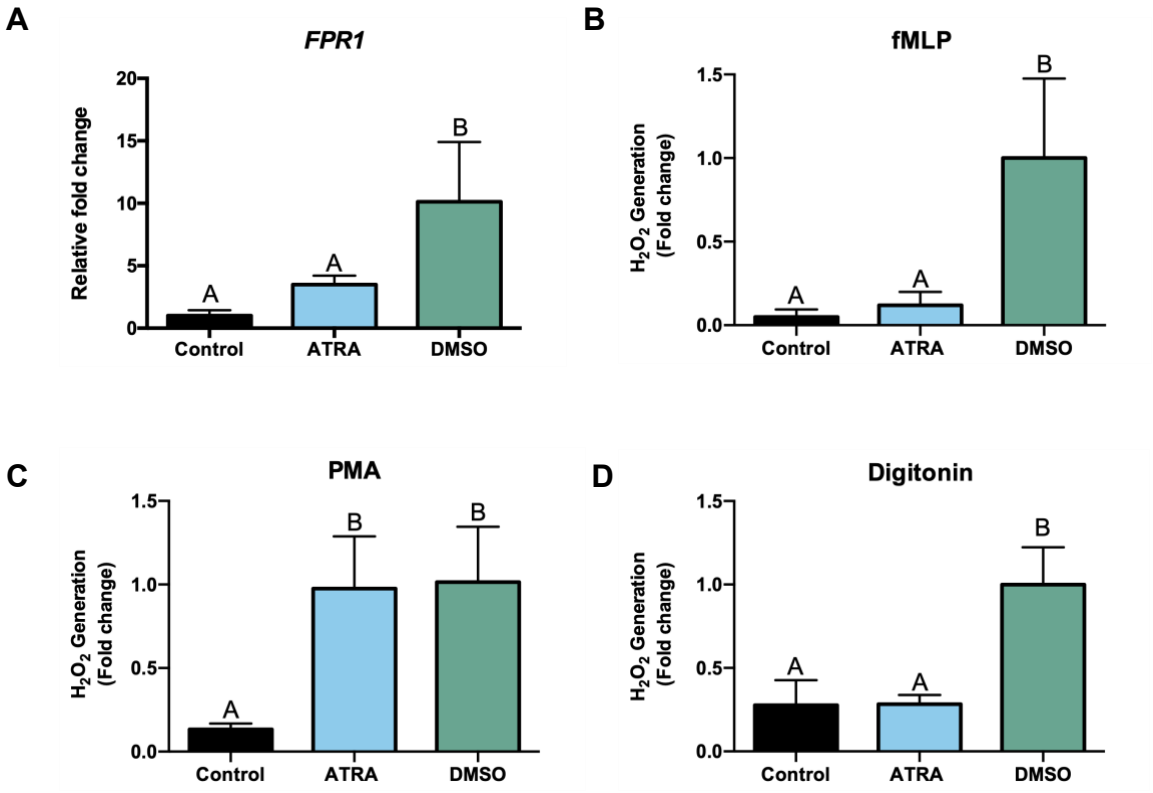

Figure 9. Generation of respiratory burst differs between ATRA- and DMSO-differentiated HL-60 cells.

HL-60 cells were differentiated with 1 µM ATRA or 1.3% DMSO for 72 h. Expression of formyl peptide receptor 1 (*FPR1*) was quantified through RT-qPCR using the Livak method ($2^{-\Delta\Delta CT}$) with *ACTB* as a reference gene. HL-60 cells were stimulated with (B) fMLP, (C) PMA and (D) digitonin where hydrogen peroxide generation (as seen by the reduction of scopoletin fluorescence) was measured relative to DMSO differentiated cells. Data are presented as mean ± SD, n=3-5. Significant differences are represented as different letters for treatments, where $p<0.05$ and were determined using one-way ANOVA with Tukey's multiple comparisons test.

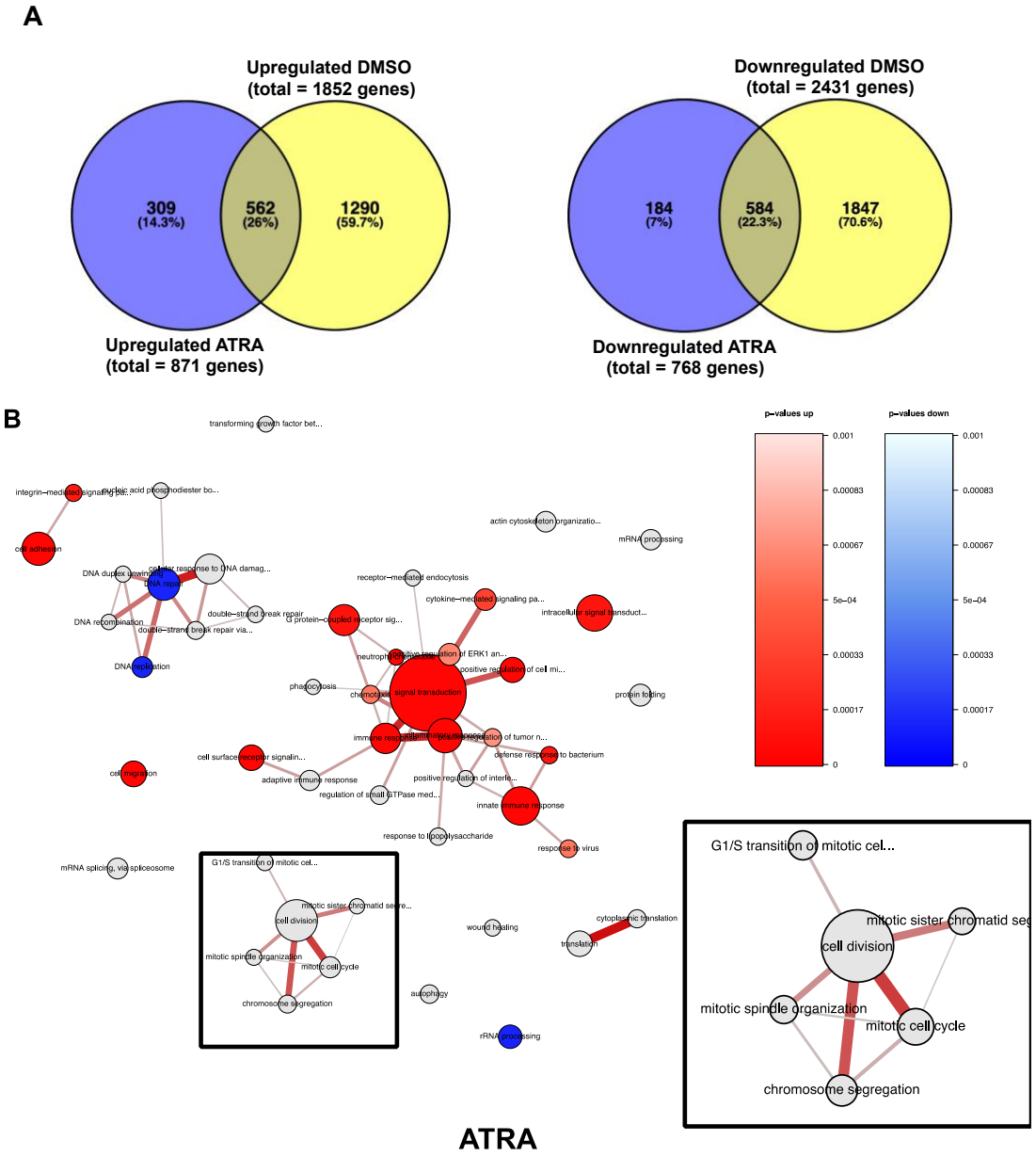
A
Upregulated DMSO
(total = 1852 genes)
309
(14.3%)
562
(26%)
1290
(59.7%)
Upregulated ATRA
(total = 871 genes)
Downregulated DMSO
(total = 2431 genes)
184
(7%)
584
(22.3%)
1847
(70.6%)
Downregulated ATRA
(total = 768 genes)
B
p−values up
p−values down
0.001
0.00083
0.00067
5e−04
0.00033
0.00017
0
transforming growth factor bet...
integrin−mediated signaling pa...
cell adhesion
actin cytoskeleton organizatio...
mRNA processing
DNA duplex unwinding
DNA repair
cellular response to DNA damag...
DNA recombination
double−strand break repair
double−strand break repair via...
DNA replication
receptor−mediated endocytosis
cytokine−mediated signaling pa...
intracellular signal transduct...
G protein−coupled receptor sig...
neutrophil activation involved ...
positive regulation of ERK1 an...
positive regulation of cell mi...
phagocytosis
chemotaxis
signal transduction
protein folding
immune response
inflammatory response
positive regulation of tumor n...
cell surface receptor signalin...
defense response to bacterium
cell migration
adaptive immune response
positive regulation of interle...
regulation of small GTPase med...
innate immune response
response to lipopolysaccharide
response to virus
mRNA splicing, via spliceosome
G1/S transition of mitotic cel...
mitotic sister chromatid segre...
cell division
mitotic spindle organization
mitotic cell cycle
chromosome segregation
wound healing
cytoplasmic translation
translation
autophagy
rRNA processing
G1/S transition of mitotic cel...
mitotic sister chromatid seg
cell division
mitotic spindle organization
mitotic cell cycle
chromosome segregation
ATRA

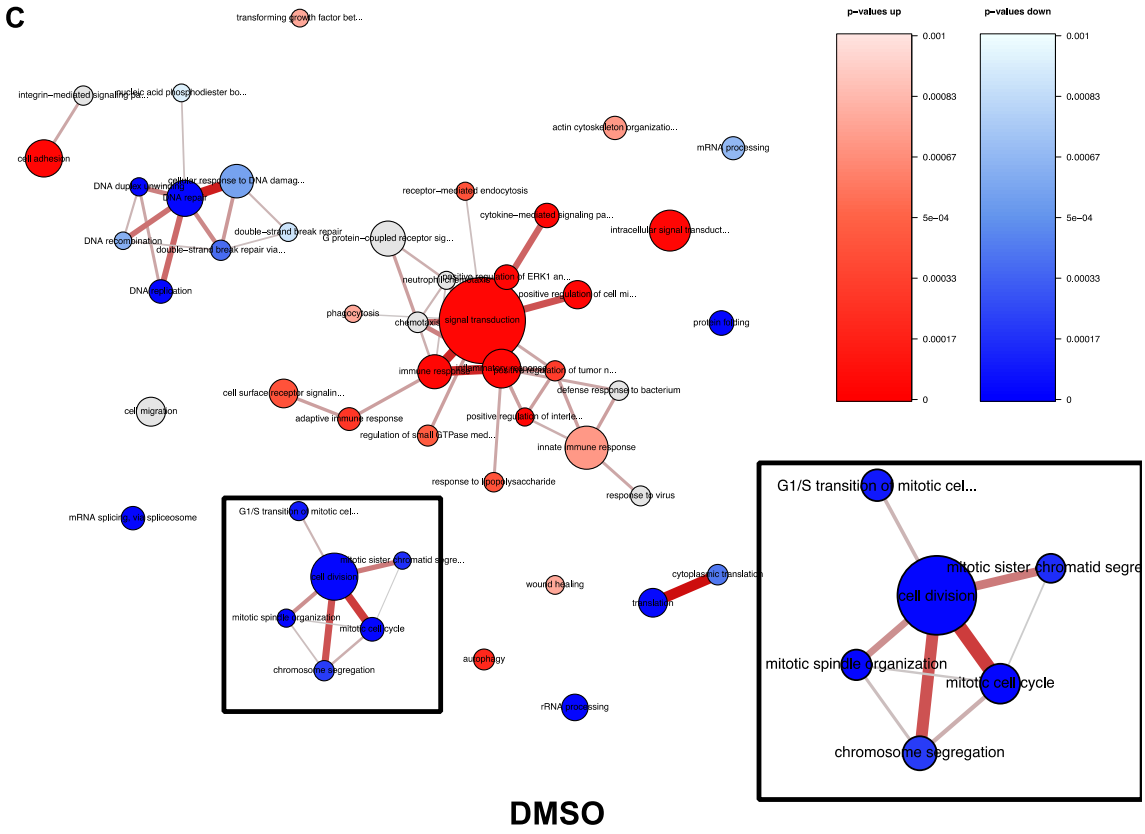
C
p−values up
p−values down
0.001
0.00083
0.00067
5e−04
0.00033
0.00017
0
transforming growth factor bet...
integrin−mediated signaling pa...
cell adhesion
actin cytoskeleton organizatio...
mRNA processing
cellular response to DNA damag...
receptor−mediated endocytosis
cytokine−mediated signaling pa...
intracellular signal transduct...
double−strand break repair
G protein−coupled receptor sig...
DNA recombination
double−strand break repair via...
positive regulation of cell mi...
phagocytosis
protein folding
cell surface receptor signalin...
defense response to bacterium
cell migration
adaptive immune response
positive regulation of interle...
innate immune response
response to lipopolysaccharide
response to virus
mRNA splicing, via spliceosome
G1/S transition of mitotic cel...
mitotic sister chromatid segre...
cell division
mitotic spindle organization
mitotic cell cycle
chromosome segregation
wound healing
cytoplasmic translation
translation
autophagy
rRNA processing
DMSO

Figure 10. ATRA and DMSO activate distinct neutrophil differentiation pathways in HL-60 cells.

Differential gene expression analysis was conducted for RNA-Seq data from GEO (GSE103706 and GSE93996) comparing ATRA- and DMSO-differentiated HL-60 cells. (A) Overlap in upregulated and downregulated genes was compared between the two differentiation stimuli with the minimum cut off being a $\log_2$ fold change of ± 1 and FDR-adjusted $p<0.01$. Group union networks were generated for gene ontology terms covering biological processes and were compared between (B) ATRA and (C) DMSO treatment groups. Red nodes represent upregulated terms while blue nodes are downregulated. The color intensity reflects the p-value of the up or downregulation, with darker colors having a smaller p-value.

Table 3. Transcription factors predicted to bind to the *LGALS12* promoter region with opposing changes in gene expression between ATRA and DMSO-differentiated HL-60 cells when comparing to control cells.

Transcription Factor	**ATRA (log_2FC)**	**DMSO (log_2FC)**
RXRA	-1.18	1.07
NR3C1	-0.09	1.61
TFAP2A	-0.92	0.33
MIB2	-0.12	1.35
NFE2	-0.55	0.82
SREBF1	0.39	-2.54
FOSL1	0.28	-1.88
RUNX3	1.71	-0.90
SAP30	-1.76	0.31
TBL1XR1	0.45	-0.63

3.1.5 Examining the roles of RXR-α, SREBP1 and SP1 in *LGALS12* transcriptional regulation

My next objective was to examine the potential transcriptional regulation of *LGALS12* within the two phenotypes of neutrophilic differentiation. Following the differential gene expression analysis of RNA-seq data from GEO, three transcription factors (*RXRA*, *SP1*, and *SREBP1*) were selected for further examination. Selection was based on overall transcript level, magnitude of change in expression observed, and other preliminary work. RT-qPCR analysis further supported that the gene expression of RXR-α (*RXRA*) significantly differed between ATRA- and DMSO-differentiated HL-60 cells ($p<0.05$) where it was upregulated 4.1-fold only in the case of DMSO (**Figure 11A**). However, treatment with RXR-α antagonist HX 531 at concentrations of 250-1000 nM for 24 hours resulted in no significant changes in *LGALS12* expression (**Figure 11B**). Similarly, cells were treated with RXR-α agonist CD3254 for 24 hours which resulted in a small but significant increase (1.7-fold, $p<0.05$) in *LGALS12* expression at 500 nM with no significant changes observed at other tested concentrations (**Figure 11D**). Both agents induced significant changes in the expression of neutrophilic differentiation marker *NCF1* (**Figure 11C, 11E**). A significant decrease (2.3-fold, $p<0.01$) in *NCF1* expression was observed in cells treated with 1000 nM of HX 531 while a significant increase (9.3-fold, $p<0.01$) was observed in those treated with 1000 nM of CD3254.

Next, the expression of transcription factor SREBP1 (*SREBF1*) was compared between ATRA- and DMSO-differentiated cells (**Figure 12A**). DMSO treatment resulted in a significant drop in expression compared to both control (8.0-fold, $p<0.01$) and ATRA cells ($p<0.01$). Subsequently, betulin was used as an inhibitor of SREBP1 to test the potential role this transcription factor plays in *LGALS12* regulation (**Figure 12B**). Treatment with 10 µM betulin resulted in a significant increase in *LGALS12* (2.9-fold, $p<0.01$) expression with a non-significant but dose-dependent increase being observed at lower concentrations. Betulin also led to a significant increase in *NCF1* expression at 10 µM (5.9-fold, $p<0.0001$) (**Figure 12C**). Finally, the expression of transcription factor SP1 (*SP1*) was compared between ATRA- and DMSO-differentiated cells (**Figure 13A**). DMSO led to a significant

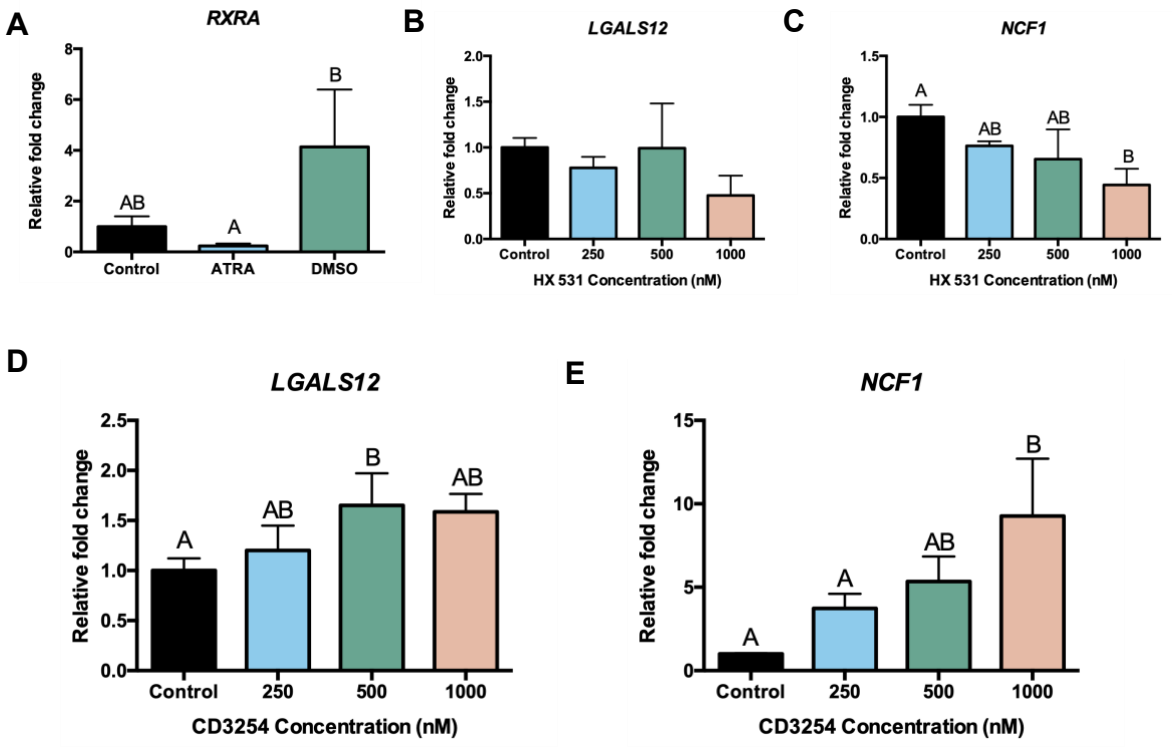

Figure 11. RXR-α is not involved in *LGALS12* transcriptional regulation based on agonist/antagonist effects.

(A) RT-qPCR was conducted to evaluate the gene expression of RXR-α (*RXRA*) between ATRA- and DMSO-differentiated cells. HL-60 cells were treated with RXR-α agonist CD3254 and antagonist HX 531 at various concentrations for 24 h and gene expression of (B, D) *LGALS12* and (C, E) neutrophilic differentiation marker *NCF1* were measured through RT-qPCR using the Livak method ($2^{-\Delta\Delta CT}$) with *ACTB* as a reference gene. Data are presented as mean ± SD, n=3. Significant differences are represented as different letters for treatments, where $p<0.05$ and were determined using one-way ANOVA with Tukey's multiple comparisons test.

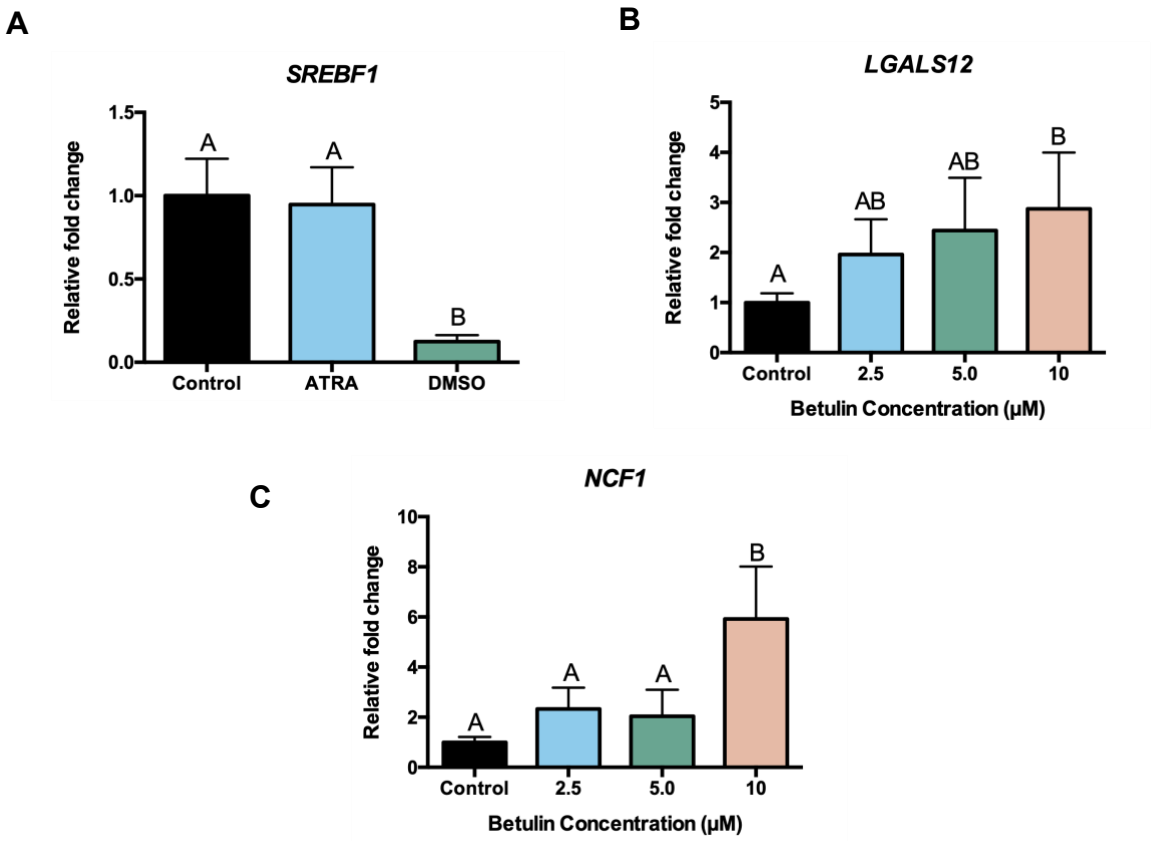

Figure 12. SREBP1 is potentially involved in *LGALS12* transcriptional regulation based on upregulation observed with betulin.

(A) RT-qPCR was conducted to evaluate the gene expression of SREBP1 (*SREBF1*) between ATRA- and DMSO-differentiated cells. HL-60 cells were treated with SREBP1 pharmacological inhibitor betulin at various concentrations for 24 h and gene expression of (B) *LGALS12* and (C) neutrophilic differentiation marker *NCF1* were measured through RT-qPCR using the Livak method ($2^{-\Delta\Delta CT}$) with *ACTB* as a reference gene. Data are presented as mean ± SD, n=3-5. Significant differences are represented as different letters for treatments, where $p<0.05$ and were determined using one-way ANOVA with Tukey's multiple comparisons test.

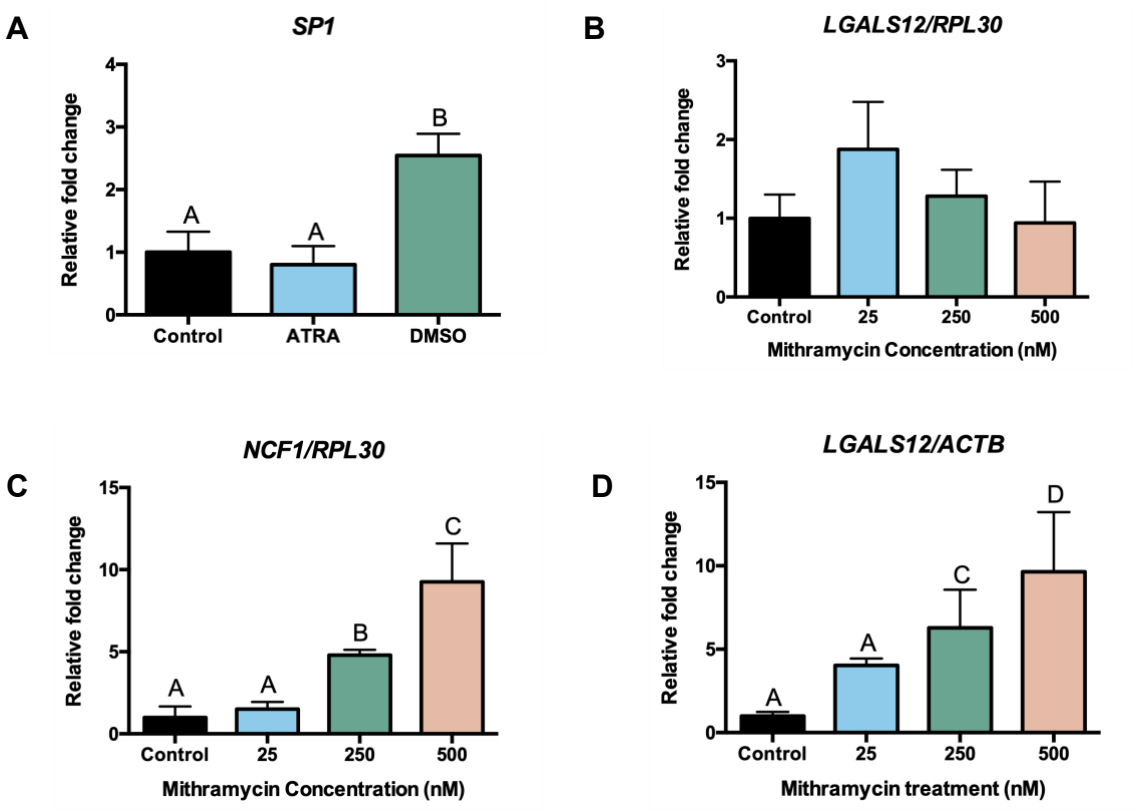

Figure 13. SP1 inhibitor mithramycin does not have an effect on *LGALS12* expression.

(A) RT-qPCR was conducted to evaluate the gene expression of SP1 (*SP1*) between ATRA- and DMSO-differentiated cells. HL-60 cells were treated with SP1 inhibitor mithramycin at various concentrations for 24 h and gene expression of (B) *LGALS12* and (C) neutrophilic differentiation marker *NCF1* were measured through RT-qPCR using the Livak method ($2^{-\Delta\Delta CT}$) with *RPL30* as a reference gene. (D) Mithramycin was observed to destabilize β-actin (*ACTB*) making it an unsuitable reference gene as it artificially elevated relative *LGALS12* expression. Data are presented as mean ± SD, n=3. Significant differences are represented as different letters for treatments, where $p<0.05$ and were determined using one-way ANOVA with Tukey's multiple comparisons test.

upregulation in *SP1* expression (2.5-fold, $p<0.01$), while ATRA did not produce a significant change in expression. Next, HL-60 cells were treated with known SP1 inhibitor mithramycin for 24 hours (**Figure 13B, 13C**). Mithramycin did not produce any significant changes in *LGALS12* expression, however it did induce a significant dose-dependent upregulation of neutrophilic differentiation marker *NCF1* with the highest increase observed at 500 nM (9.3-fold, $p<0.001$). It should be noted that mithramycin caused a destabilization of the initial reference gene used β-actin (*ACTB*) leading to an artificial upregulation of *LGALS12* (**Figure 13D**). Caution should be taken when selecting housekeeping/reference genes when used alongside mithramycin.

3.2 Characterizing galectin-12 secretion

3.2.1 Galectin-12 secretion is blocked by neutrophil-like differentiation

Following the genetic and transcriptional examination of *LGALS12*, the next aim was to evaluate galectin-12 at the protein level and its secretion out of HL-60 cells. All commercially available galectin-12 antibodies that were tested by western blot analysis either did not produce protein bands or did not produce the proper protein size (**Appendix – Figure 1S**), therefore both intracellular and secreted galectin-12 were measured through ELISA (detection range 0.31-20 ng/mL). ELISA was performed using cell supernatant and lysates for analysis of secreted and intracellular galectin-12, respectively. Galectin-12 was shown to be secreted out of HL-60 cells in a time-dependent manner becoming detectable at the six hour mark when using an initial cell concentration of $0.6x10^6$ cells/mL (**Figure 14A**). Galectin-12 secretion was fairly low as one of the control values fell below the minimal ELISA detection limit (0.18 ng/mL). Intracellularly, galectin-12 was significantly upregulated with DMSO ($p<0.05$) compared to control cells while ATRA-treated cells were not significantly different at 72 hours (**Figure 14B**). Remarkably, both ATRA and DMSO-induced differentiation led to a complete and significant ($p<0.05$) inhibition of galectin-12 secretion after 48 hours (**Figure 14C**). My next objective was to evaluate the role of *O*-GlcNAcylation in the regulation of galectin-12 secretion. Treatment with inhibitors of *O*-GlcNAc cycle components (AC, DON, TG) did not significantly alter intra-

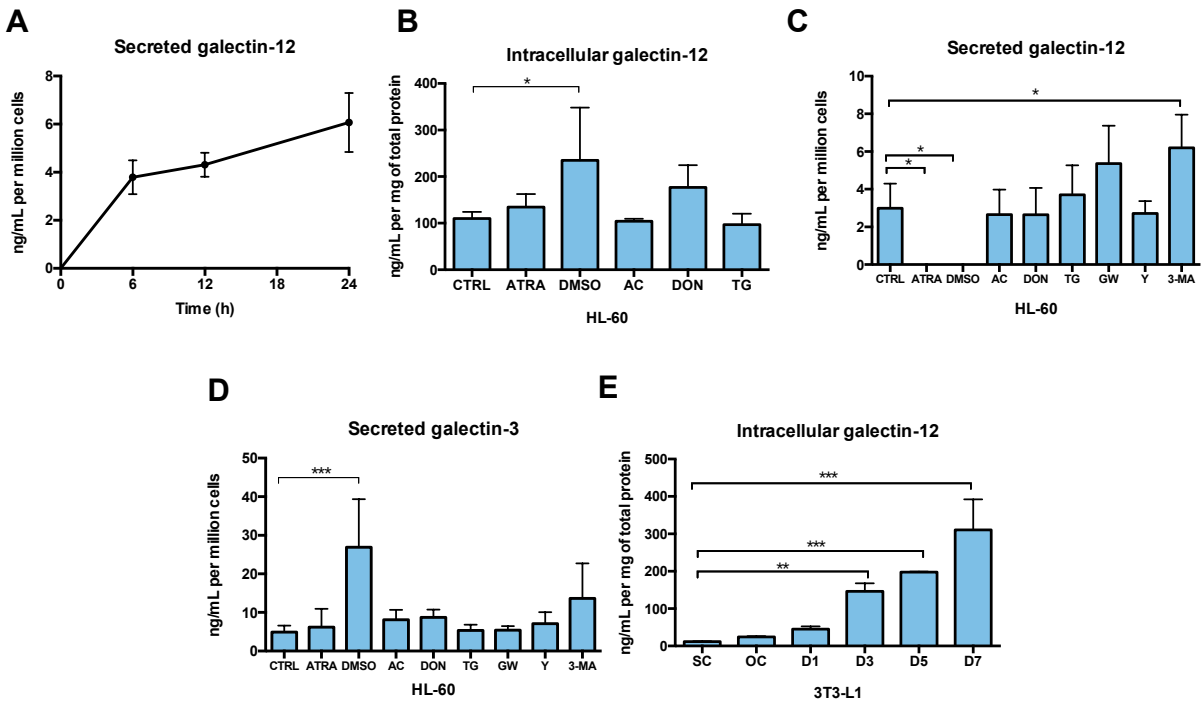

Figure 14. Galectin-12 secretion is blocked by neutrophil-like differentiation and is not sensitive to changes in *O*-GlcNAcylation.

(A) Time-dependent secretion of galectin-12 in HL-60 cells over a 24 h period was measured using ELISA. HL-60 cells were treated for 48-72 h with differentiation agents (1 µM ATRA, 1.3% DMSO), inhibitors of *O*-GlcNAc cycle enzymes (40 µM AC, 12.5 µM DON, 10 µM TG) and inhibitors of unconventional secretion pathways (20 µM GW4689, 10 µM Y-27632, 2 mM 3-MA) where (B) intracellular galectin-12, (C) secreted galectin-12 and (D) secreted galectin-3 were measured. (E) Intracellular galectin-12 levels were measured in mouse 3T3-L1 cells that were subconfluent (SC), overconfluent (OC) and between days one to seven of differentiation (D1-D7). Data are presented as mean ± SD, n=3-4. One-way ANOVA with Dunnett's multiple comparisons test was conducted where each treatment group was compared against the control. Significant differences are represented as * $p<0.05$, ** $p<0.01$, *** $p<0.001$, *** $p<0.0001$.

cellular or secreted galectin-12 levels (**Figure 14B, 14C**). Given that galectins are secreted through unconventional mechanisms, my third objective was to evaluate the role of extracellular vesicles in the secretion of galectin-12. Inhibitors of exosome (20 μM GW4869) and microvesicle (10 μM Y-27632) formation both led to no significant changes in galectin-12 secretion (**Figure 14C**). Unexpectedly, treatment with inhibitor of secretory autophagy 3-MA (2 mM) resulted in a significant increase of galectin-12 secretion ($p<0.05$). It should be noted that extended exposure to 3-MA in nutrient-rich conditions can instead increase autophagic flux (Wu et al., 2010).

Galectin-3 secretion at 48 hours was also measured (detection range 58.8-2000 pg/mL) to serve as a reference point for the magnitude of galectin-12 secretion (**Figure 14D**). In untreated HL-60 cells, galectin-3 secretion was approximately 2-fold higher than that of galectin-12. Galectin-3 secretion was observed to be significantly elevated under DMSO-induced differentiation ($p<0.001$) while ATRA produced no significant changes. Inhibitors of *O*-GlcNAc cycle enzymes and unconventional secretion did not significantly alter galectin-3 secretion.

Finally, intracellular and secreted galectin-12 were measured in mouse 3T3-L1 pre-adipocyte cells undergoing differentiation to serve as a positive control (Yang et al., 2004; Yang et al., 2011). Indeed, upon induction of adipocytic differentiation intracellular galectin-12 was significantly ($p<0.0001$) increased at three to five days of differentiation (**Figure 14E**). Galectin-12 secretion was negligible with all samples falling below the minimal detection limit (18.75 pg/mL).

3.2.2 Adipocytic differentiation induces an increase in lipid droplet content and galectin-12

My next objective was to evaluate the potential role of lipid droplets in the regulation of galectin-12 secretion. Mouse 3T3-L1 cells were used as a positive control for galectin-12 upregulation. 3T3-L1 cells were differentiated into adipocytes and the accumulation of lipid droplets was observed using brightfield (oil red O) and fluorescence (BODIPY 493/503) microscopy (**Figure 15A**). Undifferentiated 3T3-L1 cells at a subconfluent pre-

adipocyte state had no observable lipid droplet staining with oil red O and only background staining with BODIPY 493/503. At day five of differentiation, clusters of lipid droplets can be observed in red for oil red O stained cells and in green surrounding the perimeter of DAPI-stained blue nuclei in BODIPY 493/503 stained cells. In parallel, *Lgals12* expression was measured with a significant 2905-fold upregulation ($p<0.0001$) observed at day four of adipocyte differentiation when comparing to subconfluent (SC) and overconfluent (OC) cells (**Figure 15B**). Expression of adipocytic differentiation marker *Fabp4* was also significantly upregulated 204-fold ($p<0.0001$) when comparing to subconfluent cells (**Figure 15C**). 3T3-L1 cells differentiated for one day or for seven days were compared and a significant decrease ($p<0.01$) in global *O*-GlcNAcylation levels was observed at seven days (**Figure 15D**).

3.2.3 Neutrophil-like differentiation increases intracellular lipid droplet content in HL-60 cells

Gene set enrichment analysis for lipid-related gene ontology terms was conducted using RNA-Seq data from GEO covering ATRA- and DMSO-differentiated HL-60 cells (**Table 4**). There were seven gene ontology terms that were significantly ($p<0.05$) enriched with both ATRA and DMSO, while an additional six and nine terms were enriched with ATRA or DMSO only, respectively (**Figure 16**). Two of the seven mutually enriched terms included ‘response to lipid’ and ‘regulation of lipase activity’. Thus, it was then necessary to determine whether differentiated HL-60 cells experience an increase of lipid droplet content similar to 3T3-L1 cells. Intracellular lipid droplets in differentiated HL-60 cells were stained with BODIPY 493/503 and imaged using fluorescence microscopy (**Figure 17A**). The average number of lipid droplets per cell were determined using ImageJ and compared between ATRA and DMSO-differentiated HL-60 cells (**Figure 17B**). A significant increase ($p<0.05$) in the number of lipid droplets per cell was observed in DMSO-differentiated cells while a small non-significant ($p=0.644$) increase was observed with ATRA. Flow cytometry with BODIPY 493/503 was conducted to further validate the observed increase in lipid droplet content. Once again, DMSO-differentiated cells demonstrated a significant increase ($p<0.05$) in the total percentage of medium (mean GFP fluorescence intensity of 10^5-10^6 on biex scale) and high (10^6-10^7 intensity) fluorescence

cells compared to untreated cells, but ATRA-differentiated cells did not (**Figure 17C, 17D**). Next, I wanted to determine whether a change in lipid droplet accumulation independent of neutrophilic differentiation can have an impact on galectin-12. HL-60 cells were treated with oleic acid or isoproterenol for 48 h to stimulate or inhibit lipid droplet production, respectively (**Figure 17E, 17F**). Treatment with oleic acid significantly ($p<0.001$) increased galectin-12 secretion compared to untreated cells and significantly decreased ($p<0.05$) intracellular galectin-12. Treatment with isoproterenol showed no significant differences compared to untreated cells for both intracellular and secreted levels of galectin-12.

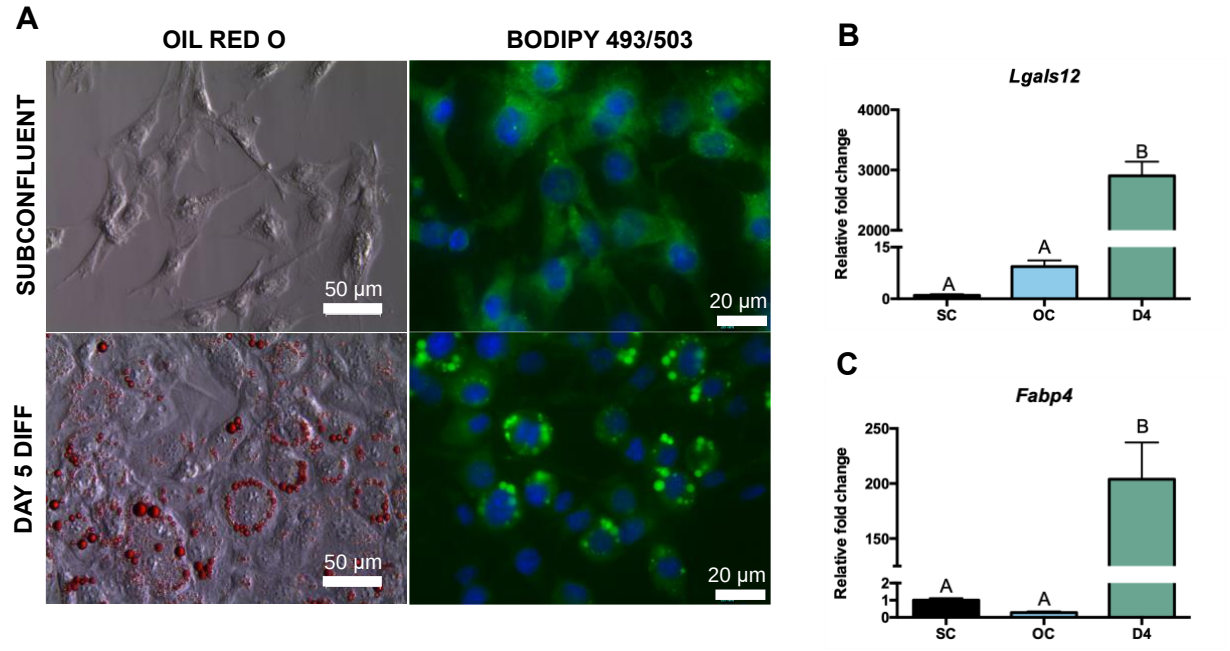
A
OIL RED O
BODIPY 493/503
SUBCONFLUENT
DAY 5 DIFF
50 µm
20 µm
50 µm
20 µm
B
Lgals12
Relative fold change
4000
3000
2000
15
0
A
A
B
SC
OC
D4
C
Fabp4
Relative fold change
250
200
150
2
1
0
A
A
B
SC
OC
D4

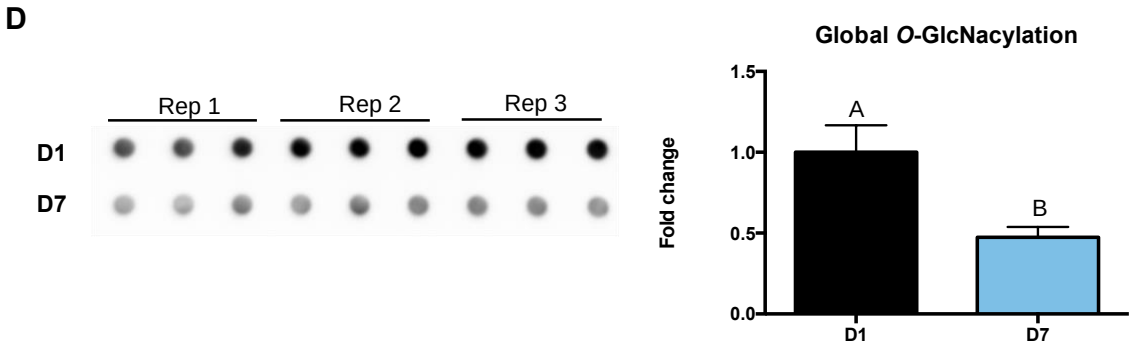
D
Rep 1
Rep 2
Rep 3
D1
D7
Global O-GlcNacylation
Fold change
1.5
1.0
0.5
0.0
A
B
D1
D7

Figure 15. Adipocyte differentiation of 3T3-L1 cells leads to an increase in *Lgals12* expression and lipid droplet content.

(A) Intracellular neutral lipids were stained using oil red O and BODIPY 493/503 in undifferentiated 3T3-L1 cells and those that were differentiated into adipocytes for five days. Oil red O staining was observed in red using brightfield IMC microscopy, while BODIPY 493/503 (green) was observed through fluorescence microscopy alongside DAPI-stained cell nuclei (blue). (B) *Lgals12* and (C) *Fabp4* gene expression were measured in 3T3-L1 cells that were subconfluent (SC), overconfluent (OC) and differentiated for four days through RT-qPCR using the Livak method ($2^{-\Delta\Delta CT}$) with *Gapdh* as a reference gene. (D) Global *O*-GlcNAcylation levels were quantified from an immunodot blot for 3T3-L1 cells at day 1 (D1) and day 7 (D7) of adipocyte differentiation. Data are presented as mean ± SD, n=3. Significant differences are represented as different letters for treatments, where $p<0.05$ and were determined using one-way ANOVA with Tukey's multiple comparisons test or with an unpaired t-test.

Table 4. Significantly enriched lipid gene ontology terms in differentiated HL-60 cells.

GO ID	Name	GO	NES	AdjP
ATRA				
GO:004512	membrane raft	CC	2.03	4E-06
GO:004801	inositol lipid-mediated signaling	BP	2.08	2E-05
GO:004646	membrane lipid catabolic process	BP	2.01	0.004
GO:003399	response to lipid	BP	1.47	0.005
GO:004355	regulation of lipid kinase activity	BP	1.90	0.005
GO:190595	positive regulation of lipid localization	BP	1.81	0.014
GO:190595	regulation of lipid localization	BP	1.68	0.02
GO:009021	positive regulation of lipid kinase	BP	1.78	0.032
GO:006019	regulation of lipase activity	BP	1.68	0.034
GO:006019	negative regulation of lipase activity	BP	1.76	0.034
GO:007139	cellular response to lipid	BP	1.40	0.034
GO:001991	lipid storage	BP	1.65	0.034
GO:007172	lipopeptide binding	MF	1.58	0.034
DMSO				
GO:004512	membrane raft	CC	2.15	9E-08
GO:000042	autophagosome membrane	CC	2.24	1E-04
GO:000664	phospholipid metabolic process	BP	1.73	1E-04
GO:004648	glycerolipid metabolic process	BP	1.70	2E-04
GO:000865	phospholipid biosynthetic process	BP	1.65	0.002
GO:000664	membrane lipid metabolic process	BP	1.60	0.011
GO:001629	lipase activity	MF	1.69	0.011
GO:003399	response to lipid	BP	1.36	0.011
GO:004501	glycerolipid biosynthetic process	BP	1.55	0.011
GO:004646	membrane lipid catabolic process	BP	1.88	0.011
GO:004801	inositol lipid-mediated signaling	BP	1.63	0.011
GO:007172	lipopeptide binding	MF	1.63	0.018
GO:004355	regulation of lipid kinase activity	BP	1.65	0.029
GO:006019	regulation of lipase activity	BP	1.65	0.029
GO:009021	negative regulation of lipid kinase	BP	1.73	0.045
GO:014035	lipid import into cell	BP	-1.67	0.049

Note: NES=Normalized enrichment score.

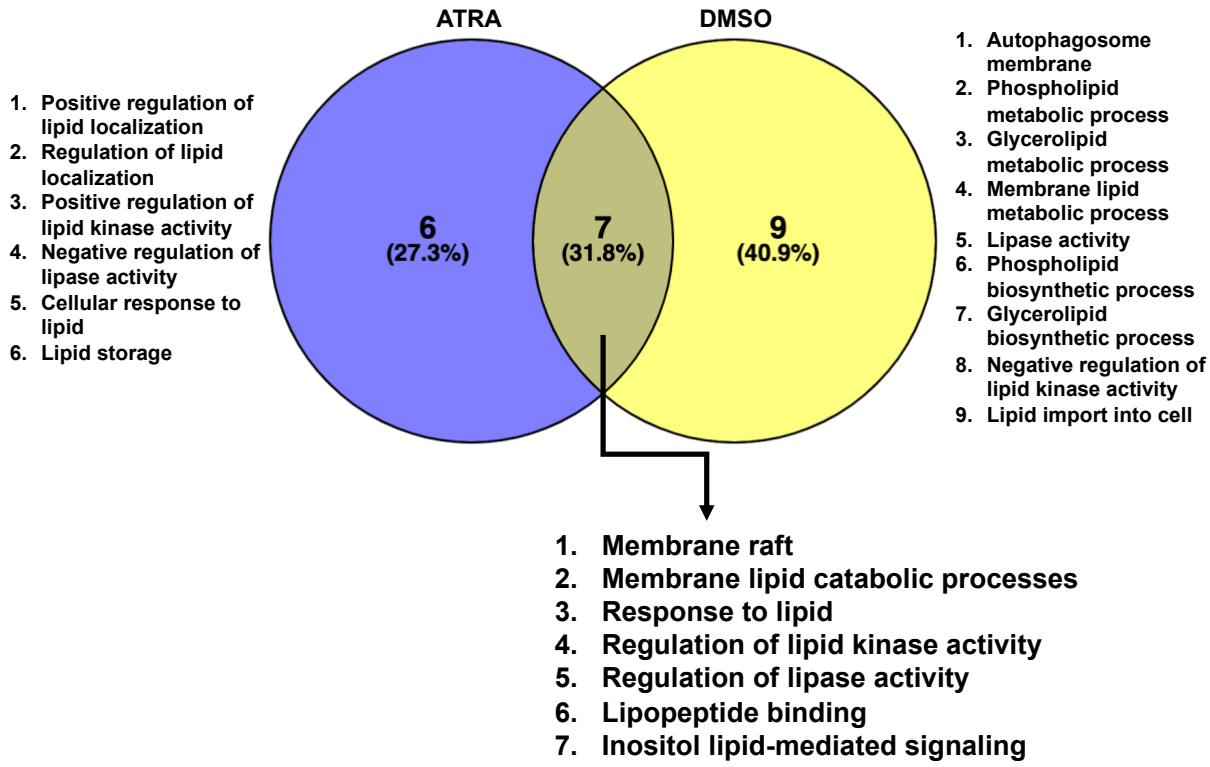

Figure 16. Lipid-related gene ontology terms are enriched upon ATRA- and DMSO-induced differentiation.

Gene set enrichment analysis of all gene ontology terms related to the keyword ‘lipid’ was conducted using RNA-Seq data from GEO (GSE103706 and GSE93996). Expression of HL-60 cells differentiated with ATRA and DMSO were compared to untreated cells. A minimum p-value cut off of $p<0.05$ was used.

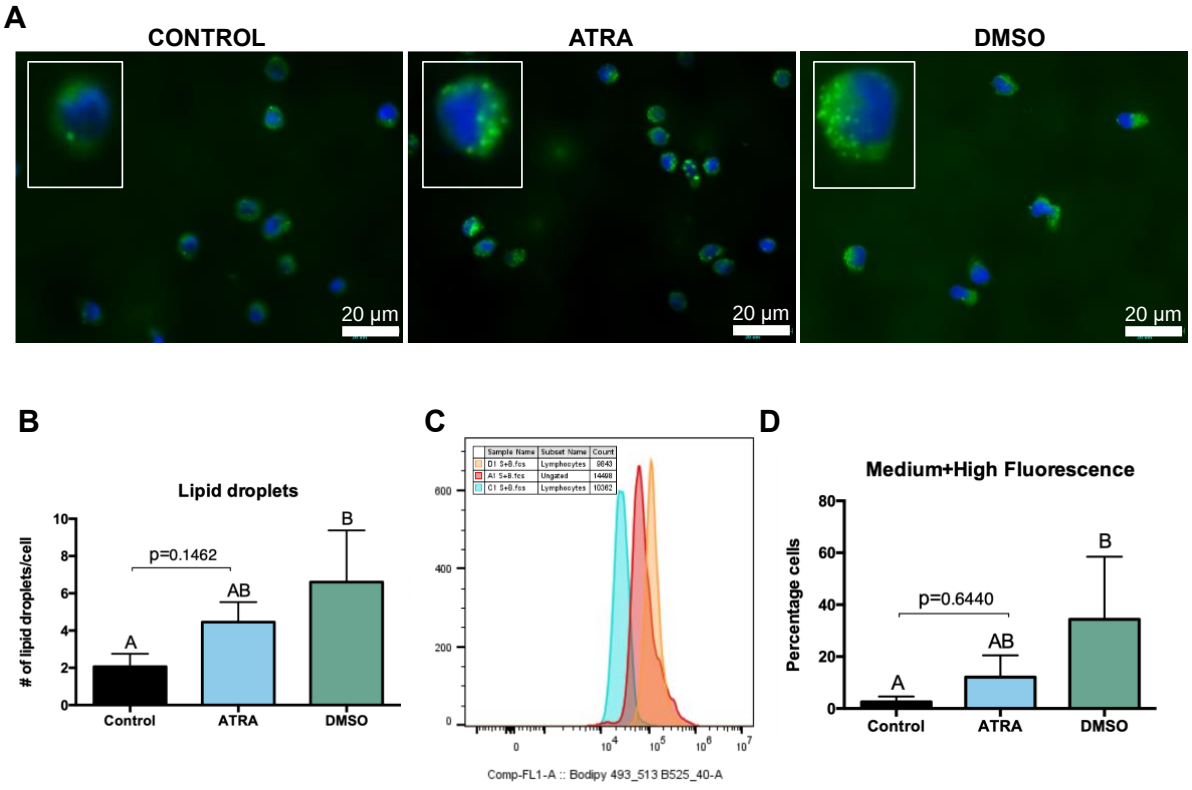
A
CONTROL
ATRA
DMSO
20 µm
20 µm
20 µm
B
Lipid droplets
# of lipid droplets/cell
p=0.1462
A
AB
B
Control
ATRA
DMSO
C
Comp-FL1-A :: Bodipy 493_513 B525_40-A
D
Medium+High Fluorescence
Percentage cells
p=0.6440
A
AB
B
Control
ATRA
DMSO
E
Secreted galectin-12
ng/mL per million cells
***
Control
Oleic Acid
Isoproterenol
F
Intracellular galectin-12
ng/mL per mg of total protein
*
Control
Oleic Acid
Isoproterenol

Figure 17. Neutrophil-like differentiation of HL-60 cells results in increased lipid droplet content.

(A) Intracellular neutral lipids were stained using BODIPY 493/503 in HL-60 cells that were differentiated with ATRA or DMSO for 72 h and imaged using fluorescence microscopy using a 40x objective lens. (B) The number of lipid droplets per cell were measured in ImageJ. (C, D) BODIPY 493/503 fluorescence was compared between undifferentiated and ATRA/DMSO-differentiated cells using flow cytometry. (E) Secreted and (F) intracellular levels of galectin-12 were measured through ELISA for HL-60 cells treated with 100 µM oleic acid or 10 µM isoproterenol for 48 h. Data are presented as mean ± SD, n=3. Significant differences in (B) and (D) are represented as different letters for treatments, where $p<0.05$ and were determined using one-way ANOVA with Tukey's multiple comparisons test. For ELISA data, one-way ANOVA with Dunnett's multiple comparisons test was conducted where each treatment group was compared against the control. Significant differences are represented as * $p<0.05$, ** $p<0.01$, *** $p<0.001$, *** $p<0.0001$.

3.3 Differentiation with ATRA leads to an increase in *LGALS12* in MDA-MB-231 cells

My last objective was to examine the levels of *LGALS12* in various breast cancer cell lines upon differentiation with ATRA. Galectin-12 gene expression was measured in four different breast cancer cell lines covering three different breast cancer subtypes. MCF-7 (luminal A subtype), SK-BR-3 (HER2-enriched), MDA-MB-231 (triple negative – basal B), and MDA-MB-468 (triple negative – basal A) cells were treated with ATRA for 72 hours. Untreated MCF-7 cells had negligible levels of *LGALS12* detected while the other three cell lines had low expression (**Figure 18A**). However, differentiation with ATRA for 72 hours induced a significant 57-fold ($p<0.0001$) upregulation of *LGALS12* in MDA-MB-231 cells (**Figure 18B**). The remaining cell lines did not show any significant changes in *LGALS12* expression. Intracellular galectin-12 in MDA-MB-231 cells was measured through ELISA and demonstrated a non-significant ($p=0.1541$) increase after treatment with ATRA (**Figure 18C**). Secretion of galectin-12 was negligible in both untreated and ATRA-treated cells with all samples falling below the minimal detection limit (0.18 ng/mL). MDA-MB-231 cells also developed a flattened morphology with the cell extensions becoming less pronounced (**Figure 18D**). ICAM-1 (*ICAM1*) was used as a marker for differentiation and was found to be significantly upregulated in MDA-MB-231 cells (12.2-fold, $p<0.05$) and SK-BR-3 cells (6.9-fold, $p<0.0001$) upon treatment with ATRA (**Figure 18E**). Global *O*-GlcNAcylation levels were also measured and a minor non-significant ($p=0.2026$) decrease was observed in ATRA-treated cells (**Figure 18F).**

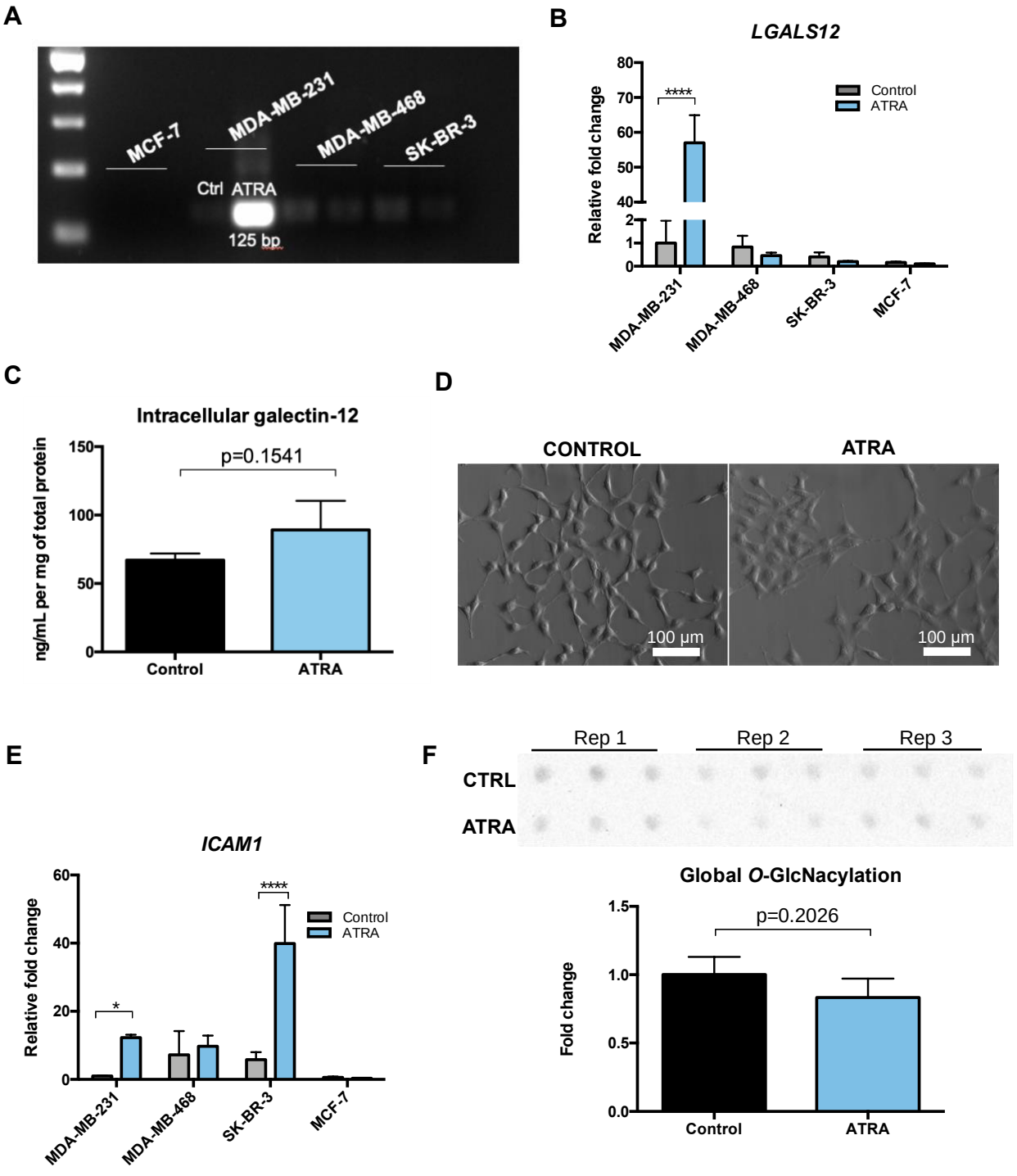
A
MCF-7
MDA-MB-231
MDA-MB-468
SK-BR-3
Ctrl ATRA
125 bp
B
LGALS12
Relative fold change
****
Control
ATRA
MDA-MB-231
MDA-MB-468
SK-BR-3
MCF-7
C
Intracellular galectin-12
ng/mL per mg of total protein
p=0.1541
Control
ATRA
D
CONTROL
ATRA
100 µm
100 µm
E
ICAM1
Relative fold change
*
****
Control
ATRA
MDA-MB-231
MDA-MB-468
SK-BR-3
MCF-7
F
Rep 1
Rep 2
Rep 3
CTRL
ATRA
Global O-GlcNacylation
Fold change
p=0.2026
Control
ATRA

Figure 18. Differentiation with ATRA induces an upregulation of *LGALS12* in MDA-MB-231 cells.

Four breast cancer cell lines were treated with 1 µM ATRA for 72 hours and *LGALS12* was measured through (A) endpoint PCR and (B) RT-qPCR using the Livak method ($2^{-\Delta\Delta CT}$) with *ACTB* as a reference gene. (C) Intracellular galectin-12 in MDA-MB-231 cells was measured through ELISA **(**D) MDA-MB-231 cell morphology was examined using brightfield IMC microscopy. (E) Differentiation marker ICAM-1 (*ICAM1*) expression was measured in all cell lines. (F) Global *O*-GlcNAcylation levels were measured using an immunodot blot for MDA-MB-231 cells treated with ATRA and compared relative to untreated cells. Data are presented as mean ± SD, n=3. Two-way ANOVA with Sidak's multiple comparisons test was conducted within each cell line where significant differences are represented as * $p<0.05$, ** $p<0.01$, *** $p<0.001$, *** $p<0.0001$.

Chapter 4

4 Discussion

This study aimed to investigate the role of galectin-12 in two distinctive cell differentiation models. My findings indicate that ATRA and DMSO produce different phenotypes of neutrophil-like HL-60 cells with unique gene expression profiles. *LGALS12* was found to be differentially expressed between these two phenotypes which could allow it to serve as a marker to distinguish these phenotypes. These cells also differed in their functional response to fMLP and digitonin and the expression of certain nuclear envelope genes like lamin A/C and LBR. The role of three putative transcription (RXR-α, SP1 and SREBP1) factors in *LGALS12* regulation were also assessed using chemical inhibitors.

Next, I demonstrated that galectin-12 activity is *O*-GlcNAc-independent as treatment with inhibitors of *O*-GlcNAc cycle enzymes did not produce any change in intracellular/secreted galectin-12 levels. I also showed that neutrophil-like differentiation blocked the secretion of galectin-12 out of HL-60 cells which was accompanied by an increase in lipid droplet accumulation. Directly targeting lipid droplet formation using oleic acid and isoproterenol found that galectin-12 secretion is likely not dependent on lipid droplets and that the decrease in secretion during differentiation occurs through other mechanisms. The mechanism of galectin-12 secretion is still unknown as inhibitors of both exosome and microvesicle formation did not produce any effect. However, secretory autophagy inhibitor 3-MA increased galectin-12 secretion suggesting a potential role of this pathway.

Finally, I aimed to characterize *LGALS12* expression in breast cancer cell lines upon ATRA-induced differentiation. *LGALS12* in four breast cancer cell lines (MDA-MB-231, MDA-MB-468, SK-BR-3, MCF-7) was assessed after treatment with ATRA to reverse EMT and induce differentiation. I revealed that MDA-MB-231 cells experience an increase in *LGALS12* expression upon ATRA treatment which was accompanied by an increase in differentiation marker *ICAM1*. These early findings suggest that the activity of galectin-12 differs between various molecular subtypes of breast cancer and that it may serve as a

tumor suppressor gene. Overall, my study findings demonstrate that galectin-12 is involved in the regulation of differentiation of leukemia and breast cancer cell lines.

4.1 Interpretation

4.1.1 ATRA- and DMSO-induced neutrophil-like HL-60 cells vary in gene expression profiles.

ATRA and DMSO are two well-established models of inducing neutrophil-like differentiation in HL-60 cells. In this study, both agents produced cells that exhibited the key characteristics of neutrophilic differentiation. This includes cells which developed lobulation of the nucleus, a drop in global *O*-GlcNAcylation, upregulation of *NCF1*/*NCF2,* and generation of hydrogen peroxide. However, the pathways of differentiation used are distinct, converging at a later point which results in gene expression profiles that vary. Although both agents produce terminally differentiated neutrophil-like cells, the expression of galectin-12 is opposite between the two models. ATRA-induced differentiation led to an upregulation of *LGALS12* while DMSO led to a downregulation which matches the previously observed contradictory findings in the literature (Xue et al., 2016; Vinnai et al., 2017; McTague et al., 2022). This suggests that there are different signaling pathways at play and that the transcription regulation of galectin-12 varies depending on how neutrophilic differentiation is induced.

My first objective was to study the molecular mechanisms and transcriptional regulation governing galectin-12 expression in HL-60 cells under two neutrophilic differentiation models. I began by comparing the gene expression profiles of the two differentiation models using existing RNA-Seq data. DMSO-differentiated cells had more DEGs than with ATRA. There was also overlap of DEGs between the two phenotypes, reflecting that both agents have differentiation mechanisms that converge at a certain point. However, there were more DEGs that were uniquely associated with DMSO, and fewer that were unique to ATRA only. These findings suggest that the ATRA-induced pathway of differentiation is more streamlined while DMSO produces an effect on a wider range of processes. ATRA binds directly to nuclear RAR resulting in the formation of a heterodimer

with RXR. This RAR-RXR heterodimer binds to specific cis-acting DNA sites known as RAREs within the promoter region of target genes (Lawson and Berliner, 1999). One target gene is p21 which inhibits cyclin D/CDK2 and causes cell cycle arrest (Mar and Quackenbush, 2009). Other target genes include those relevant to neutrophilic functions.

On the other hand, the manner by which DMSO induces neutrophilic differentiation is still not well-defined, potentially due to the shift in focus to ATRA which has shown high success as a treatment for APL. HL-60 cells control cell cycle progression through the PI3K/Akt pathway involving activation of forkhead transcription factors (Cappellini et al., 2003). DMSO upregulates the tumor suppressor PTEN via NF-κB activation which leads to a decrease in Akt phosphorylation. This reduces phosphorylation of FOXO3 which inhibits its role in cell survival and also causes it to translocate to the nucleus producing an increase in p27 (Lee et al., 2005; Mar and Quackenbush, 2009). Upregulation of p27 seems to be the key factor for both DMSO and vitamin D3-induced G_1/S transition blockade in HL-60 cells (Wang et al., 1996; Mar and Quackenbush, 2009). My GSEA found that processes related to cell division, G_1/S transition, and mitotic cell cycle were all downregulated only in DMSO. Therefore, DMSO has an effect on growth arrest more broadly than ATRA. GSEA found DMSO also downregulated processes related to DNA damage repair, protein folding, and mRNA processing more than ATRA. Recent work found that cell treatment with low-dose (0.1-1.5%) DMSO affects DNA conformation, total nucleic acid content, and protein secondary structure (Tunçer et al., 2018). These off-target effects could produce a wide range of consequences on other cellular processes beyond differentiation initiation.

The gene expression profile of nuclear envelope proteins seems to also vary between the two models. Nuclear lamins compose part of the nuclear envelope where they provide mechanical support and influence nuclear shape through interactions with other cytoskeletal components (Manley et al., 2018). Changes in expression occur during neutrophilic differentiation resulting in a uniquely flexible nucleus. Upon differentiation, LBR is upregulated while lamin A/C and lamin B1 are downregulated which leads to a nucleus that is malleable and lobulated (Olins and Olins, 2004; Manley et al., 2018). LBR in particular is directly linked to lobulation where low expression causes hypolobulation in

those with Pelger-Huët Anomaly (Zwerger et al., 2008). The downregulation of *LBR* and upregulation of *LMNA* in DMSO-differentiated cells may explain why ATRA-differentiated cells had a bigger decrease in both nuclear circularity and roundness than DMSO. DMSO-differentiated cells were not able to develop the same level of segmentation as with ATRA. The strong downregulation of *LMNB2* with both ATRA and DMSO is inconsistent with the literature which states that lamin B2 is stably expressed or even upregulated upon differentiation (Manley et al., 2018). It would be necessary to confirm these findings at the protein level to see if this downregulation goes beyond gene expression.

4.1.2 Defining ATRA- and DMSO-induced phenotypes of neutrophil-like cells

In 2009, a novel model characterizing tumor-associated neutrophils as N1 and N2 was proposed (Fridlender et al., 2009). This model paralleled the terminology used to characterize M1/M2 macrophage polarization creating a simplified approach for describing anti-tumor (N1) and pro-tumor (N2) neutrophils in cancer. This model can be generalized to classify the ATRA and DMSO phenotypes I observed in this study. Classification of ATRA/DMSO phenotypes as pro or anti-tumor can be centered around the following criteria: expression of *LGALS12*, presence of FPR1, and inflammatory potential. The ATRA phenotype can be considered N1 and anti-tumorigenic, with high *LGALS12*, low *FPR1*, and low inflammatory response. In contrast, the DMSO phenotype would be N2 and pro-tumorigenic, with low *LGALS12*, high *FPR1*, and high inflammatory response.

A parallel can be drawn to the role of *LGALS12* in macrophage polarization, where galectin-12 plays a role in neutrophil polarization in the same manner as in macrophages. Knockdown of *LGALS12* led to M2 polarization (Wan et al., 2016), which mirrors what is observed with DMSO producing a downregulation of *LGALS12*. M2 macrophages themselves are considered to be pro-tumorigenic due to their immunosuppressive properties and role in tumor cell proliferation (Boutilier and Elsawa, 2021). Additionally, low *LGALS12* is associated with poorer prognosis in AML while those patients with higher expression had better outcomes (El Leithy et al., 2015). Similar downregulations of

LGALS12 are found in other forms of cancer like CRC and breast carcinoma (Katzenmaier et al., 2017; Tazhitdinova and Timoshenko, 2021). High or ectopic expression of *LGALS12* is also linked to cell cycle inhibition and growth arrest (Hotta et al., 2001; Yang et al., 2001). These points together suggest low *LGALS12* is representative of pro-tumor effects, while high *LGALS12* can have a protective function and regulate proliferation.

Some evidence also points to aging neutrophils being pro-tumorigenic. Mature neutrophils are released from the bone marrow and enter into circulation where they are considered 'fresh' neutrophils. These cells undergo an ageing process where they acquire changes in the expression of surface markers like various chemokine receptors (Ai and Udalova, 2020). Aged neutrophils have been linked to proliferation of tumor cells and promotion of metastasis due to reasons like excessive release of ROS, NETs and metalloproteinases (MMP-9) (Mittmann et al., 2021; Peng et al., 2021). FPR1 is considered a late marker of neutrophilic differentiation (Rincón et al., 2018). Therefore, it can be argued that the DMSO phenotype is more functionally mature and could embody 'aged' neutrophils. Aged neutrophils are often the first line of defense at the site of infection/inflammation being highly reactive with the ability to activate immune responses faster than fresh neutrophils (Uhl et al., 2016). As neutrophils age, their molecular signature changes and they acquire elevated expression of surface markers like toll-like receptor 4 (TLR-4) and macrophage-1 antigen (Mac-1) that help produce higher responsiveness to various stimuli. The actual magnitude of ROS generation does not vary compared to fresh neutrophils but the aged cells phagocytize bacteria more efficiently. In my study, DMSO-differentiated cells generated respiratory burst in response to fMLP, PMA, and digitonin while ATRA-differentiated cells only to PMA. The lack of response in ATRA cells to fMLP is due to the absence of active FPR1 receptors on the cell surface, which was reflected in these cells having less *FPR1* expression than DMSO cells. Digitonin leads to calcium influx which activates PKC signaling but ATRA has been shown to decrease total calcium in the cells upon differentiation (Reiterer and Yen, 2007). Therefore, there is potentially an insufficient level of calcium influx by digitonin to activate PKC and respiratory burst in these cells. My findings support a model where DMSO-differentiated cells have more inflammatory potential than ATRA and act more aged. However, this reasoning could be contested as

previous work has also shown ATRA producing higher phagocytic index and more ROS than DMSO (Sham et al., 1995; Manda-Handzlik et al., 2018).

Another factor linking the DMSO phenotype to pro-tumor effects is the role of FPR1 in cancer. High expression of *FPR1* has been associated with tumorigenesis in certain contexts, albeit *FPR1* is usually only measured in the tumor cells themselves and not tumor-associated neutrophils. In one instance, *FPR1* was found to be elevated in both the colorectal epithelium and tumor-associated neutrophils in CRC patients (Li et al., 2017). Put together, this sets up a model where the DMSO phenotype represents aged neutrophils with potential pro-tumor effects due to high *FPR1*/low *LGALS12*, while the ATRA phenotype are fresh neutrophils that have anti-tumor properties and low *FPR1*/high *LGALS12*.

Some researchers intentionally extend the definition of N1 and N2 neutrophils to the pro- and anti-inflammatory designations used with macrophages. This would then characterize N2 neutrophils are being pro-tumor and anti-inflammatory, which would not match the high inflammatory potential associated with the DMSO phenotype. However, the idea of only anti-inflammation/immunosuppression being linked to pro-tumor effects has been criticized as the role of chronic inflammation is well-established in cancer (Antuamwine et al., 2023). DMSO-differentiated cells being highly reactive can therefore also be considered a pro-tumor feature. One study found that decreasing the number of aged neutrophils in circulation reduced inflammation-related tissue damage in models of sickle cell disease (Zhang et al., 2015).

The model of N1/N2 neutrophils is a simple approach that can serve as a starting point to characterizing the neutrophil-like cells that arise from ATRA- and DMSO-induced differentiation. This attempt at characterization also does not imply that these neutrophil-like cells are the same as those tumor-associated neutrophils observed *in vivo*, but that they could embody certain qualities of them.

4.1.3 Transcriptional regulation of galectin-12

Given that galectin-12 expression varies between ATRA and DMSO phenotypes, my next objective was to determine potential differences in transcriptional regulation. Predicted transcription factors that bind to the promoter region of *LGALS12* were identified and those that had opposite changes in expression after ATRA- and DMSO-induced differentiation were selected for further examination. Three transcription factors were chosen to be targeted with chemical inhibition, SP1 (*SP1*), RXR-α (*RXRA*), and SREBP1 (*SREBF1*).

My findings do not suggest a role of RXR-α and SP1 in galectin-12 transcriptional regulation but do suggest a potential involvement of SREBP1. Both *RXRA* and *SP1* were found to be strongly upregulated in DMSO-induced differentiation but not with ATRA. While treatment with an RXR-α agonist did impact *LGALS12* expression, it did not match the expected gene expression of the DMSO phenotype and no effect was observed with an RXR-α antagonist. In concept, increasing RXR-α activity with an agonist would mimic what was observed with DMSO and therefore lead to a drop in *LGALS12* if this transcription factor is involved in regulation. However, treatment with CD3254 led to an upregulation of *LGALS12* instead alongside *NCF1* upregulation.

RXR-α is both a nuclear receptor and a transcription factor. RXR-α itself is implicated in the initial steps of ATRA-induced differentiation as it forms a heterodimer with RAR that activates downstream signaling. RXR-α is highly abundant in myeloid cells where it is upregulated during differentiation (Lehmann et al., 2001). The observed changes in RXR-α expression within neutrophilic differentiation seem to be inconsistent. Generally, RXR works synergistically with RAR but it may be able to induce neutrophilic differentiation in an RAR-independent manner (Robertson et al., 1992; Benoit, 1999). However, one paper found that RXR-α has to be downregulated during granulocyte colony-stimulating factor (G-CSF)-dependent neutrophil differentiation of myeloid progenitor cells, and that ectopic expression of RXR-α impairs both proliferation and terminal differentiation (Taschner et al., 2007). Ultimately, my findings do not establish a direct role of RXR-α in *LGALS12* transcriptional regulation.

Inhibition of SP1 with mithramycin did not produce any changes in *LGALS12* expression but it did strongly increase *NCF1* which may reflect induction of differentiation. Indeed, mithramycin has been shown to induce some level of differentiation in patients with leukemia (Koller and Miller, 1986). Mithramycin binds to GC regions of DNA (which blocks SP1 binding) and so its inhibitory effect may be too broad with large off-target effects. SP1 is a ubiquitous transcription factor and has been implicated in regulation of myeloid-specific gene expression and terminal neutrophil differentiation (Friedman, 2002). It has been directly involved with activating the promoters of neutrophil differentiation markers CD11b, CD14, and lactoferrin (Khanna-Gupta et al., 2000; Friedman, 2002). SP1 has predicted binding sites in the promoter region of *LGALS12* but my findings with mithramycin do not implicate a direct role in *LGALS12* regulation.

SREBF1 was found to be downregulated in DMSO-differentiated cells but not ATRA. The use of SREBP1 inhibitor betulin led to an increase in *LGALS12* expression and *NCF1* which was unexpected as this does not match the effect of low SREBP1 in DMSO-induced differentiation. SREBP1 is a transcription factor typically implicated in lipid and cholesterol synthesis (Horton et al., 2002). No direct role of SREBP1 in neutrophil activity or differentiation has been noted in the literature. Galectin-12 co-localizes with lipid droplets in adipocytes, and there is an increase in lipid droplets upon neutrophilic differentiation (Xue et al., 2016). Therefore, the upregulation of *LGALS12* may be a compensatory mechanism by the cells if there is impairment of triglyceride production due to inhibition of SREBP1. The involvement of SREBP1 in *LGALS12* transcriptional regulation cannot be completely ruled out.

4.1.4 Neutrophilic differentiation of HL-60 cells blocks secretion of galectin-12

Galectin-12 secretion was found to be completely blocked during neutrophilic differentiation induced by ATRA and DMSO in HL-60 cells. The level of galectin-12 secretion itself was low in these cells being close to the detection limit of the ELISA kit used. It was also much lower than galectin-3 which was used as a reference control. Galectin-3 secretion showed a trend-wise increase in secretion with ATRA, DON and AC

and a large significant increase with DMSO which matched previous findings (McTague et al., 2022). Unexpectedly, the intracellular level of galectin-12 rose with DMSO but not ATRA, which does not match the gene expression data. This may be due to differences in mRNA stability or other factors that create an inconsistency between gene expression and protein level. The lack of a reliable galectin-12 antibody makes it difficult to confirm this finding through immunoblotting.

Intracellular galectin-12 was found to increase in a time-dependent manner in 3T3-L1 cells upon adipocyte differentiation, however secretion was negligible being below the minimal detection limit. This is in line with previous work that observed no secretion of galectin-12 in adipocytes despite such a high intracellular level (Yang et al., 2011). Therefore, galectin-12 secretion seems to be tissue-specific as it is more easily detectable in neutrophil-like cells. This also implies that in adipocytes, galectin-12 possibly has no extracellular functions and does not interact with cell surface molecules.

Next, my objective was to determine which mechanism of unconventional secretion governs galectin-12 release in HL-60 cells. Chemical inhibitors were used to block key steps in the formation and release of exosomes, microvesicles, and autophagosomes. My findings do not suggest a role of exosomes and microvesicles in the secretion of galectin-12. However, galectin-3 secretion was also tested for these treatments and no changes were observed despite strong evidence suggesting both processes involved with its secretion (Popa et al., 2018; Bänfer and Jacob, 2020). Either the mechanism of galectin-3 secretion is cell-type specific or the inhibitory effect cannot be detected at the given 48 hour time point and inhibitor concentration. Additionally, there is both ESCRT-dependent and -independent formation of multivesicular bodies (MVBs) which contain the exosomes destined for release (Catalano and O'Driscoll, 2020). GW4869 only blocks the independent pathway, so these findings demonstrate that galectin-3 is probably secreted primarily through ESCRT-dependent mechanisms. Indeed, the N-terminal tail of galectin-3 has been shown to interact with ESCRT machinery which allows it to be packaged into exosomes within MVBs (Bänfer et al., 2018). There is currently no tangible evidence that galectin-12 is secreted through exosomes at all and galectin-12 also lacks an N-terminal tail.

However, these initial findings imply that if exosomal secretion of galectin-12 does occur it is likely not through ESCRT-independent mechanisms.

On the other hand, secretory autophagy may be involved in galectin-12 secretion. 3-MA has been shown to have a dual role in autophagic flux where in certain conditions it can increase autophagy instead of inhibiting it (Wu et al., 2010). Treatment with 3-MA in full medium for over 9 hours was found to increase autophagy. HL-60 cells were grown in complete media and treated with 3-MA for 48 hours which would fall into the conditions necessary for promoting autophagy. Therefore, the observed increase in galectin-12 secretion may reflect secretory autophagy being a viable mechanism. An increasing trend was also found for galectin-3 secretion upon 3-MA treatment, which suggests that this galectin may also be secreted through autophagy. Secretory autophagy could represent one mechanism of unconventional secretion in these cells, especially during situations of cell stress or damage. Many galectins have been associated with damaged lysosomes like galectin-1, -3, -8, and -9 but not galectin-12 previously (Popa et al., 2018). It is difficult to gauge whether the elevated autophagic flux is representative of galectin-12 secretion during normal cell conditions. To date, galectin-1 is the only member of the family that has been confirmed to be secreted through the use of autophagy (Davuluri et al., 2021).

4.1.5 Galectin-12 secretion may be modulated but not dependent on intracellular lipid droplet accumulation

Another study objective was to evaluate the role of lipid droplets in the secretion of galectin-12. Leukocytes including neutrophils, have been shown to accumulate lipid droplets in response to inflammatory conditions and stimuli (Melo and Weller, 2016). While in adipocytes these organelles serve as energy storage, in leukocytes lipid droplets can hold important signaling molecules like cytokines. Adipocytes experience a large increase in lipid droplet content as they differentiate and mature. By now, it is well-established that galectin-12 is involved with regulation of lipolysis and that it co-localizes to lipid droplets (Yang et al., 2011, 2016). Therefore, I initially proposed that galectin-12 regulation is influenced or regulated by its association with lipid droplets. My findings suggest a link between suppression of galectin-12 secretion and elevated intracellular lipid

content. Adipocytes by nature have higher lipid content than the average cell, so it is not surprising that galectin-12 secretion is always negligible. For neutrophils this secretion blockade only occurs upon a differentiation-induced increase in lipid droplet content. Knockdown of galectin-12 reduced lipid droplet formation in ATRA-differentiated NB4 cells which suggests that the association to lipid droplets exists beyond the adipocyte cell model (Xue et al., 2016).

There is little information surrounding the presence and regulation of lipid droplets in HL-60 cells. Therefore, I sought to establish whether neutrophil-like differentiation of HL-60 cells induces the accumulation of lipid droplets like in NB4 cells which can also differentiate into neutrophils. GSEA of existing HL-60 RNA-Seq data demonstrated that many lipid-related ontology terms were positively enriched upon differentiation with ATRA or DMSO. Enriched terms common to both ATRA and DMSO included 'response to lipid' and 'regulation of lipase activity'. Furthermore, both fluorescence microscopy and flow cytometry found a significant increase in lipid droplets upon differentiation with DMSO and an increasing trend with ATRA. The non-significant increase in lipid droplets with ATRA was not unexpected. One study found that lipid droplets in ATRA-differentiated HL-60 cells are not detectable until stimulation with *Porphyromonas gingivalis* LPS which increased both size and number of observable droplets (Nose et al., 2013). This suggests that differentiation with ATRA may prime machinery for lipid droplet synthesis but that there needs to be an inflammatory signal for their formation.

These initial findings proposed an association of lipid droplets with regulation of galectin-12 secretion. However, it is not yet established whether galectin-12 actually co-localizes to lipid droplets at all in neutrophils like in adipocytes. The composition of lipid droplet-associated proteins varies between cell types and are not fully described, especially for neutrophils. In adipocytes, galectin-12 co-localizes with perilipin-1 which is not expressed in neutrophils (Nose et al., 2013; Itabe et al., 2017). Perilipins are found on the surface of lipid droplets and play a role in droplet formation and stabilization. Perilipin-1 is primarily found on the surface of large lipid droplets in mature adipocytes, while other members of the family have different distribution. Perilipin-2 and -3 have ubiquitous expression with perilipin-2 having a well-documented role in droplet stability (Itabe et al., 2017).

Remarkably, no expression of perilipin-1, -2, and -5 was measured in HL-60 cells while perilipin-3 increased upon stimulation with LPS (Nose et al., 2013). The absence of perilipin-2 in HL-60 cells is unexpected as it has been used as a marker for leukocyte lipid droplets previously (Melo and Weller, 2016). Knockdown of perilipin-3 in HL-60 cells was found to suppress lipid droplet formation. Therefore, in this particular cell line perilipin-3 is crucial for droplet stability and can compensate for the absence of perilipin-2. Whether galectin-12 interacts with perilipin-3 in HL-60 cells in a manner similar to what is observed with perilipin-1 in adipocytes is currently unknown.

Additionally, the increase in lipid droplet content may be a secondary effect and not what is directly impacting galectin-12 secretion. Potentially, it is the neutrophilic differentiation process itself that is suppressing galectin-12 secretion. To test this, I used agents that stimulate or inhibit lipid droplet formation without inducing neutrophilic differentiation. Unexpectedly, stimulation of lipid droplet formation with oleic acid increased galectin-12 secretion, while droplet disruption with isoproterenol had no effect. Isoproterenol induces lipolysis which cause the breakdown of large lipid droplets and results in the formation of relatively small droplets instead (Chitraju et al., 2017). While galectin-12 co-localizes to large droplets in adipocytes, this may not be the case in neutrophils which have a smaller droplet size in the first place. Thus, the continued presence of small droplets here may be sufficient to not impact galectin-12 secretion. Additionally, treatment of 3T3-L1 cells with isoproterenol has previously resulted in a decrease of *Lgals12*, so potentially this effect is cell type-specific (Fasshauer et al., 2002).

On the other hand, cell treatment with oleic acid results in lipid droplet formation due to the activation of free-fatty acid receptor-4 (FFAR4) (Rohwedder et al., 2014). The increase in galectin-12 secretion despite elevated lipid droplet formation suggests that its secretion is not solely regulated by lipid droplets. In fact, the increase in galectin-12 secretion was accompanied by a drop of intracellular protein, which may represent flux of excess galectin-12 out of the cell. Potentially, cells are attempting to maintain homeostasis by reducing intracellular galectin-12 through secretion because an external stimulus is inducing lipid droplet formation. In that context, there is no need for any additional galectin-12 to modulate lipogenesis. It would be interesting to evaluate the level of

LGALS12 and whether it was also downregulated to compensate for the high level of lipid droplet synthesis by oleic acid.

4.1.6 Galectin-12 functions in an *O*-GlcNAc-independent manner

The next objective of my study was to evaluate whether *O*-GlcNAc homeostasis had a regulatory role in controlling the expression and secretion of galectin-12 in HL-60 cells. *O*-GlcNAcylation is a post-translational protein modification that is implicated in various cellular processes and is sensitive to stress and nutrient availability (Lee et al., 2021). Oftentimes, a drop in *O*-GlcNAcylation is observed upon differentiation, while an increase is found in cancer. My findings currently propose that galectin-12 is regulated by *O*-GlcNAc-independent mechanisms. Previous work using inhibitors of *O*-GlcNAc cycle enzymes demonstrated alterations in *LGALS12* expression (Sherazi et al., 2018; McTague et al., 2022) however, these changes do not seem to translate to protein and secretion levels.

A model where low *O*-GlcNAc favors galectin secretion has been proposed based on the findings observed in the galectins that have been tested thus far. *O*-GlcNAcylated proteins tend to remain in the cell, while deglycosylation leads to their release. Both ATRA and DON increased secretion of galectin-1, -3, -9, and -10 in HL-60 cells (McTague et al., 2022). Inhibition of GFAT with DON leads to a deficiency in the sugar substrate UDP-GlcNAc which ultimately produces low global *O*-GlcNAcylation. DON treatment also induces neutrophilic differentiation in HL-60 cells, demonstrated by changes in gene expression and secretion of galectins that mimic the effects of ATRA (McTague et al., 2022). Of the galectins evaluated thus far, galectin-12 is the first to have a decrease in secretion upon differentiation with both ATRA and DMSO and no changes with DON. Inhibition of the *O*-GlcNAc cycle enzymes did not produce any effect on galectin-12 secretion or intracellular protein levels, which suggests it functions in an *O*-GlcNAc-independent manner. Galectin-12 likely does not fit the model of deglycosylation being required for its secretion as observed with galectin-3 (Mathew et al., 2022). This was unexpected as many transcription factors involved with adipogenesis like C/EBP-β and PPARγ are known to be *O*-GlcNAc-sensitive and act downstream of galectin-12 (Özcan et al., 2010; Ji et al., 2012). These transcription factors are suggested to have transactivation

with galectin-12 so changes in their *O*-GlcNAcylation could impact galectin-12 too (Yang et al., 2004). However, this regulation could be cell-type specific and not occur in neutrophils. It is potentially the unique tissue and subcellular localization of galectin-12 that makes it function in an *O*-GlcNAc-independent manner.

Unexpectedly, a decrease in global *O*-GlcNAcylation was observed in 3T3-L1 cells upon adipocyte differentiation which is inconsistent with the literature. 3T3-L1 cells were reported to experience a time-dependent increase in *O*-GlcNAcylation during adipocyte differentiation (Ishihara et al., 2010; Hsieh et al., 2012). In fact, inhibition of GFAT in 3T1-L1 cells blocked both adipocyte differentiation and the formation of lipid droplets due to the impact on adipogenesis-related transcriptions factors like C/EBPα and β. The 3T3-L1 cells in my study demonstrated other key characteristics of mature adipocytes like high expression of adipocyte marker fatty acid binding protein 4 (*Fabp4*) and lipid droplet accumulation. It is uncertain why I was unable to replicate the strong and sustained increase in global *O*-GlcNAcylation in 3T3-L1 cells.

4.1.7 ATRA-induced differentiation of MDA-MB-231 cells upregulates *LGALS12* expression

My final objective was to characterize the expression and secretion of *LGALS12* in breast cancer cell lines upon differentiation with ATRA. My previous *in silico* analysis reported a downregulation of *LGALS12* in all subtypes of breast cancer when comparing to normal tissue (Tazhitdinova and Timoshenko, 2021). The widespread downregulation suggests that galectin-12 could serve as a tumor suppressor gene where its expression prevents tumorigenesis. My study is only the second instance where *LGALS12* expression has been evaluated in any breast cancer cell lines after the study where galectin-12 was first described (Yang et al., 2001). I aimed to measure the basal level of *LGALS12* expression in four breast cancer cell lines and after treatment with ATRA. Promising *in vitro* findings suggest differentiation therapy with ATRA could reverse the EMT process and tumor progression (Bobal et al., 2021).

The cell lines tested in this study cover different subtypes of breast cancer including luminal A (MCF-7), HER2-enriched (SK-BR-3), and triple negative/basal-like (MDA-MB-231 and MDA-MB-468). These subtypes vary in their outcomes with luminal A tumors having the most favorable prospects and triple negative having the worst (Dai et al., 2017). An upregulation of *LGALS12* was observed in MDA-MB-231 cells upon differentiation with ATRA, while the other three had low or unchanged expression. To my knowledge, this is the first time that *LGALS12* expression has been detected in MDA-MB-231, MDA-MB-468 and SK-BR-3 cells. Given that no effect on *LGALS12* was observed in three out of four cell lines, galectin-12 likely functions in a breast cancer subtype-specific manner. This provides a novel cell model where galectin-12 may be involved in the regulation of differentiation. The overall low basal expression of *LGALS12* and the upregulation due to differentiation with ATRA further supports that this protein could also serve a tumor-suppressor gene where it is inhibited during tumorigenesis. This once again, is in line with the downregulation of *LGALS12* in AML and CRC (El Leithy et al., 2015; Katzenmaier et al., 2017). In addition to *LGALS12*, gene expression of ICAM-1 was also upregulated in MDA-MB-231 cells along with SK-BR-3 cells. ICAM-1 has been previously used as a marker of differentiation in breast cancer cells (Yu et al., 2019). One paper reported that ATRA seems to inhibit growth of breast cancer cells through upregulation of ICAM-1 suggesting this could be a key regulator in MDA-MB-231 differentiation (Baj et al., 1999).

LGALS12 was induced by ATRA in only one of the triple negative cell lines tested. This subtype can be further divided into different classes where MDA-MB-468 are classified as basal A and MDA-MB-231 are classified as basal B/mesenchymal stem-like (Lehmann et al., 2011; Dai et al., 2017). Triple negative tumors have the worst outcomes due to their aggressive nature and lack of treatment targets. Within this, basal B/mesenchymal stem-like are the most invasive with the least differentiated features. Therefore, MDA-MB-231 cells could potentially be the most impacted by treatment with ATRA, reversing any mesenchymal characteristics into a more epithelial-like or differentiated phenotype. Basal A cells on the other hand possess more differentiated epithelial characteristics which could explain the lack of response in MDA-MB-468 cells. MDA-MB-231 and MDA-MB-468 cells also seem to have diverging transcriptional responses to ATRA that are produced

through RARE-independent signaling. For example, interferon regulatory factor 1 (IRF1) expression was induced by ATRA and this allowed for the activation of cathepsin S in MDA-MB-231 but not MDA-MB-468 cells (Coyle et al., 2017). It should be noted that in this tumor xenograft study, ATRA was reported to have a pro-tumor effect in MDA-MB-231 but anti-tumor in MDA-MB-468, which is the opposite of my findings (Marcato et al., 2015). The effect of ATRA on differentiation or tumor growth is still not well-defined and results may vary between xenograft and *in vitro* models.

Treatment with ATRA has also shown anti-proliferative and pro-differentiation effects in both MCF-7 and SK-BR-3 cells in the literature (Byers et al., 1996; Yan et al., 2016). ATRA treatment led to the induction of apoptosis and downregulation of proteins linked to tumor progression (Bobal et al., 2021). The lack of *LGALS12* expression observed in my study implies that differentiation in other breast cancer cell lines occurs through galectin-12-independent mechanisms.

No changes in global *O*-GlcNAcylation levels were observed during ATRA treatment of MDA-MB-231 cells which was unexpected. Breast cancer like many other cancers has been reported to have elevated *O*-GlcNAcylation levels (Caldwell et al., 2010; Akella et al., 2020). In particular, overexpression of OGT has been observed in breast cancer cells and its subsequent knockdown inhibited tumor growth and cell cycle progression (Caldwell et al., 2010). Therefore, in breast cancer high *O*-GlcNAcylation is associated with a more stem-like phenotype which would be decreased upon differentiation. However, the basal level of global *O*-GlcNAcylation was already low in MDA-MB-231 cells and the ATRA-induced differentiation process may be *O*-GlcNAc-independent. There was also negligible secretion of galectin-12 suggesting like in adipocytes, this protein functions primarily inside the cell with limited extracellular signaling. All together, these findings present a novel model of MDA-MB-231 cells to study galectin-12 regulation, where it may serve as a marker of differentiation and as a tumor suppressor gene.

4.2 Conclusions and applications

This study provided further insight into the role and regulation of galectin-12 in cell differentiation using myeloid and breast cancer cell lines (**Figure 19**). The findings here suggest that galectin-12 could serve as a marker of neutrophil polarization as its expression varied between two distinct phenotypes of neutrophil-like cells. Further work featuring galectin-12 as a marker can be used to help characterize ATRA and DMSO-induced phenotypes of neutrophils. The N1/N2 model of anti- and pro-tumorigenic neutrophils is one set of observed phenotypes but galectin-12 expression can also potentially be linked to defining immature vs. mature neutrophils, low-density vs. high-density neutrophils, and other populations of neutrophils (Rosales, 2018; Ai and Udalova, 2020).

This study also established that galectin-12 is a unique member of the galectin family with regards to its sensitivity to changes in *O*-GlcNAcylation and secretion. This is the only galectin tested in HL-60 cells thus far, that had inhibition of secretion upon neutrophilic differentiation (McTague et al., 2022). Overall, galectin-12 seems to be minimally secreted as negligible secretion was observed in both adipocytes and breast cancer cell lines. There is currently only one study that has measured galectin-12 in human serum, looking at patients with pancreatic cancer (Galdino et al., 2021). The increase in lipid droplet accumulation upon neutrophilic differentiation of HL-60 cells helps expand the potential regulatory role of galectin-12 in lipogenesis within a new cell model beyond adipocytes, sebocytes, and the previously tested APL NB4 cells (Yang et al., 2004; Harrison et al., 2007; Xue et al., 2016).

Presently, little is known about the mechanisms of unconventional secretion for the majority of the galectin family. This is the first study to observe secretion of galectin-12 and to attempt to uncover the mechanism used, showing the potential involvement of secretory autophagy. The lack of secretion in other cell models also raises the question of whether galectin-12 has any extracellular functions in neutrophils. If galectin-12 does bind to ligands on the surface of neutrophils, it would be necessary to determine what these targets are and the purpose of these interactions.

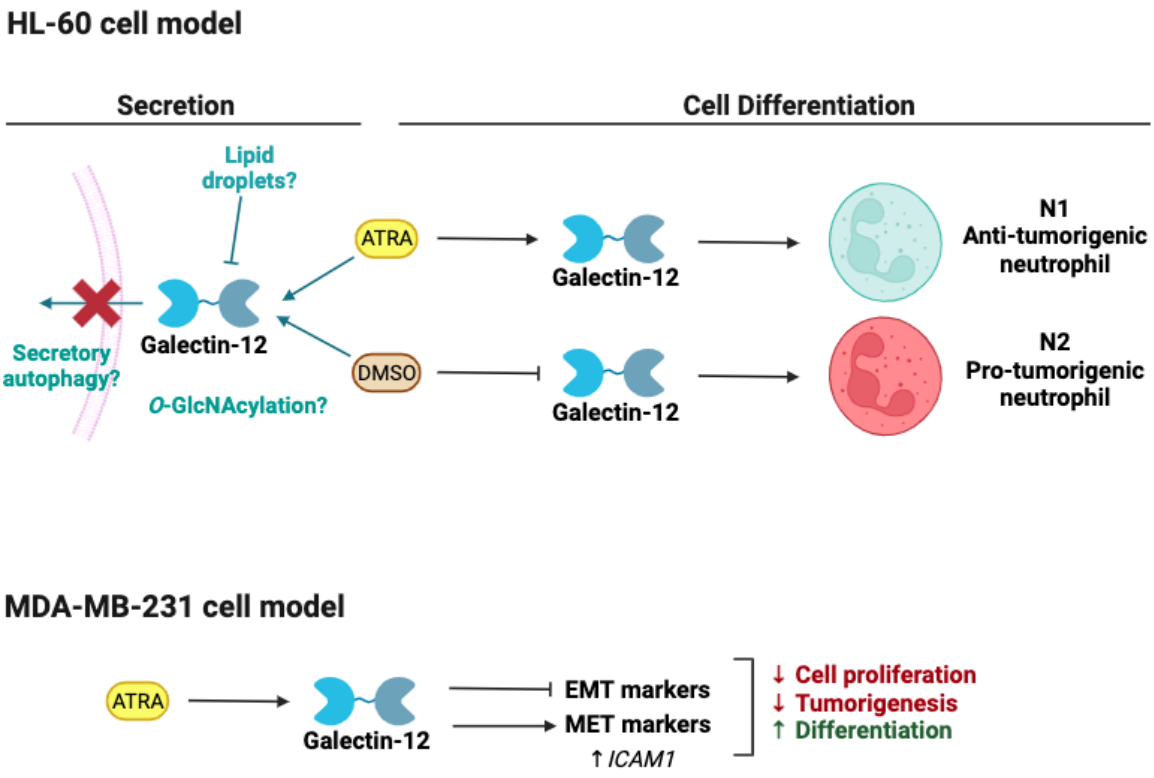

Figure 19. Proposed role and regulation of galectin-12 in HL-60 and MDA-MB-231 cells.

In HL-60 cells, galectin-12 is suggested to be involved with the polarization of neutrophils into N1/anti-tumorigenic and N2/pro-tumorigenic phenotypes. The neutrophilic differentiation of HL-60 cells also blocked galectin-12 secretion, which is suggested to be regulated by secretory autophagy. The exact roles of lipid droplets and *O*-GlcNAcylation in the regulation of galectin-12 are still not defined. Galectin-12 is suggested to act in a subtype-specific manner in breast cancer cells where it is upregulated upon ATRA-induced differentiation in MDA-MB-231 cells acting as a tumor suppressor gene. If galectin-12 is involved with the regulation of cell differentiation, then it will inhibit epithelial-mesenchymal transition (EMT) markers and induce those involved with mesenchymal-epithelial transition (MET). Figure was generated using BioRender.

Finally, this study measured *LGALS12* expression in breast cancer cell lines, providing a new model and context to further study galectin-12. My findings point to galectin-12 functioning in a subtype-specific manner within breast cancer cell lines which can be explored further. It would also be essential to measure *LGALS12* in other breast cancer cell lines and a normal mammary epithelial control like MCF-10A cells to determine whether this downregulation occurs broadly across all subtypes of breast cancer (Qu et al., 2015). The ability to restore *LGALS12* expression upon treatment with ATRA in MDA-MB-231 cells parallels the epigenetic silencing of galectin-12 in CRC (Katzenmaier et al., 2017). Additionally, in pancreatic cancer samples, some positive staining for galectin-12 was observed in the stroma but not the tumor cells (Galdino et al., 2021). When galectin-12 was initially discovered, its functions were described in relation to proliferation, apoptosis, and cell cycle regulation (Hotta et al., 2001; Yang et al., 2001). However, there has been little development on these early findings observed using ectopic and overexpression models. If galectin-12 is silenced in cancer, it could be due to its involvement in these particular processes that can impede tumorigenesis. Altogether, galectin-12 is a unique and tissue-specific member of the galectin family that is implicated in cell differentiation.

4.3 Study limitations and future directions

Nearly all my experimental work assessed galectin-12 RNA levels only, which does not always reflect protein abundance. A major limitation I face with galectin-12 is the lack of a reliable commercially available antibody for western blots and immunofluorescence microscopy. So far, I have only evaluated protein levels through ELISA which does not allow for validation of protein molecular size. This also prevented me from being able to conduct fluorescence microscopy to determine the localization of galectin-12 within neutrophils and breast cancer cell lines. A connection between lipid droplet level and galectin-12 secretion was made based off the present study findings and past knowledge in an adipocyte model. However, galectin-12 may be localized completely differently in neutrophils or breast cancer cell lines. There is a need to produce a human galectin-12 antibody or use a Flag-tag system with transfected cells to determine the subcellular localization in cells. Additionally, this study has made some preliminary observations with regards to the mechanism of unconventional secretion at play through the use of chemical

inhibitors. However, these can have off-target effects and only give an estimation of whether the level of galectin-12 secretion is associated with the mechanism. Isolation of exosomes, microvesicles, autophagosomes, and lipid droplets using ultracentrifugation would validate whether galectin-12 is actually present in these vesicles.

Current findings point to galectin-12 being involved with regulation of neutrophilic differentiation and lipogenesis (Xue et al., 2016). To determine whether galectin-12 plays a major role in neutrophilic differentiation, a knockdown or knockout model needs to be developed. HL-60 cells are known to be a difficult to transfect cell line. My attempts at lipofectamine-based transfection and other attempts using electroporation in the Timoshenko lab were unsuccessful. Nucleofection is a new electroporation-based transfection approach that is greatly improving transfection efficiency (Distler et al., 2005). Currently an shRNA-based knockdown of *LGALS12* is being optimized for nucleofection. Once knockdown cells are created then their ability to differentiate into neutrophils with ATRA/DMSO will be assessed and their ability to generate ROS in response to various stimuli.

Finally, I proposed a model where the DMSO phenotype represent neutrophils that are N2 and pro-tumor, while those differentiated with ATRA are N1 and anti-tumor. The surface markers of different neutrophil phenotypes vary, and these could be evaluated next through flow cytometry. This includes comparing surface markers related to N1 vs. N2 neutrophils and also between fresh and aged neutrophils. The surface markers related to various neutrophil phenotypes are not strictly defined but seem to be context-dependent (Shaul and Fridlender, 2019). I may observe a combination of markers that is unique solely to ATRA or DMSO-induced neutrophils.

Due to time constraints, only one differentiation marker was tested in the breast cancer cell lines. However, a comprehensive gene expression profile would be necessary to assess whether there is an overall change in EMT markers with a shift towards a more differentiated epithelial-like phenotype. Some well-known markers associated with EMT like E-cadherin and N-cadherin cannot be used for all cell lines. For example, E-cadherin is not expressed in MDA-MB-231 cells due to promoter hypermethylation (Chao et al.,

2010). Therefore, starting with an RT^2 Profiler PCR Array or conducting RNA-Seq can help determine whether ATRA-induced changes have an effect on EMT.

References

Ai, Z., and Udalova, I. A. (2020). Transcriptional regulation of neutrophil differentiation and function during inflammation. *J. Leukoc. Biol.* 107, 419–430.

Akella, N. M., Ciraku, L., and Reginato, M. J. (2019). Fueling the fire: emerging role of the hexosamine biosynthetic pathway in cancer. *BMC Biol.* 17, 52.

Akella, N. M., Le Minh, G., Ciraku, L., Mukherjee, A., Bacigalupa, Z. A., Mukhopadhyay, D., et al. (2020). *O*-GlcNAc transferase regulates cancer stem–like potential of breast cancer cells. *Mol. Cancer Res.* 18, 585–598.

Alexa, A., Rahnenführer, J., and Lengauer, T. (2006). Improved scoring of functional groups from gene expression data by decorrelating GO graph structure. *Bioinformatics* 22, 1600–1607.

Anders, S., Pyl, P. T., and Huber, W. (2015). HTSeq—a Python framework to work with high-throughput sequencing data. *Bioinformatics* 31, 166–169.

Antuamwine, B. B., Bosnjakovic, R., Hofmann-Vega, F., Wang, X., Theodosiou, T., Iliopoulos, I., et al. (2023). N1 versus N2 and PMN-MDSC: A critical appraisal of current concepts on tumor-associated neutrophils and new directions for human oncology. *Immunol. Rev.* 314, 250–279.

Assem, M., El-Araby, R. E., Al-Karmalawy, A. A., Nabil, R., Kamal, M. A. M., Belal, A., et al. (2023). Promoter methylation might shift the balance of Galectin-3 & 12 expression in de novo adult acute myeloid leukemia patients. *Front. Genet.* 14, 1122864.

Baj, G., Arnulfo, A., Deaglio, S., Tibaldi, E., Surico, N., and Malavasi, F. (1999). All-trans retinoic acid inhibits the growth of breast cancer cells by up-regulating ICAM-1 expression. *J. Biol. Regul. Homeost. Agents* 13, 115–122.

Bänfer, S., and Jacob, R. (2020). Galectins in intra- and extracellular vesicles. *Biomolecules* 10, 1232.

Bänfer, S., Schneider, D., Dewes, J., Strauss, M. T., Freibert, S.-A., Heimerl, T., et al. (2018). Molecular mechanism to recruit galectin-3 into multivesicular bodies for polarized exosomal secretion. *Proc. Natl. Acad. Sci.* 115, E4396-E4405.

Baudoin, L., and Issad, T. (2015). *O*-GlcNAcylation and inflammation: A vast territory to explore. *Front. Endocrinol.* 5, 235.

Belambri, S. A., Rolas, L., Raad, H., Hurtado-Nedelec, M., Dang, P. M.-C., and El-Benna, J. (2018). NADPH oxidase activation in neutrophils: Role of the phosphorylation of its subunits. *Eur. J. Clin. Invest.* 48, e12951.

Benjamini, Y., and Hochberg, Y. (1995). Controlling the false discovery rate: A practical and powerful approach to multiple testing. *J. R. Stat. Soc. Ser. B Methodol.* 57, 289–300.

Benoit, G. (1999). RAR-independent RXR signaling induces t(15;17) leukemia cell maturation. *EMBO J.* 18, 7011–7018.

Birnie, G. D. (1988). The HL60 cell line: a model system for studying human myeloid cell differentiation. *Br. J. Cancer. Suppl.* 9, 41–45.

Bobal, P., Lastovickova, M., and Bobalova, J. (2021). The role of ATRA, natural ligand of retinoic acid receptors, on EMT-related proteins in breast cancer: Minireview. *Int. J. Mol. Sci.* 22, 13345.

Boutilier, A. J., and Elsawa, S. F. (2021). Macrophage polarization states in the tumor microenvironment. *Int. J. Mol. Sci.* 22, 6995.

Breitman, T. R., Selonick, S. E., and Collins, S. J. (1980). Induction of differentiation of the human promyelocytic leukemia cell line (HL-60) by retinoic acid. *Proc. Natl. Acad. Sci.* 77, 2936–2940.

Brenner, D. R., Weir, H. K., Demers, A. A., Ellison, L. F., Louzado, C., Shaw, A., et al. (2020). Projected estimates of cancer in Canada in 2020. *Can. Med. Assoc. J.* 192, E199–E205.

Byers, S., Pishvaian, M., Crockett, C., Peer, C., Tozeren, A., Sporn, M., et al. (1996). Retinoids increase cell-cell adhesion strength, beta-catenin protein stability, and localization to the cell membrane in a breast cancer cell line: a role for serine kinase activity. *Endocrinology* 137, 3265–3273.

Caldwell, S. A., Jackson, S. R., Shahriari, K. S., Lynch, T. P., Sethi, G., Walker, S., et al. (2010). Nutrient sensor *O*-GlcNAc transferase regulates breast cancer tumorigenesis through targeting of the oncogenic transcription factor FoxM1. *Oncogene* 29, 2831–2842.

Cappellini, A., Tabellini, G., Zweyer, M., Bortul, R., Tazzari, P. L., Billi, A. M., et al. (2003). The phosphoinositide 3-kinase/Akt pathway regulates cell cycle progression of HL60 human leukemia cells through cytoplasmic relocalization of the cyclin-dependent kinase inhibitor p27Kip1 and control of cyclin D1 expression. *Leukemia* 17, 2157–2167.

Catalano, M., and O'Driscoll, L. (2020). Inhibiting extracellular vesicles formation and release: a review of EV inhibitors. *J. Extracell. Vesicles* 9, 1703244.

Chao, Y. L., Shepard, C. R., and Wells, A. (2010). Breast carcinoma cells re-express E-cadherin during mesenchymal to epithelial reverting transition. *Mol. Cancer* 9, 179.

Chitraju, C., Mejhert, N., Haas, J. T., Diaz-Ramirez, L. G., Grueter, C. A., Imbriglio, J. E., et al. (2017). Triglyceride synthesis by DGAT1 protects adipocytes from lipid-Induced ER stress during lipolysis. *Cell Metab.* 26, 407-418.e3.

Cluntun, A. A., Lukey, M. J., Cerione, R. A., and Locasale, J. W. (2017). Glutamine metabolism in cancer: Understanding the heterogeneity. *Trends Cancer* 3, 169–180.

Congleton, J., Jiang, H., Malavasi, F., Lin, H., and Yen, A. (2011). ATRA-induced HL-60 myeloid leukemia cell differentiation depends on the CD38 cytosolic tail needed for membrane localization, but CD38 enzymatic activity is unnecessary. *Exp. Cell Res.* 317, 910–919.

Cooper, D. N., and Barondes, S. H. (1990). Evidence for export of a muscle lectin from cytosol to extracellular matrix and for a novel secretory mechanism. *J. Cell Biol.* 110, 1681–1691.

Coyle, K. M., Maxwell, S., Thomas, M. L., and Marcato, P. (2017). Profiling of the transcriptional response to all-trans retinoic acid in breast cancer cells reveals RARE-independent mechanisms of gene expression. *Sci. Rep.* 7, 16684.

Cummings, R., Liu, F.-T., Rabinovich, G. A., and Stowell, Sean R, V., Gerardo R. (2022). Galectins in *Essentials of Glycobiology* (NY: Cold Spring Harbor), Chapter 36.

Dai, X., Cheng, H., Bai, Z., and Li, J. (2017). Breast cancer cell line classification and its relevance with breast tumor subtyping. *J. Cancer* 8, 3131–3141.

Dalton, W. J., Ahearn, M., McCredie, K., Freireich, E., Stass, S., and Trujillo, J. (1988). HL-60 cell line was derived from a patient with FAB-M2 and not FAB-M3. *Blood* 71, 242–247.

Davuluri, G. V. N., Chen, C.-C., Chiu, Y.-C., Tsai, H.-W., Chiu, H.-C., Chen, Y.-L., et al. (2021). Autophagy drives galectin-1 secretion from tumor-associated macrophages facilitating hepatocellular carcinoma progression. *Front. Cell Dev. Biol.* 9, 741820.

Delacour, D., Gouyer, V., Zanetta, J.-P., Drobecq, H., Leteurtre, E., Grard, G., et al. (2005). Galectin-4 and sulfatides in apical membrane trafficking in enterocyte-like cells. *J. Cell Biol.* 169, 491–501.

Distler, J. H. W., Jungel, A., Kurowska-Stolarska, M., Michel, B. A., Gay, R. E., Gay, S., et al. (2005). Nucleofection: a new, highly efficient transfection method for primary human keratinocytes. *Exp. Dermatol.* 14, 315–320.

Dobin, A., Davis, C. A., Schlesinger, F., Drenkow, J., Zaleski, C., Jha, S., et al. (2013). STAR: ultrafast universal RNA-seq aligner. *Bioinformatics* 29, 15–21.

Duncan, R. E., Ahmadian, M., Jaworski, K., Sarkadi-Nagy, E., and Sul, H. S. (2007). Regulation of Lipolysis in Adipocytes. *Annu. Rev. Nutr.* 27, 79–101.

Edgar, J. R. (2016). Q&A: What are exosomes, exactly? *BMC Biol.* 14, 46.

El Leithy, A. A., Helwa, R., Assem, M. M., and Hassan, N. H. A. (2015). Expression profiling of cancer-related galectins in acute myeloid leukemia. *Tumor Biol.* 36, 7929–7939.

Eliyatkin, N., Yalcin, E., Zengel, B., Aktaş, S., and Vardar, E. (2015). Molecular Classification of Breast Carcinoma: From Traditional, Old-Fashioned Way to A New Age, and A New Way. *J. Breast Health* 11, 59–66.

Farre, D. (2003). Identification of patterns in biological sequences at the ALGGEN server: PROMO and MALGEN. *Nucleic Acids Res.* 31, 3651–3653.

Fasshauer, M., Klein, J., Lossner, U., and Paschke, R. (2002). Negative regulation of adipose-expressed galectin-12 by isoproterenol, tumor necrosis factor alpha, insulin and dexamethasone. *Eur. J. Endocrinol.*, 553–559.

Felipe Lima, J., Nofech-Mozes, S., Bayani, J., and Bartlett, J. (2016). EMT in breast carcinoma—A review. *J. Clin. Med.* 5, 65.

Fillion, I., Ouellet, N., Simard, M., Bergeron, Y., Sato, S., and Bergeron, M. G. (2001). Role of chemokines and formyl peptides in pneumococcal pneumonia-induced monocyte/macrophage recruitment. *J. Immunol.* 166, 7353–7361.

Fridlender, Z. G., Sun, J., Kim, S., Kapoor, V., Cheng, G., Ling, L., et al. (2009). Polarization of tumor-associated neutrophil phenotype by TGF-β: "N1" versus "N2" TAN. *Cancer Cell* 16, 183–194.

Friedman, A. D. (2002). Transcriptional regulation of granulocyte and monocyte development. *Oncogene* 21, 3377–3390.

Funes, S. C., Rios, M., Escobar-Vera, J., and Kalergis, A. M. (2018). Implications of macrophage polarization in autoimmunity. *Immunology* 154, 186–195.

Galdino, L. V., Albuquerque, A. P. B., Lira, M. M. de M., de Lima, L. R. A., Pitta, M. G. da R., and Rêgo, M. J. B. M. (2021). Galectin-12 in pancreatic cancer: A new player in the microenvironment? *Pancreas* 50, e78–e79.

Gatie, M. I., Spice, D. M., Garha, A., McTague, A., Ahmer, M., Timoshenko, A. V., et al. (2022). *O*-GlcNAcylation and regulation of galectin-3 in extraembryonic endoderm differentiation. *Biomolecules* 12, 623.

Ginestier, C., Wicinski, J., Cervera, N., Monville, F., Finetti, P., Bertucci, F., et al. (2009). Retinoid signaling regulates breast cancer stem cell differentiation. *Cell Cycle* 8, 3297–3302.

Gloster, T. M., Zandberg, W. F., Heinonen, J. E., Shen, D. L., Deng, L., and Vocadlo, D. J. (2011). Hijacking a biosynthetic pathway yields a glycosyltransferase inhibitor within cells. *Nat. Chem. Biol.* 7, 174–181.

Gopalan, V., Saremi, N., Sullivan, E., Kabir, S., Lu, C.-T., Salajegheh, A., et al. (2016). The expression profiles of the galectin gene family in colorectal adenocarcinomas. *Hum. Pathol.* 53, 105–113.

Grazier, J. J., and Sylvester, P. W. (2022). Role of galectins in metastatic breast cancer in *Breast Cancer* (Brisbane, AU: Exon Publications), Chapter 8.

Grosset, A.-A., Labrie, M., Vladoiu, M. C., Yousef, E. M., Gaboury, L., and St-Pierre, Y. (2016). Galectin signatures contribute to the heterogeneity of breast cancer and provide new prognostic information and therapeutic targets. *Oncotarget* 7, 18183–18203.

Groth, C., Weber, R., Lasser, S., Özbay, F. G., Kurzay, A., Petrova, V., et al. (2021). Tumor promoting capacity of polymorphonuclear myeloid-derived suppressor cells and their neutralization. *Int. J. Cancer* 149, 1628–1638.

Guerrini, V., and Gennaro, M. L. (2019). Foam cells: One size doesn't fit all. *Trends Immunol.* 40, 1163–1179.

Hanover, J. A., Chen, W., and Bond, M. R. (2018). *O*-GlcNAc in cancer: An Oncometabolism-fueled vicious cycle. *J. Bioenerg. Biomembr.* 50, 155–173.

Harrison, W. J., Bull, J. J., Seltmann, H., Zouboulis, C. C., and Philpott, M. P. (2007). Expression of lipogenic factors galectin-12, resistin, SREBP-1, and SCD in human sebaceous glands and cultured sebocytes. *J. Invest. Dermatol.* 127, 1309–1317.

Hart, G. W., Slawson, C., Ramirez-Correa, G., and Lagerlof, O. (2011). Cross Talk Between *O*-GlcNAcylation and phosphorylation: roles in signaling, transcription, and chronic disease. *Annu. Rev. Biochem.* 80, 825–858.

Hekmatirad, S., Moloudizargari, M., Moghadamnia, A. A., Kazemi, S., Mohammadnia-Afrouzi, M., Baeeri, M., et al. (2021). Inhibition of exosome release sensitizes U937 cells to PEGylated liposomal doxorubicin. *Front. Immunol.* 12, 692654.

Horton, J. D., Goldstein, J. L., and Brown, M. S. (2002). SREBPs: activators of the complete program of cholesterol and fatty acid synthesis in the liver. *J. Clin. Invest.* 109, 1125–1131.

Hotta, K., Funahashi, T., Matsukawa, Y., Takahashi, M., Nishizawa, H., Kishida, K., et al. (2001). Galectin-12, an adipose-expressed galectin-like molecule possessing apoptosis-inducing activity. *J. Biol. Chem.* 276, 34089–34097.

Hsieh, T.-J., Lin, T., Hsieh, P.-C., Liao, M.-C., and Shin, S.-J. (2012). Suppression of Glutamine:Fructose-6-phosphate amidotransferase-1 inhibits adipogenesis in 3T3-L1 adipocytes. *J. Cell. Physiol.* 227, 108–115.

Hughes, R. (1999). Secretion of the galectin family of mammalian carbohydrate-binding proteins. *Biochim. Biophys. Acta* 1473, 172–185.

Ilmer, M., Mazurek, N., Gilcrease, M. Z., Byrd, J. C., Woodward, W. A., Buchholz, T. A., et al. (2016). Low expression of galectin-3 is associated with poor survival in node-positive breast cancers and mesenchymal phenotype in breast cancer stem cells. *Breast Cancer Res.* 18, 97.

Ishihara, K., Takahashi, I., Tsuchiya, Y., Hasegawa, M., and Kamemura, K. (2010). Characteristic increase in nucleocytoplasmic protein glycosylation by O-GlcNAc in 3T3-L1 adipocyte differentiation. *Biochem. Biophys. Res. Commun.* 398, 489–494.

Itabe, H., Yamaguchi, T., Nimura, S., and Sasabe, N. (2017). Perilipins: a diversity of intracellular lipid droplet proteins. *Lipids Health Dis.* 16, 83.

Ji, S., Park, S. Y., Roth, J., Kim, H. S., and Cho, J. W. (2012). *O*-GlcNAc modification of PPARγ reduces its transcriptional activity. *Biochem. Biophys. Res. Commun.* 417, 1158–1163.

Johannes, L., Jacob, R., and Leffler, H. (2018). Galectins at a glance. *J. Cell Sci.* 131, jcs208884.

Johnson, W. E., Li, C., and Rabinovic, A. (2007). Adjusting batch effects in microarray expression data using empirical Bayes methods. *Biostatistics* 8, 118–127.

Ju, M.-H., Byun, K.-D., Park, E.-H., Lee, J.-H., and Han, S.-H. (2021). Association of galectin 9 expression with immune cell infiltration, programmed cell death Ligand-1 expression, and patient's clinical outcome in triple-negative breast cancer. *Biomedicines* 9, 1383.

Kalluri, R., and Weinberg, R. A. (2009). The basics of epithelial-mesenchymal transition. *J. Clin. Invest.* 119, 1420–1428.

Katzenmaier, E.-M., André, S., Kopitz, J., and Gabius, H.-J. (2014). Impact of sodium butyrate on the network of adhesion/growth-regulatory galectins in human colon cancer *in vitro*. *Anticancer Res.*, 10, 5429–5438.

Katzenmaier, E.-M., Fuchs, V., Warnken, U., Schnölzer, M., Gebert, J., and Kopitz, J. (2019). Deciphering the galectin-12 protein interactome reveals a major impact of galectin-12 on glutamine anaplerosis in colon cancer cells. *Exp. Cell Res.* 379, 129–139.

Katzenmaier, E.-M., Kloor, M., Gabius, H.-J., Gebert, J., and Kopitz, J. (2017). Analyzing epigenetic control of galectin expression indicates silencing of galectin-12 by promoter methylation in colorectal cancer. *IUBMB Life* 69, 962–970.

Katzenmaier, E.-M., Stark, H.-J., Gebert, J., and Kopitz, J. (2018). Galectin-12 colocalizes with splicing factor-rich speckles and shuttles between the nucleus and cytoplasm in colon cancer cells. *J Mol Biochem* 7, 28–40.

Khanna-Gupta, A., Zibello, T., Simkevich, C., Rosmarin, A. G., and Berliner, N. (2000). Sp1 and C/EBP are necessary to activate the lactoferrin gene promoter during myeloid differentiation. *Blood* 95, 3734–3741.

Kimura, T., Jia, J., Kumar, S., Choi, S. W., Gu, Y., Mudd, M., et al. (2017). Dedicated SNARE s and specialized TRIM cargo receptors mediate secretory autophagy. *EMBO J.* 36, 42–60.

Kinkel, A. D., Fernyhough, M. E., Helterline, D. L., Vierck, J. L., Oberg, K. S., Vance, T. J., et al. (2004). Oil red-O stains non-adipogenic cells: a precautionary note. *Cytotechnology* 46, 49–56.

Koller, C. A., and Miller, D. M. (1986). Preliminary observations on the therapy of the myeloid blast phase of chronic granulocytic leukemia with plicamycin and hydroxyurea. *N. Engl. J. Med.* 315, 1433–1438.

Korotkevich, G., Sukhov, V., Budin, N., Shpak, B., Artyomov, M. N., and Sergushichev, A. (2016). Fast gene set enrichment analysis. BioRxiv. doi: 10.1101/060012.

Laczy, B., Hill, B. G., Wang, K., Paterson, A. J., White, C. R., Xing, D., et al. (2009). Protein *O*-GlcNAcylation: a new signaling paradigm for the cardiovascular system. *Am. J. Physiol. Heart Circ. Physiol.* 296, H13–H28.

Law, C. W., Chen, Y., Shi, W., and Smyth, G. K. (2014). voom: precision weights unlock linear model analysis tools for RNA-seq read counts. *Genome Biol.* 15, R29.

Lawson, N. D., and Berliner, N. (1999). Neutrophil maturation and the role of retinoic acid. *Exp. Hematol.* 27, 1355–1367.

Lee, J. B., Pyo, K.-H., and Kim, H. R. (2021). Role and function of *O*-GlcNAcylation in cancer. *Cancers* 13, 5365.

Lee, J.-L., Wang, Y.-C., Hsu, Y.-A., Chen, C.-S., Weng, R.-C., Lu, Y.-P., et al. (2023). Galectin-12 modulates Kupffer cell polarization to alter the progression of non-alcoholic fatty liver disease. *Glycobiology*, cwad062.

Lee, Y.-R., Shim, H.-J., Yu, H.-N., Song, E.-K., Park, J., Kwon, K.-B., et al. (2005). Dimethylsulfoxide induces upregulation of tumor suppressor protein PTEN through nuclear factor-κB activation in HL-60 cells. *Leuk. Res.* 29, 401–405.

Leek, J. T., Johnson, W. E., Parker, H. S., Jaffe, A. E., and Storey, J. D. (2012). The sva package for removing batch effects and other unwanted variation in high-throughput experiments. *Bioinformatics* 28, 882–883.

Lehmann, B. D., Bauer, J. A., Chen, X., Sanders, M. E., Chakravarthy, A. B., Shyr, Y., et al. (2011). Identification of human triple-negative breast cancer subtypes and preclinical models for selection of targeted therapies. *J. Clin. Invest.* 121, 2750–2767.

Lehmann, S., Paul, C., and Törmä, H. (2001). Retinoid receptor expression and its correlation to retinoid sensitivity in non-M3 acute myeloid leukemia blast cells. *Clin. Cancer Res.* 7, 367–373.

Li, S.-Q., Su, N., Gong, P., Zhang, H.-B., Liu, J., Wang, D., et al. (2017). The expression of formyl peptide receptor 1 is correlated with tumor invasion of human colorectal cancer. *Sci. Rep.* 7, 5918.

Li, X., Molina, H., Huang, H., Zhang, Y., Liu, M., Qian, S., et al. (2009). *O*-Linked N-acetylglucosamine modification on CCAAT enhancer-binding protein β. *J. Biol. Chem.* 284, 19248–19254.

Liberzon, A., Subramanian, A., Pinchback, R., Thorvaldsdóttir, H., Tamayo, P., and Mesirov, J. P. (2011). Molecular signatures database (MSigDB) 3.0. *Bioinformatics* 27, 1739–1740.

Lin, E.-S., Hsu, Y.-A., Chang, C.-Y., Lin, H.-J., Chen, C. S., and Wan, L. (2020). Ablation of Galectin-12 Inhibits Atherosclerosis through Enhancement of M2 Macrophage Polarization. *Int. J. Mol. Sci.* 21, 5511.

Lin, F.-J., Huang, Y.-H., Tsao, C.-H., Hsieh, W.-C., Lo, Y.-H., Zouboulis, C. C., et al. (2023). Galectin-12 regulates immune responses in the skin through sebaceous glands. *J. Invest. Dermatol.*, S0022202X23020602.

Liu, D., Zhu, H., and Li, C. (2023). Galectins and galectin-mediated autophagy regulation: new insights into targeted cancer therapy. *Biomark. Res.* 11, 22.

Livak, K. J., and Schmittgen, T. D. (2001). Analysis of relative gene expression data using real-time quantitative PCR and the 2−ΔΔCT method. *Methods* 25, 402–408.

Lukyanov, P., Furtak, V., and Ochieng, J. (2005). Galectin-3 interacts with membrane lipids and penetrates the lipid bilayer. *Biochem. Biophys. Res. Commun.* 338, 1031–1036.

Maller, S. M., Cagnoni, A. J., Bannoud, N., Sigaut, L., Pérez Sáez, J. M., Pietrasanta, L. I., et al. (2020). An adipose tissue galectin controls endothelial cell function via preferential recognition of 3-fucosylated glycans. *FASEB J.* 34, 735–753.

Manda-Handzlik, A., Bystrzycka, W., Wachowska, M., Sieczkowska, S., Stelmaszczyk-Emmel, A., Demkow, U., et al. (2018). The influence of agents differentiating HL-60 cells toward granulocyte-like cells on their ability to release neutrophil extracellular traps. *Immunol. Cell Biol.* 96, 413–425.

Manley, H. R., Keightley, M. C., and Lieschke, G. J. (2018). The Neutrophil Nucleus: An Important Influence on Neutrophil Migration and Function. *Front. Immunol.* 9, 2867.

Mar, J. C., and Quackenbush, J. (2009). Decomposition of gene expression state space trajectories. *PLoS Comput. Biol.* 5, e1000626.

Marcato, P., Dean, C. A., Liu, R.-Z., Coyle, K. M., Bydoun, M., Wallace, M., et al. (2015). Aldehyde dehydrogenase 1A3 influences breast cancer progression via differential retinoic acid signaling. *Mol. Oncol.* 9, 17–31.

Mathew, M. P., Abramowitz, L. K., Donaldson, J. G., and Hanover, J. A. (2022). Nutrient-responsive *O*-GlcNAcylation dynamically modulates the secretion of glycan-binding protein galectin 3. *J. Biol. Chem.* 298, 101743.

Mayadas, T. N., Cullere, X., and Lowell, C. A. (2014). The multifaceted functions of neutrophils. *Annu. Rev. Pathol. Mech. Dis.* 9, 181–218.

McTague, A., Tazhitdinova, R., and Timoshenko, A. V. (2022). *O*-GlcNAc-mediated regulation of galectin expression and secretion in human promyelocytic HL-60 cells undergoing neutrophilic differentiation. *Biomolecules* 12, 1763.

Melo, R. C. N., and Weller, P. F. (2016). Lipid droplets in leukocytes: Organelles linked to inflammatory responses. *Exp. Cell Res.* 340, 193–197.

Messeguer, X., Escudero, R., Farré, D., Núñez, O., Martínez, J., and Albà, M. M. (2002). PROMO: detection of known transcription regulatory elements using species-tailored searches. *Bioinformatics* 18, 333–334.

Mittmann, L. A., Haring, F., Schaubächer, J. B., Hennel, R., Smiljanov, B., Zuchtriegel, G., et al. (2021). Uncoupled biological and chronological aging of neutrophils in cancer promotes tumor progression. *J. Immunother. Cancer* 9, e003495.

Modenutti, C. P., Capurro, J. I. B., Di Lella, S., and Martí, M. A. (2019). The structural biology of galectin-ligand recognition: Current advances in modeling tools, protein engineering, and inhibitor design. *Front. Chem.* 7, 823.

Nguyen, G. T., Green, E. R., and Mecsas, J. (2017). Neutrophils to the ROScue: Mechanisms of NADPH oxidase activation and bacterial resistance. *Front. Cell. Infect. Microbiol.* 7, 373.

Nose, F., Yamaguchi, T., Kato, R., Aiuchi, T., Obama, T., Hara, S., et al. (2013). Crucial role of perilipin-3 (TIP47) in formation of lipid droplets and PGE2 production in HL-60-derived neutrophils. *PLoS ONE* 8, e71542.

Olins, A. L., and Olins, D. E. (2004). Cytoskeletal influences on nuclear shape in granulocytic HL-60 cells. *BMC Cell Biol.* 5, 30.

Özcan, S., Andrali, S. S., and Cantrell, J. E. L. (2010). Modulation of transcription factor function by O-GlcNAc modification. *Biochim. Biophys. Acta* 1799, 353–364.

Peng, Z., Liu, C., Victor, A. R., Cao, D.-Y., Veiras, L. C., Bernstein, E. A., et al. (2021). Tumors exploit CXCR4 ^{hi} CD62L ^{lo} aged neutrophils to facilitate metastatic spread. *OncoImmunology* 10, 1870811.

Perou, C. M., Sørlie, T., Eisen, M. B., Van De Rijn, M., Jeffrey, S. S., Rees, C. A., et al. (2000). Molecular portraits of human breast tumours. *Nature* 406, 747–752.

Pohl, E., and Tomlinson, C. W. E. (2020). Classical pathways of gene regulation by retinoids. *Methods in Enzymology* 637, 151–173.

Popa, S. J., Stewart, S. E., and Moreau, K. (2018). Unconventional secretion of annexins and galectins. *Semin. Cell Dev. Biol.* 83, 42–50.

Qiu, B., and Simon, M. (2016). BODIPY 493/503 Staining of neutral lipid droplets for microscopy and quantification by flow cytometry. *Bio Protoc.* 6, e1912.

Qu, Y., Han, B., Yu, Y., Yao, W., Bose, S., Karlan, B. Y., et al. (2015). Evaluation of MCF10A as a reliable model for normal human mammary epithelial cells. *PLOS ONE* 10, e0131285.

R Core Team (2022). R: A language and environment for statistical computing. *R Found. Stat. Comput. Vienna Austria*. Available at: URL https://www.R-project.org/.

Reiterer, G., and Yen, A. (2007). Platelet-derived growth factor receptor regulates myeloid and monocytic differentiation of HL-60 cells. *Cancer Res.* 67, 7765–7772.

Rincón, E., Rocha-Gregg, B. L., and Collins, S. R. (2018). A map of gene expression in neutrophil-like cell lines. *BMC Genomics* 19, 573.

Robertson, K. A., Emami, B., Mueller, L., and Collins, S. J. (1992). Multiple members of the retinoic acid receptor family are capable of mediating the granulocytic differentiation of HL-60 cells. *Mol. Cell. Biol.* 12, 3743–3749.

Rohwedder, A., Zhang, Q., Rudge, S. A., and Wakelam, M. J. O. (2014). Lipid droplet formation in response to oleic acid in Huh-7 cells is a fatty acid receptor mediated event. *J. Cell Sci.* 127, 3104–3115.

Rosales, C. (2018). Neutrophil: A cell with many roles in inflammation or several cell types? *Front. Physiol.* 9, 113.

Rouillard, A. D., Gundersen, G. W., Fernandez, N. F., Wang, Z., Monteiro, C. D., McDermott, M. G., et al. (2016). The harmonizome: a collection of processed datasets gathered to serve and mine knowledge about genes and proteins. *Database* 2016, baw100.

Sapet, C., Simoncini, S., Loriod, B., Puthier, D., Sampol, J., Nguyen, C., et al. (2006). Thrombin-induced endothelial microparticle generation: identification of a novel pathway involving ROCK-II activation by caspase-2. *Blood* 108, 1868–1876.

Schäfer, T., Zentgraf, H., Zehe, C., Brügger, B., Bernhagen, J., and Nickel, W. (2004). Unconventional secretion of fibroblast growth factor 2 is mediated by direct translocation across the plasma membrane of mammalian cells. *J. Biol. Chem.* 279, 6244–6251.

Schneider, M. R., and Paus, R. (2010). Sebocytes, multifaceted epithelial cells: Lipid production and holocrine secretion. *Int. J. Biochem. Cell Biol.* 42, 181–185.

Sham, R. L., Phatak, P. D., Belanger, K. A., and Packman, C. H. (1995). Functional properties of HL60 cells matured with all-trans-retinoic acid and DMSO: Differences in response to interleukin-8 and fMLP. *Leuk. Res.* 19, 1–6.

Shaul, M. E., and Fridlender, Z. G. (2019). Tumour-associated neutrophils in patients with cancer. *Nat. Rev. Clin. Oncol.* 16, 601–620.

Sherazi, A. A., Jariwala, K. A., Cybulski, A. N., Lewis, J. W., Karagiannis, J., Cumming, R. C., et al. (2018). Effects of global *O*-GlcNAcylation on galectin gene-expression profiles in human cancer cell lines. *Anticancer Res.* 38, 6691–6697.

Skubitz, K., Zhen, Y., and August, J. (1982). Dexamethasone synergistically induces chemotactic peptide receptor expression in HL-60 cells. *Blood* 59, 586–593.

Stahl, M., and Tallman, M. S. (2019). Acute promyelocytic leukemia (APL): remaining challenges towards a cure for all. *Leuk. Lymphoma* 60, 3107–3115.

Stewart, S. E., Menzies, S. A., Popa, S. J., Savinykh, N., Harrison, A. P., Lehner, P. J., et al. (2017). A genome-wide CRISPR screen reconciles the role of N-linked glycosylation in galectin-3 transport to the cell surface. *J. Cell Sci.* 130, 3234–3247.

Tanaka, T., Kaneda, Y., Li, T.-S., Matsuoka, T., Zempo, N., and Esato, K. (2001). Digitonin enhances the antitumor effect of cisplatin during isolated lung perfusion. *Ann. Thorac. Surg.* 72, 1173–1178.

Taschner, S., Koesters, C., Platzer, B., Jörgl, A., Ellmeier, W., Benesch, T., et al. (2007). Down-regulation of RXRα expression is essential for neutrophil development from granulocyte/monocyte progenitors. *Blood* 109, 971–979.

Tasseff, R., Jensen, H. A., Congleton, J., Dai, D., Rogers, K. V., Sagar, A., et al. (2017). An effective model of the retinoic acid induced HL-60 differentiation program. *Sci. Rep.* 7, 14327.

Tazhitdinova, R., and Timoshenko, A. V. (2020). The emerging role of galectins and *O*-GlcNAc homeostasis in processes of cellular differentiation. *Cells* 9, 1792.

Tazhitdinova, R., and Timoshenko, A. V. (2021). The glycobiological landscape of breast cancer: insights into galectins and *O*-GlcNAc homeostasis-related genes. 14 September 2021, PREPRINT (Version 1) available at Research Square https://doi.org/10.21203/rs.3.rs-898135/v1.

Thijssen, V. L., Heusschen, R., Caers, J., and Griffioen, A. W. (2015). Galectin expression in cancer diagnosis and prognosis: A systematic review. *Biochim. Biophys. Acta* 1855, 235–247.

Timoshenko, A. V. (2015). Towards molecular mechanisms regulating the expression of galectins in cancer cells under microenvironmental stress conditions. *Cell. Mol. Life Sci.* 72, 4327–4340.

Trebo, A., Ditsch, N., Kuhn, C., Heidegger, H. H., Zeder-Goess, C., Kolben, T., et al. (2020). High galectin-7 and low galectin-8 expression and the combination of both are negative prognosticators for breast cancer patients. *Cancers* 12, 953.

Tribulatti, M. V., Figini, M. G., Carabelli, J., Cattaneo, V., and Campetella, O. (2012). Redundant and antagonistic functions of galectin-1, -3, and -8 in the elicitation of T cell responses. *J. Immunol.* 188, 2991–2999.

Tsao, C.-H., Hsieh, W.-C., Lin, F.-J., Yang, R.-Y., Chang, M.-T., Apaya, M. K., et al. (2022a). The critical role of galectin-12 in modulating lipid metabolism in sebaceous glands. *J. Invest. Dermatol.* 143, 913-924.e4.

Tsao, C.-H., Hsieh, W.-C., Yang, R.-Y., Lo, Y.-H., Tu, T.-J., Ke, L.-Y., et al. (2022b). Galectin-12 modulates sebocyte proliferation and cell cycle progression by regulating cyclin A1 and CDK2. *Glycobiology* 32, 73–82.

Tunçer, S., Gurbanov, R., Sheraj, I., Solel, E., Esenturk, O., and Banerjee, S. (2018). Low dose dimethyl sulfoxide driven gross molecular changes have the potential to interfere with various cellular processes. *Sci. Rep.* 8, 14828.

Uhl, B., Vadlau, Y., Zuchtriegel, G., Nekolla, K., Sharaf, K., Gaertner, F., et al. (2016). Aged neutrophils contribute to the first line of defense in the acute inflammatory response. *Blood* 128, 2327–2337.

Uhlén, M., Fagerberg, L., Hallström, B. M., Lindskog, C., Oksvold, P., Mardinoglu, A., et al. (2015). Tissue-based map of the human proteome. *Science* 347, 1260419.

Väremo, L., Nielsen, J., and Nookaew, I. (2013). Enriching the gene set analysis of genome-wide data by incorporating directionality of gene expression and combining statistical hypotheses and methods. *Nucleic Acids Res.* 41, 4378–4391.

Vinnai, J. R., Cumming, R. C., Thompson, G. J., and Timoshenko, A. V. (2017). The association between oxidative stress-induced galectins and differentiation of human promyelocytic HL-60 cells. *Exp. Cell Res.* 355, 113–123.

Wan, L., Lin, H.-J., Huang, C.-C., Chen, Y.-C., Hsu, Y.-A., Lin, C.-H., et al. (2016). Galectin-12 enhances inflammation by promoting M1 polarization of macrophages and reduces insulin sensitivity in adipocytes. *Glycobiology* 26, 732–744.

Wang, B., Yan, Y., Zhou, J., Zhou, Q., Gui, S., and Wang, Y. (2013). A novel all-trans retinoid acid derivatives inhibits the migration of breast cancer cell lines MDA-MB-231 via myosin light chain kinase involving p38-MAPK pathway. *Biomed. Pharmacother.* 67, 357–362.

Wang, Q., Jones, J., and Studzinski, G. P. (1996). Cyclin-dependent kinase inhibitor p27 as a mediator of the G1-S phase block induced by 1,25-dihydroxyvitamin D3 in HL60 cells. *Cancer Res.* 56, 264-7.

Wang, Y., and Zhou, B. P. (2011). Epithelial-mesenchymal transition in breast cancer progression and metastasis. *Chin. J. Cancer* 30, 603–611.

Wu, Y.-T., Tan, H.-L., Shui, G., Bauvy, C., Huang, Q., Wenk, M. R., et al. (2010). Dual role of 3-methyladenine in modulation of autophagy via different temporal patterns of inhibition on Class I and III phosphoinositide 3-kinase. *J. Biol. Chem.* 285, 10850–10861.

Xue, H., Yang, R.-Y., Tai, G., and Liu, F.-T. (2016). Galectin-12 inhibits granulocytic differentiation of human NB4 promyelocytic leukemia cells while promoting lipogenesis. *J. Leukoc. Biol.* 100, 657–664.

Yan, Y., Li, Z., Xu, X., Chen, C., Wei, W., Fan, M., et al. (2016). All-trans retinoic acids induce differentiation and sensitize a radioresistant breast cancer cells to chemotherapy. *BMC Complement. Altern. Med.* 16, 113.

Yang, R.-Y., Hsu, D. K., Yu, L., Chen, H.-Y., and Liu, F.-T. (2004). Galectin-12 is required for adipogenic signaling and adipocyte differentiation. *J. Biol. Chem.* 279, 29761–29766.

Yang, R.-Y., Hsu, D. K., Yu, L., Ni, J., and Liu, F.-T. (2001). Cell cycle regulation by galectin-12, a new member of the galectin superfamily. *J. Biol. Chem.* 276, 20252–20260.

Yang, R.-Y., Rabinovich, G. A., and Liu, F.-T. (2008). Galectins: structure, function and therapeutic potential. *Expert Rev. Mol. Med.* 10, e17.

Yang, R.-Y., Xue, H., Yu, L., Velayos-Baeza, A., Monaco, A. P., and Liu, F.-T. (2016). Identification of VPS13C as a galectin-12-binding protein that regulates galectin-12 protein stability and adipogenesis. *PLOS ONE* 11, e0153534.

Yang, R.-Y., Yu, L., Graham, J. L., Hsu, D. K., Lloyd, K. C. K., Havel, P. J., et al. (2011). Ablation of a galectin preferentially expressed in adipocytes increases lipolysis, reduces adiposity, and improves insulin sensitivity in mice. *Proc. Natl. Acad. Sci.* 108, 18696–18701.

Yang, X., and Qian, K. (2017). Protein O-GlcNAcylation: emerging mechanisms and functions. *Nat. Rev. Mol. Cell Biol.* 18, 452–465.

Yasinska, I. M., Sakhnevych, S. S., Pavlova, L., Teo Hansen Selnø, A., Teuscher Abeleira, A. M., Benlaouer, O., et al. (2019). The Tim-3-galectin-9 pathway and its regulatory mechanisms in human breast cancer. *Front. Immunol.* 10, 1594.

You, H., Yu, W., Sanders, B. G., and Kline, K. (2001). RRR-α-tocopheryl succinate induces MDA-MB-435 and MCF-7 human breast cancer cells to undergo differentiation. *Cell Growth Differ.* 12, 471–480.

Yu, B., Yuan, B., Kiyomi, A., Kikuchi, H., Hayashi, H., Hu, X., et al. (2019). Differentiation induction of human breast cancer cells by arsenite in combination with tetrandrine. *Am. J. Transl. Res.* 11, 7310–7323.

Zhang, D., Chen, G., Manwani, D., Mortha, A., Xu, C., Faith, J. J., et al. (2015). Neutrophil ageing is regulated by the microbiome. *Nature* 525, 528–532.

Zwerger, M., Herrmann, H., Gaines, P., Olins, A. L., and Olins, D. E. (2008). Granulocytic nuclear differentiation of lamin B receptor–deficient mouse EPRO cells. *Exp. Hematol.* 36, 977–987.

Appendix: Supplementary Material

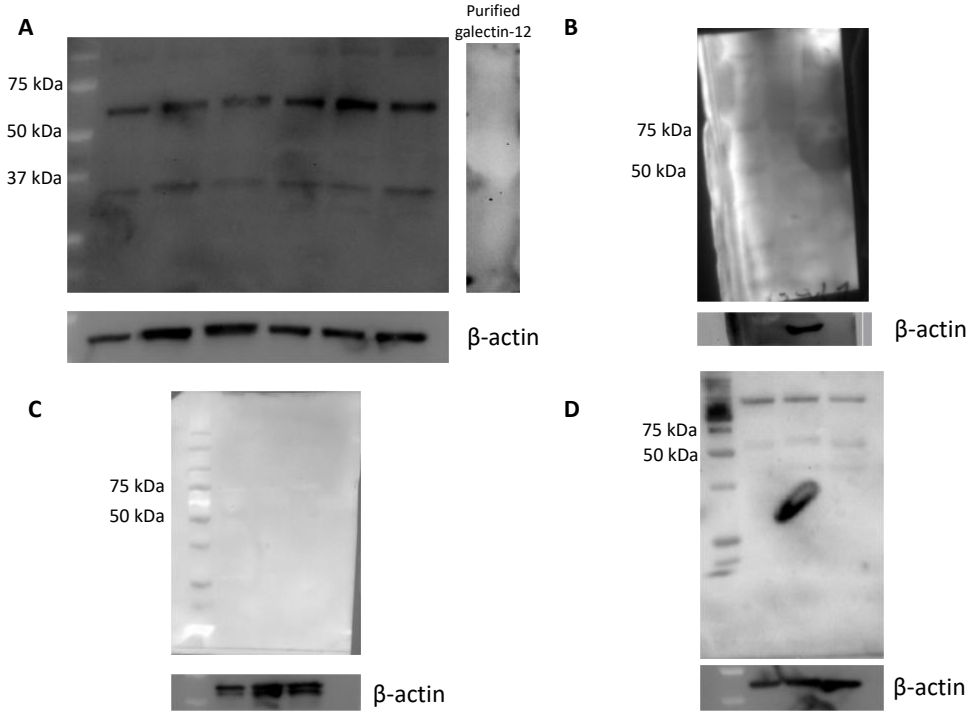

Figure 1S. Tested commercially available galectin-12 antibodies.

The expected molecular size of galectin-12 is 37 kDa (Hotta et al., 2001). (A) Invitrogen galectin-12 antibody (PA5-113236, 1:500) was tested using control HL-60 cells and those treated with ATRA, DMSO, TG, AC and DON. Purified galectin-12 from a human ELISA kit was also tested. (B) Bioss galectin-12 antibody (BS-8413R, 1:500) was tested using differentiated mouse 3T3-L1 cells and purified galectin-12. (C) Santa Cruz galectin-12 antibody (sc-67294, 1:200) was tested using control HL-60 cells and those treated with ATRA and DMSO. (D) Abnova galectin-12 antibody (H00085329-B02P, 2 µg/mL) was tested using control HL-60 cells and those treated with ATRA and AC. β-actin (sc-47778, 1:200) was used as a control for all tested samples.

Curriculum Vitae

Name: Rada Tazhitdinova

Post-secondary Education and Degrees:

The University of Western Ontario
London, Ontario, Canada
2021-2023 M.Sc. in Biology
2016-2021 B.Sc. Honours Specialization in Genetics

Honours and Awards:

2022-2023 Canada Graduate Scholarship – NSERC CGS-M
2021-2022 Ontario Graduate Scholarship
2021 The University of Western Ontario Gold Medal
Honours Specialization in Genetics
2020, 2021 Bennie and Shirley Bradshaw Award in Science

Related Work Experience:

2022-2023 Teaching Assistant – The University of Western Ontario
2020 Western Undergraduate Student Research Internship
2019 Undergraduate Student – Research Work (V9518)

Publications:

McTague, A., **Tazhitdinova, R.**, and Timoshenko, A. V. (2022). *O*-GlcNAc-mediated regulation of galectin expression and secretion in human promyelocytic HL-60 cells undergoing neutrophilic differentiation. *Biomolecules* 12, 1763.

Tazhitdinova, R., and Timoshenko, A. V. (2021). The glycobiological landscape of breast cancer: insights into galectins and *O*-GlcNAc homeostasis-related genes. 14 September 2021, Preprint (Version 1) available at Research Square https://doi.org/10.21203/rs.3.rs-898135/v1.

Tazhitdinova, R., and Timoshenko, A. V. (2020). The emerging role of galectins and *O*-GlcNAc homeostasis in processes of cellular differentiation. *Cells* 9, 1792.

Jariwala, K. A., Sherazi, A. A., **Tazhitdinova, R.** , Shum, K., Guevorguian, P., Karigiannis, J., Staples, J. F., and Timoshenko, A. V. (2020). The association between increasing levels of *O*-GlcNAc and galectins in the liver tissue of hibernating thirteen-lined ground squirrels (*Ictidomys tridecemlineatus*). *Cell and Tissue Res*. 381, 115-123.

Abstracts and Posters:

Tazhitdinova, R., Laus, K., and Timoshenko, A. V. (2023). The potential role of tissue-specific galectins as tumor suppressors. 19th Annual Oncology Research and Education Day, London, Ontario, June 9th.

Tazhitdinova, R., Cristiano, S., Zhurov, V., and Timoshenko, A. V. (2023). Investigating the role and regulation of galectin-12 in a model of neutrophil-like differentiation of human acute promyelocytic leukemia HL-60 cells. 4th Annual Immuno-Oncology Symposium, London, Ontario, March 29th.

Tazhitdinova, R., and Timoshenko, A. V. (2022). Investigating the molecular mechanisms of galectin-12 regulation in human acute promyelocytic leukemia HL-60 cells. 18th Annual Oncology Research and Education Day, London, Ontario, June 10th.

Tazhitdinova R., Timoshenko, A.V. (2021). The glycobiological landscape of breast cancer: galectins and *O*-GlcNAc homeostasis-related genes. Canadian Cancer Research Conference, virtual, November 8-11th.

Tazhitdinova, R., and Timoshenko, A. V. (2021). Examining the glycobiological landscape of breast cancer: Galectins and *O*-GlcNAc homeostasis-related genes. 17th Annual Oncology Research and Education Day, virtual, June 14-18th.

Tazhitdinova, R., and Timoshenko, A. V. (2019). HL-60 cells as a new model of cell differentiation in serum-free medium. Western Cell Stress Symposium, London, Ontario, August 27th.